SET-THEORETIC ANALYSIS OF MULTI-LINK SYSTEMS WITH APPLICATIONS TO GAIT

by

ZVI LADIN

B.Sc., Technion, Israel, 1974
M.Sc., Technion, Israel, 1978

SUBMITTED TO THE DEPARTMENT OF HEALTH SCIENCES AND TECHNOLOGY IN PARTIAL FULFILLMENT OF THE REQUIREMENTS FOR THE DEGREE OF

DOCTOR OF PHILOSOPHY

at the

MASSACHUSETTS INSTITUTE OF TECHNOLOGY

July 1985

Signature of Author _____
Department of Health Sciences and Technology
July 11, 1985

Certified by _____
Woodie C. Flowers
Thesis Supervisor

Accepted by _____
Ernie G. Cravalho
Chairman, Dept. Committee of Graduate Studies

to

RIVKA

KEREN

DROR

Set-Theoretic Analysis of Multi-Link
Systems With Applications To Gait

by

ZVI LADIN

Submitted to the Department of Health Sciences and Technology on July 11, 1985 in partial fulfillment of the requirements for the degree of Doctor of Philosophy.

Abstract

The introduction of powered prostheses for lower-limb amputees may improve mobility and increase the ability to safely respond to stumbles and other disturbances. Set-Theoretic analysis has been applied to a basic mode of an amputee-prosthesis system in order to examine how gait disturbances or uncertainties propagate through the gait cycle and ultimately affect the likelihood that the next step can be taken.

This thesis presents the first extension of Set-Theoretic analysis to the study of the propagation of uncertainties in multi-link systems. The mathematical formulation involves the local linearization of the state-equations of a multi-link system around its nominal trajectory, and the description of bounded sets of states by ellipsoids in the state-space.

An automated procedure to generate the linearized symbolic version of the state-equations using the MACSYMA program is described. A double pendulum, affected by two constant-torque actuators at the joints has been studied. The direction of the joint-torques and the initial conditions have a strong effect on the propagation of the initial uncertainties.

A three-link, two-degree-of-freedom model has been analyzed, and the results suggest that disturbances tend to die-out at the end of swing phase. Hence, the geometric coupling created by the joints has a beneficial effect at the critical state of load transfer.

Thesis Committee:

Prof. Woodie Flowers, Chairman
Associate Professor of Mechanical Engineering, M.I.T.

Prof. Fred Schweppe
Professor of Electrical Engineering and Computer Science, M.I.T.

Prof. Neville Hogan
Associate Professor of Mechanical Engineering, M.I.T.

Prof. Robert Mann
Professor of Mechanical Engineering, M.I.T.

Dr. Eugene Record
Chief of Staff, VA Outpatient Clinic, Boston, Massachusetts

Thesis Supervisor: Woodie C. Flowers
Title: Associate Professor of Mechanical Engineering

Acknowledgements

With my tenure as a graduate student at M.I.T coming to an end, I look back at the past years, realizing the enormous change I have gone through. The educational process I participated in will always have a very special place in my heart. So many people have contributed so much for so long toward the success of this process, that no matter how hard I try, I will never be able to thank them all.

First I would like to thank Professor Woodie Flowers who always encouraged me to ask questions and to try out new answers and ideas, even if initially they seem somewhat far-fetched.

Professor Fred Schweppe deserves special thanks. He was a constant source of moral and professional support, and by keeping his door, mind and heart always open and available helped me to overcome quite a few difficult moments (or rather days).

Thanks to Professors Hogan, Mann and Doctor Record for their assistance. Despite their busy schedules they always found time to answer my questions.

My appreciation goes to my office mates, past and present, Jeff Stein, Cary Abul-Haj, Ed Colgate and Joe Belot for making this office such a wonderful environment. Special thanks to Bill Murray who was always there to lend a helping hand, and was so generous with his time and experience.

Thanks also to Ralph Burgess and to George Darlymple on their help in solving electronic and computer hardware problems.

There could not be a better opportunity to thank my parents. My mother

who gave so much of herself for my well-being, and my father for teaching me the importance of being an autodidact.

Last but in many respects first, special thanks to my wife Rivka. Her love, support and understanding throughout the years helped to overcome many difficult, and seemingly unsurmountable obstacles. And finally thanks to my children Dror and Keren, who revealed to me the new and wonderful dimension of life - parenthood.

The support for this work was provided by a Whitaker Fellowship, and by NSF Grant No. ECS8023193, and is gratefully acknowledged.

Table of Contents

List of Figures

List of Tables

Chapter 1
Introduction

1.1 Control Issues In Gait Research

Gait is the process by which a human being, an animal or a walking mechanism moves over the ground by periodically and discretely establishing support. The supporting links (legs) serve the dual purpose of supporting the body weight and propelling it in the desired direction. It is clear from this defintion that gait must be a controllable process. The control aspects of gait could be organized hierarchically into three levels:

1. the decision how to progress (i.e. direction, mode)
2. the exact sequence of neuromuscular activity required to execute the above decision
3. the execution of the above sequence given environmental disturbances

The first level involves strategic decisions. These include decisions about the direction of locomotion, the kind of surface that has to be negotiated and its slope in the field of gravity.

The second level includes the time sequences of actuator activation and deactivation, the patterns of sensor input that are required to maintain the planned trajectory (either for switching purposes, or for analog input required as a part of feedback loops).

The third level deals with the sensitivity and stability of the process. In the

human (and animal) it includes spinal reflexes (like the cat's placement reflex) which are aimed at overcoming local (and small) disturbances, without the need for involving higher level information processing centers.

Most gait research can be divided into three different categories:

1. synthetic gait and analytic modeling
2. experimental measurements
3. walking machines and prosthetic research

Since a successful characterization of the gait process has to address all the control issues listed above (explicitly or implicitly), an organizational framework that consists of the following table has thus been constructed.

gait research category / hierarchical level	synthetic gait and analytic modeling	experimental measurements	walking machines and prosthetic research
decision making level			
trajectory planning			
sensitivity and stability			

Table 1-I: An organizational framework for gait research

Table 1-I is a useful framework to chracterize and evaluate individual contributions in the field of gait. This work attempts to fill a void in the left bottom square of

the above table, by supplying a theoretical tool to examine the sensitivity of gait models to disturbances. A more comprehensive discussion of the above table can be found in chapter 2.

1.2 Research Objectives

The work presented in this thesis describes a new comprehensive method for analyzing the sensitivity of gait models (or of any multi-linkage system) to unknown-but-bounded disturbances (i.e. the only information available about the disturbances is the fact that they are smaller than or equal to an upper limit).

The mathematical tool that has been applied for this purpose is called Set-Theoretic analysis, and is aimed at describing the interrelationships between bounded disturbances, bounded (i.e. constrained) states, and bounded actuators. The research goals of this thesis can be defined as follows.

1. Develop a mathematical formulation of Set-Theoretic applied to multi-linkage systems in general, and to gait analysis in particular.

2. Study the time propagation of discrete and continuous disturbances in a multi-linkage system.

3. Examine the sensitivity of a simple gait model to disturbances.

1.3 Thesis Organization

Chapter 1 includes the introduction to the thesis. It presents an organizational framework for examining past and present contributions in the area of gait control and introduces the concept of bounded sets and the use of Set-Theoretic analysis for the sensitivity analysis of gait models. This chapter also

includes a statement of research objectives and a general outline of the thesis.

Chapter 2 elaborates on the major recent contributions to the field of gait-research, in the context of the organizational framework introduced in chapter 1.

Chpter 3 describes the geometric and dynamic issues involved in load transfer. It illustrates the need for the use of sets (as opposed to specific states or trajectories), and the study of the interrelathionship between the magnitude of the disturbances, the available actuaors and the given system.

Chapter 4 describes one approach to the study of the interrelationship between disturbances, actuators and states. The approach is based on the solution to a two-point-boundary-value problem, and uses a single pendulum as a working example.

Chapter 5 describes the Set-Theoretic formulation as apllied to multi-linkage systems. It includes a description of the unknown-but-bounded class of control problems, an overview of the historical development of Set-Theoretic, and the mathematical formulation of Set-Theoretic applications to multi-linkage systems. It gives a detailed description of the sensitivity analysis of multi-linkage systems to bounded disturbances. It includes the description of the automatic equation-generator that has been developed in this work (using Paul's algorithm [40]), the integration packages used for the numerical solution, and the non-linear geometric transformation used to display the results.

Chapter 6 describes the major results obtained by the use of Set-Theoretic analysis to study the sensitivity of a double-pendulum to disturbances. It includes the description of the verification procedures used on the results. It describes the time propagation of discrete and continuous disturbances in a double pendulum system, affected by two constant-torque actuators located at the joints.

Chapter 7 illustrates the power of using Set-Theoretic to analyze the sensitivity of a three-link gait model to disturbances.

Chapter 8 concludes the thesis, assesses the contributions of this work both in the field of gait research and Set-Theoretic control. It suggests the direction for future experimental and theoretical research in the general field of multi-linkage systems, and in the specific area of gait modeling .

The thesis has been written with the understanding that two different populations of readers may wish to read it: control engineers and gait researchers. It is recommended that people who are only interested in the Set-Theoreic applications or the issues of theoretical control, should read chapters 1, 5, 6 and 8. Gait researchers should read chapters 1, 2, 3, 4, 7 and 8.

Chapter 2
An Overview of Gait Research

2.1 Hierarchical Control

The theory of evolution describes the development of humans from lower forms of species. In addition to sociological and intellectual changes, a noticeable behavioral change (with strong anatomical ramifications) involves the change in the form of locomotion[1]. Animals use legged locomotion in a variety of modes and for different terrains; the number of legs involved is usually four or more (an exception are the Marsupials like the kangaroos which use bipedal hopping). In characterizing quadrupedal gait two terms are of special value: the duty factor and the relative phase. McGhee [25] first introduced the term "duty factor" to describe the portion of the cycle that each foot is in contact with the ground. Alexander [1] introduced the term "relative phase" to characterize the sequence of leg placement on the terrain. McMahon [26] uses those definitions to describe six distinctively different quadrupedal gaits.

Humans use bipedal gait in one of two modes: walking or running. Whether a period of double support exists or not is usually used to distinguish running from walking. If one takes a closer look at each of these modes, a finer characterization can be made. This characterization involves the grouping together of patterns of

---

[1] some interesting observations on the evolutionary development of fish movement into the locomotory cycle of the newt can be found in [14]

locomotion, for example level walking, walking up a ramp or walking down a staircase. The decision which pattern to adopt is a conscious decision, which is probably made at the high levels of the brain. Such a decision is based on integration of information from the environment with conscious decisions about intentions, and generates what can be termed as a strategy for negotiating the environment.

The result of any decision is the creation of a pattern of periodic neuromuscular activity (which can be generated at the spinal level, as some studies suggest), which moves the lower limbs (and the rest of the body) in a periodic manner. Such a pattern will produce a trajectory for all the links which make up the limbs, in order to successfully negotiate the environment.

The description up to this point is of a hierarchical system which uses afferent information coming from the environment through the sensory interface, integrates it with conscious information about the intentions, and creates a periodic activity of the neuromuscular system. The neuromuscular activity generates periodic trajectories of the limbs.

Fig. 2-1 illustrates this hierarchy described above in a graphic form: the left side describes the information processing portion of the system. The sensory information from the environment is integrated with the concious intentions and produces the first level of control - the decision making level. The resulting information outflow creates the periodic neural activity which constitutes the second level of control.

The neural activity drives the muscular system, which in turn generates physical movements of the body segments. The physical interaction between the body and the world is depicted on the right side of the figure. The figure also

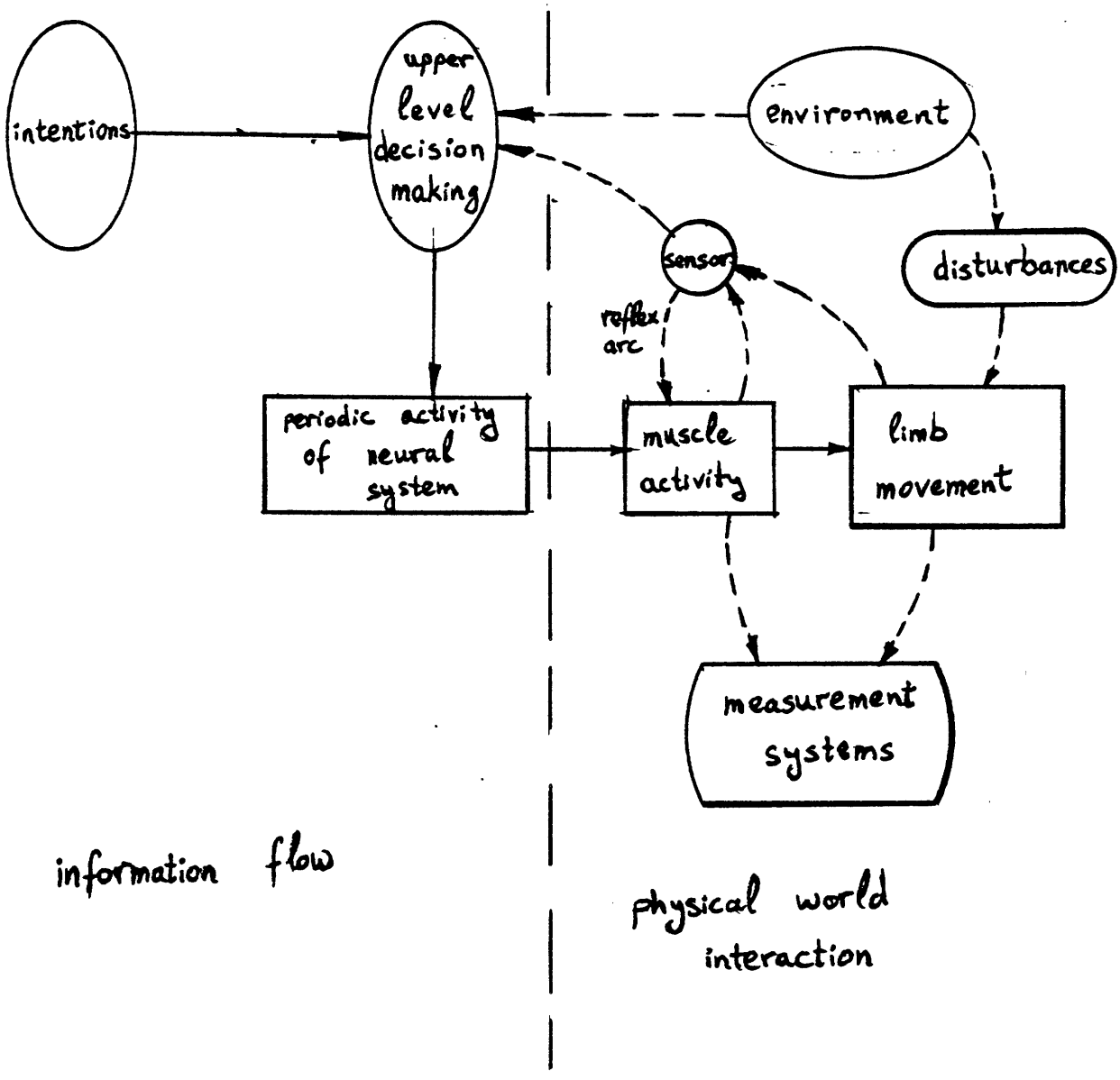

Figure 2-1: The hierarchical organization of the locomotion control system

describes the possible occurance of disturbances, which are generated by the environment and affect the limb movements. The closed loop which connects the limb movement, the sensors and the muscular activity describes the local (e.g. spinal) response to disturbances, which constitutes the third level of control.

In summary, a study of the control aspects of the gait phenomenon can involve any of the three levels of control described above:

1. the decision making level
2. the trajectory planning and execution
3. the sensitivity of the above trajectories to disturbances

The essence of this study is to describe a new and promising tool for examining the sensitivity of the gait process to disturbances.

2.2 The Different Facets of Gait Research

In reviewing the gait research that has been performed to this day, a useful categorization involves the following three areas:

1. theoretical gait models
2. experimental work
3. walking machines and prostheses

The theoretical research involves different models which were designed to generate dynamic and kinematic trajectories, to analyze possible networks of information flow and to test the stability of different models.

The experimental work involves measurements of kinematic and dynamic

variables, patterns of muscular activity, and observations of the effects of different neural defficiencies on the performance of the limbs.

The prosthetics and the walking machines area includes the prosthetic replacement of all or parts of the lower limbs on one hand, and the research and development of walking machines on the other.

The essence of the last two sections has been described in chapter 1 and has been summarized in table 2-I. The table is repeated here for completeness, and a few entries illustrate the use of the table.

	gait models	experimental work	walking machines
strategy	McGhee (quadruped gallop, trot)	Alexander (transition from walking to running)	Ozguner et al (Ohio hexapod; preview information)
patterns	Vukobratovic	Bressler & Frankel Murray	Raibert (hopper)
sensitivity and stability	this work	Nashner	Miura and Shimoyama (biper)

Table 2-I: An organizational framework for gait research

The table is made up of a 3x3 matrix. The vertical axis describes the hierarchical control of the gait process, and the horizontal axis describes the different aspects of gait research. The table organizes past and present gait research, enables the examination past contributions in the field, and permits assessments of the need for future research. The rest of this chapter examines past gait research in the context

of the organizational framework suggested above.

2.3 Theoretical Gait Models

The scope of the theoretical models that have been developed in the past 20 years touches upon the different control levels of gait analysis and synthesis. Most of the research works discuss the trajectory planning level, some examine the stability issues of different models, and only a few mention or discuss the highest control level (the decision making level). Only during the last few years has this problem been tackled, and only for statically stable walking machines (as will be described in later sections). It should be noted that the hierarchical control of gait has been mentioned by [58] (three level control) and [32], [59] (two level control).

2.3.1 Trajectory planning

Two major approaches have been taken for the purpose of generating the required trajectories: the kinematic/dynamic approach and the optimization approach.

2.3.1.1 Kinematic/dynamic models

Vukobratovic and Juricic [58] and Frank [10] synthesized two simplified forms of gait, and solved the control problem required to maintain those forms of gait. Vukobratovic and Juricic used a model which resembled a cross-country skier, using the upper body as a balancing weight to stabilize the gait. The feet were kept in contact with the ground at all time. Frank described a model which resembled a person riding a unicycle. Both models are far from describing the bi-phasic aspects of gait (i.e. the change from stance to swing and vice versa) and they

can be considered more like models of sliding than of walking. The interesting feature of the models, though, is the the mathematical description of steps, achieved by interchanging the supporting leg.

Vukobratovic et al [57] examined the above models for stability, and showed that the first model could be stabilized by either a discrete or a continuous strategy. The discrete strategy involved correcting any errors at the end of each cycle (basically setting up correct initial conditions for the next cycle). The continuous strategy suggested making continuous changes in the period and/or the amplitude of the counter-weight oscillations. The second model could be stabilized against either position or velocity errors of the mass, by using position and velocity feedback (to prevent the body mass from tipping over).

Gubina et al [17] introduced a new, linearized planar model, consisting of a planar body on top of a massless leg. This model relaxed the synchronous leg switching requirement, and suggested an asynchronous, position dependent switching (which, in effect, is step-size control[2]). Position and velocity feedback of the leg angle were used to stabilize the model against disturbances. Even though the controller design is based on a linearized model, it was shown to be effective for the nonlinear dynamic equations as well.

Morawski [32] describes a two-level hierarchy (which he terms strategy and tactics). A kinematic control of the locomotion speed (strategy) is described, while maintaining lateral stability using asynchronous switching of leg support (tactics). In spite of the simplicity of the model (an inverted pendulum), it does explain some of the features observed in bipedal gait (e.g. use of the body's attitude as a part of

---

[2]as will be described in a later section, this form of control has been adopted for dynamically stable monoped and biped walking machines

the longitudinal velocity control).

The last work to be included is that of Mochon [28], [29] which suggests that the swing phase of normal gait is ballistic in its nature. Hence, the major role of the double-support phase is to set the initial conditions for the ballistic phase.

2.3.1.2 Optimization solutions

The first works in this category are those of Nubar and Contini [37] who described a minimum principle in biomechanics, and Beckett and Chang [4] who suggested that gait is a minimum energy process.

Chow and Jacobson [8] also suggested the existence of hierarchical control, with a somewhat different task allocation between the different levels. They prescribed hip and foot center of pressure trajectories and used experimentally measured foot floor interaction forces, in order to generate a mixture of algebraic and optimization trajectories for the different state variables in their model. In their extensive paper they touched upon the sensitivity to initial conditions (and to final conditions), but no methodological treatment of disturbances is given.

Townsend [55], [53], [54] solved an optimization problem, which minimized foot placement area and energy expenditure. Their results strongly depended on the weighting function used.

Beletskii and Golubitskaya [5] synthesized a linearized oscillatory gait of a biped (moving the contact linearly with time). They found that oscillations were advantageous to minimize energy expenditure and control-moments; it is also advantageous to supply impulse torques at the moment of leg support change.

2.3.2 Stability analysis

As was shown earlier, quite a few of the researchers who were involved in attempts to generate reference trajectories for gait models, took a closer look at the issue of model stability. The results of such analyses are usually valid only for the specific model under consideration.

The most comprehensive and promising approach to the determination of whether a model is stable or not can be found in the work of Hemami and Chen [18]. They have shown that 4 out of the 6 degrees of freedom of a 2-link planar model can be stabilized by viscoelastic forces. The other 2 degrees of freedom can be stabilized using active torques. The stability was obtained around an equilibrium position using a Lyapunov function.

The work described in this thesis is aimed at generating a general formulation for dealing with the sensitivity analysis of theoretical models. It also addresses one of the major concerns raised by Hemami and Chen: it permits finding the small regions around the trajectory where arbitrary movements DO satisfy the connection constraints between the different links. Hence, any variational analysis method which is attempted must be performed inside those regions, in order not to violate the geometric connectivity constraints of the multi-linkage model.

It is interesting to note that Vukobratovic and Stokic [59] describe a different approach for analyzing and stabilizing small disturbances. That approach is based on generating decoupled linearized state equations for small deviations from a nominal trajectory. However, that approach is only valid when certain state variables can be used to generate linear state equations (with respect to the controlled actuators). This limitation does not apply to the analysis suggested in this thesis.

2.4 Experimental gait research

2.4.1 The hierarchical organization of gait control

Physiological and clinical studies have been conducted in order to study the hierarchy of gait control (this terminology has been first used by the Russian physiologist Bernstein in the early 1930's). Those studies have produced a strong physiological evidence for the role of spinal reflexes in overcoming disturbances (what has been termed as "dynamic" or "decentralized" control). There is also a growing body of clinical data which describes the role of certain brain structures (like the cerebellum) in making high-level strategic decisions about the process of locomotion (e.g. maintaining posture during level walking), but there are only conjectures for explaining the details of the trajectories exhibited in any given mode of locomotion.

McMahon [26] describes the "placing reaction": when an animal experiences a disturbance to the dorsal aspect of a paw, the limb will respond in one of three possible responses, depending on the paw's locomotion phase. If the disturbance takes place during swing phase, the limb flexes to overcome the disturbance; the same disturbance applied during stance phase generates extensor activity. The same reflex takes place if the cat is blindfolded and is held in such a way that the paw is unsupported. Since the reflex is the same for spinal cats [15], it appears likely that this is a spinal reflex, modulated by the foot position. A similar response is exhibited by a person walking in the dark.

2.4.2 Kinematic and dynamic trajectories in normal gait

The modern study of kinematic and dynamic trajectories in normal gait (both in terms of methods and findings) can be traced back to Marey [23] and to Muybridge [35]. Marey was the first to use a head mounted accelerometer to study body accelerations, and air-chambers in the shoes as the first prototype of a portable force-plate. Muybridge used multiple-camera photography to study human movements.

Numerous researchers have since dealt with the kinematics and dynamics of the gait process Murray et al [33], [34], Bressler and Frankel [7], Antonsson [3], Winter and his group [61], [60], Zarrugh [65], Simon et al [49] and many others. The methods of measurement range from using optoelectronic systems which measure position and estimate the time derivatives, to systems which use accelerometers to measure accelerations and to estimate velocities and positions. In order to generate accurate dynamic measurements, a force-plate to measure foot-floor interactions is usually used.

2.4.3 Sensitivity to disturbances in bipedal gait

The only study which tried to address directly the issue of bipedal gait sensitivity to disturbances is the study by Nashner [36]. In that study, a movable platform was incorporated in a walkway. The platform produced small position and orientation perturbations, and the EMG activity of the gastrocnemius and tibialis anterior was measured. The major finding was that the EMG patterns produced muscular activity, which tended to resist changes in the nominal rotational trajectory of the supporting (and disturbed) ankle. It is interesting to note that the EMG response pattern was similar to the response observed in a

standing subject, experiencing the same disturbances. This finding, coupled with the physiological measurements of the "placing reaction", suggests the existence of a unified strategy for handling disturbances to a person in an upright position.

The unanswered question, which relates to this thesis, is "how do the kinematic disturbances propagate through the system?, do they die out with the trajectory converging to the original trajectory, or does the control system modify the original trajectory?". If the behavior of the human body is any indication to the performance of a system that has been improved and fine-tuned in the long process of evolution, then such information is invaluable in the design process of adaptive gait controllers (either for amputees or for man-made walking machines).

2.5 Walking Machines and Prostheses

The last facet of gait research is the area of walking machines and prostheses design. Among the different walking machines that have been developed (most of them within the last 20 years), there are clearly two groups: statically stable or dynamically stable. Statically stable machines enjoy the same kind of stability that a table enjoys (the projection of the gravity vector is always inside the bonded polygon formed by the supporting legs). Dynamically stable machines allow the projection of the gravity vector to be outside the support area during some portions of the cycle.

2.5.1 Statically stable machines

Since the major problem of any walking device is to maintain its stability, it is not surprising that the very first walking device (the "Phoney Pony" built by Frank and McGhee in 1966 [24] was a quadruped. The device was able to perform

level walking under computer control at top speed 0.5 miles per hour. Of special interest is the control strategy used in this case - which is a finite state control [52]. This is a realization of the hierarchical strategy of gait control, and it involves the integration of automata theory and finite states, with continuous control required for automatic control of devices, by the introduction of the cybernetic actuator.

A further step toward the realization of a walking machine which can negotiate rough terrains has been achieved by Hirose [19]. That design is based on slowing down the walking quadruped machine, so that a stable support can be found for the swinging leg (i.e., the machine is statically stable all the time). Ozguner et al [39] present an even closer solution to the biological system by integrating preview information. The algorithm was used to correctly place the legs of a hexapod on a rough terrain.

It is interesting to contrast the above examples of hierarchical control[3] with the GE Quadruped Transporter built by Liston and Mosher in 1968 [22]. This 3000 lb hydraulic elephant was controlled by a human operator who was strapped into a seat and manually controlled each of the twelve degrees of freedom. Force feedback from the legs was provided to the operator.

The control task was so demanding that no human operator, experienced as may be, was able to "drive" it for more than a few minutes at a time.

---

[3] aimed at getting the human operator directly involved only in the high-level decisions of direction and velocity, while being removed from the task of directly controlling the degrees of freedom of each link

2.5.2 Dynamically stable machines

Since the issue of dynamic stability is the prime focus of this thesis, a detailed description of the control aspects of dynamically stable machines will be given in this subsection. The only truly dynamically stable machines are the monoped hopper developed by Raibert and his group at CMU (a research summary can be found in [41]), and the Miura and Shimoyama biped [27] (dubbed the "biper"). The hopper is made of an inverted pendulum, with the mass - also called the body, hinged to a leg. Control torques can be applied at the hinge (also termed the hip). This device represents an interesting approach to crystallize the necessary conditions for maintaining a periodic movement, while establishing only discrete and short intervals of ground support. The biper maintains stable gait (at least one leg is always in contact with the floor) using three actuators (or five in a more advanced model).

The most interesting aspect of the hopper experiments is the ability to control independently three features of a 2D hopper (i.e. a planar hopper). These features include:

1. the hopping height
2. the forward velocity
3. the body attitude

The two features that are most relevant to gait study - the forward velocity and the body attitude - are controlled by a simple PD (Proportional and Derivative) controller. The large difference in masses of the leg and that of the body, enables the utilization of only one degree of freedom (the hip) to control both the forward velocity and the body attitude.

The forward velocity is controlled by changing the "step size". This is done by changing the angle at which the hopper lands at "heel strike". Due to the mass difference between the leg and the body, torques applied during swing phase will mostly affect the leg. Applying torques during stance phase will have a very different effect, as they will affect mostly the body attitude. The control strategy described above was found to be effective - especially for slow velocities. An extension of this strategy effectively controlled a 3D hopper: a 2D control algorithm was used to control the locomotion in the plane of motion, and corrections were made to deviations from that plane.

In contrast to the hopper, where the control strategy is aimed at maintaining some average properties (like average forward velocity), the biper was designed to follow a precomputed trajectory. The trajectory itself was found as a solution to the linearized dynamic equations. In this case too, the swinging leg is assumed to be decoupled (for control purposes) from the leg in stance.

An interesting aspect of the biper research is the stability analysis that has been performed. The analysis is based on an approximation to the variational form of the linearized equations. The analysis led to the design of stride length controller (which is conceptually similar to the forward velocity controller of the hopper). The controller corrects the errors in the trajectory of the current stance leg, by modifying the placement of the swinging leg.

A second generation of the biper, which includes four aditional degrees of freedom (knees and ankles), was also successfully tested (the knees operate in hyperextension - to facilitate ground clearance problems), but no information on the stability was given.

2.6 Summary

A new organizational framework to examine gait research has been developed. The research can be described as filling a puzzle which has three categories along each of its axes.

The vertical axis includes the hierarchical organization of gait control, and the horizontal axis includes the three aspects of gait research: the theoretical modelling and synthesis of gait, the experimental measurements of gait and the design and development of walking machines.

The next chapter describes the application of Set-Theoretic analysis to the study of gait. It especially describes a framework for dealing with the sensitivity of gait models, and thereby fills a void in the left bottom square of the organizational puzzle.

Chapter 3
The Dynamic Stability of Gait

3.1 The Definition of Gait Stability

The term gait - stability or dynamic stability of gait has been used almost from the inception of gait modelling and analysis. Even though the users of these terms usually have some intuitive feeling as to their meaning, rarely has there been an attempt to actually define this term. A possible definition of dynamic stability can describe the system's ability to maintain gait in the face of disturbances. Such a definition most closely brings to mind the stability definition in the sense of Liapunov.

Stability in the sense of Liapunov (Ogata [38]) means that the system's state remains bounded for a bounded set of initial conditions (which is similar to the -- Bounded Input Bounded Output-- (BIBO) concept, as described in Franklin and Powell [11]). This definition faces quite a few obstacles if one tries to apply it directly to gait analysis.

The gait process is a complex interaction between a multi-linkage system and its environment. The interacting port (the foot) goes through a periodic motion where it supports the body weight in one part of the cycle, and swings freely forward in the other part of the cycle. Looking at the supported body from the outside, it represents an open - chain multi-linkage system in one part (the single - support phase), and a closed - chain multi-linkage system during the double - support phase.

Each one of the above descriptions carries its own implicit stress of the variables to be controlled, yet they share the bi-phasic nature of the gait process (the leg is either in stance or in swing, the body is either in double or single support). This bi-phasic nature separates the analysis of gait from that of many other dynamic systems. From physical reasoning it is clear that the initial conditions for the leg going into the stance phase are very important in determining whether the next step will be successful or not (e.g. extending the leg too much forward might require excessive knee torques in order to successfully support the body weight). Hence, if the swinging leg is disturbed in its trajectory, the success or failure of the next step may depend on establishing "acceptable" initial conditions for the next stance phase.

To address the question of gait stability, this thesis suggests looking at the recovery mechanisms that could maintain gait in the face of external or internal disturbances. External disturbances include events such as stumbling - which disturbs the swinging leg, or slipping - which disturbs the leg in stance. Internal disturbancea for a human include events such as involuntary muscle jerk or tremor, or electromechanical noise in an active prosthetic system for an amputee.

From watching and experiencing the way humans recover from stumbling one can see that the swinging leg must hit a certain target zone on the floor in order to transfer successfully into the next stance phase. By the same token, if the swinging leg hits outside the acceptable target area, the result will be a failure and a fall. This discussion suggests that having a methodological formulation which is able to address target areas or zones, will be a very important tool in analyzing the minimum requirements needed to maintain stable gait in the face of disturbances.

3.2 Control and Stability Issues in Existing Prostheses

Stable gait can be characterized as satisfying two requirements:

1. providing support
2. providing movement

Support providing pertains to the leg in stance and is of prime importance as long as the body weight is supported by that leg. Movement providing pertains mostly to the swinging leg. This leg must clear the ground (as well as any other obstacles) and get into the position required to unload the leg in stance successfully.

As in any other dynamic system that has to be controlled, the two issues that are involved in correcting errors (or recovering from disturbances) are:

1. identifying the occurence of the disturbance
2. taking the necessary measures to recover (or correct the error)

A lower limb amputee using an artificial limb is deficient on both accounts. The sensory system can recognize the occurance of disturbances only indirectly - usually from the change in pressure patterns in the stump, or from the load transferred to more proximal joints. The ability to respond to disturbances is even more limited as the amputee does not have direct control over the degree of freedom to be manipulated (e.g. an above knee amputee must manipulate the location of the prosthesis by applying hip torques).

Commercially available prostheses for lower-limb amputees are are all passive. Disturbances introduced to such devices will usually die out (as the energy gets absorbed by the passive unit), but the required target zone will usually be missed, and a fall will take place. The research work that has been done with active and

controllable prostheses was aimed at increasing the functionality of such devices. This was done by adding new modes of operation, and developing schemes for the transition between the modes (Grimes [16] and Stein [51]). Grimes was successful in implementing a controller which identified the transitions between level walking and walking up a ramp and a staircase.

That work, while a breakthrough in the research toward increasing the functionality of active prostheses, did not address the recovery issue. The safety issue was addressed by shutting the power down either voluntarily by the subject, or involuntarily by the "EMG startle reflex" ([16] page 141). Such a solution, while being conservative and preventing major disasters, fails to take advantage of the available power in order to increase the range of disturbances which can be successfully negotiated. Unilateral amputees can use such a prosthesis and in some cases revert to their sound leg in order to recover from a stumble; but bilateral amputees do not have such an option, which means that even slight disturbances will end up with a fall.

These problems illustrate the major limitations of existing prostheses, as well as point out the promise of active, controllable prostheses. One of the major contributions of such prostheses is going to be not only the ability to better tailor the nominal performance of such a prosthesis to the specific requirements of the amputee, but most of all - to successfully negotiate disturbances to those trajectories. The long range goal of such an approach is to identify the minimum conditions required to maintain stable gait, and to enhance the ability of the controlled prosthesis to satisfy those conditions.

The work presented in this thesis identifies the direction required to formulate a mathematical structure to address some of the basic questions which pertain to the dynamic stability of gait:

1. what are the requirements for a successful load transfer

2. what are the limits of a given prosthetic system

3.3 Geometric and Dynamic Issues in Load Transfer

The term gait - stability as discussed in this work relates to the ability of a walking human being to successfully recover from disturbances that take place during the walking cycle. The main focus is on the transient response of the system, and pertinent questions are whether disturbances tend to grow or diminish, what are the effects of the geometric constraints on the resulting uncertainties in the positions of the linkages, and so on.

Fig. 3-1 describes a simplified stick figure of a person in the single support phase of gait: the leg in stance makes an angle of θ_1 with the floor, the swinging thigh is at an angle θ_2 with respect to the leg in stance, and the swinging shank is at an angle θ_3 with respect to the swinging thigh.

As the hip gets closer to the floor, the range of possible contact points between the swinging foot and the floor changes. Fig. 3-2 describes the range of possible contact configurations for a high hip position. The possible knee locations that will establish foot contact are k_0 - k_2 (points beyond k_2 will the cause the foot to be above the floor). When the knee is between k_0 and k_1 the foot has to be behind the hip, in order not to violate the knee hyperextension constraint. Such foot positions cause a step back to be taken, and are not used in normal, undisturbed gait. For each knee position between k_1 and k_2, the shank can assume two possible positions (e.g. f_1 and f_3 are possible foot positions for the knee position k_1). The limit is reached at the k_2 knee position, where the shank is perpendicular to the floor (and obviously only one foot position is possible).

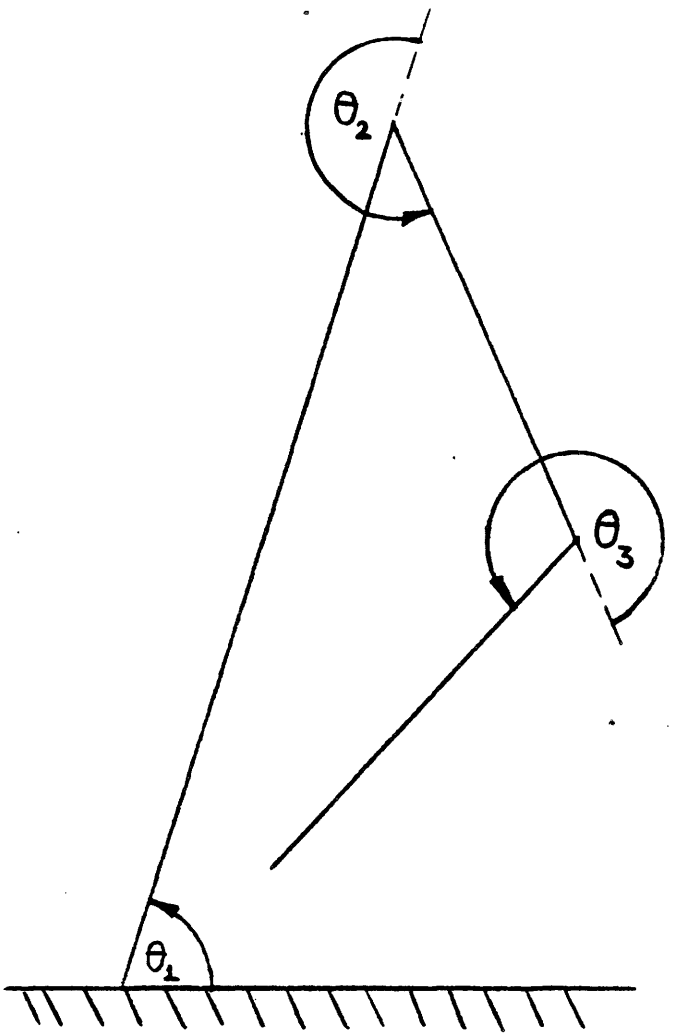

Figure 3-1: Angle nomenclature for the 3-link stick figure

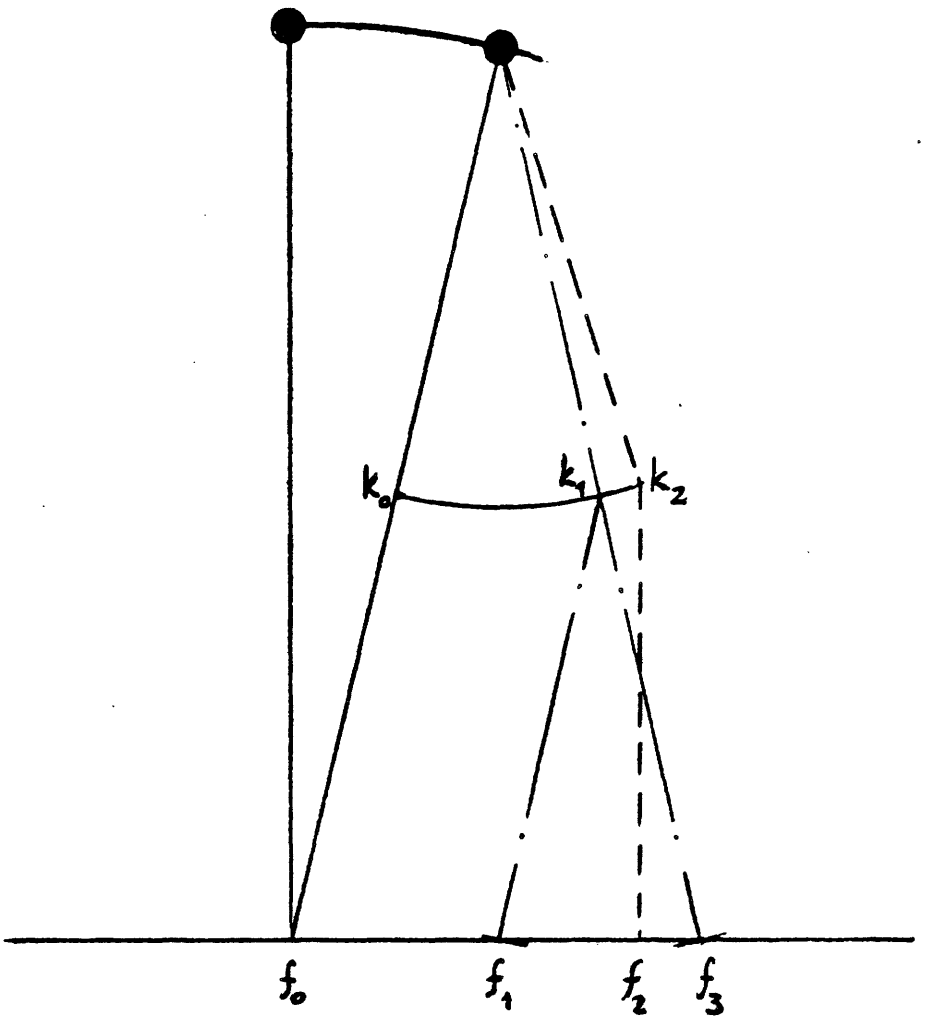

Figure 3-2: Foot-floor contact at high hip position

If the hip is allowed to fall farther (Fig. 3-3), the range of acceptable knee and foot positions increases. Note that with the increase in the acceptable target zone the knee becomes more flexed, which means that larger torques will now be experienced by the knee joint. The difference in the target zones for the two hip positions is described in Fig. 3-4. This plot is made in the joint space (i.e. each axis is made of one of the joint angles).

In addition to the geometric issues involved in establishing contact with the floor, the dynamic issues in load transfer have to be addressed. If an assumption of a quasi-static equilibrium is made, the required knee torques at the two configurations (high and low hip positions) can be compared. As the hip is allowed to fall, the moment arm of the hip with respect to the knee increases, and hence larger knee torques are required to balance the body weight (most of the body mass is assummed to be concentrated at the hip). Hence, the increased target area for the low hip position involves larger knee torque requirements as well.

In summary, a higher hip position for load transfer involves tighter bounds on the geometric target zone, but is less demanding in terms of joint reactions and energy loss (could this be the reason for the smaller step size taken by older people?).

3.4 Problem formulation

The simplest model that has been developed to describe some aspects of the gait process, is the inverted pendulum model ([30], [51], [2]). This model is used in this thesis to illustrate some aspects of the gait recovery problem. Gait recovery involves overcoming unpredictable disturbances, so that a regular periodeic movement can resume. As in any other controlled movement, there must exist a

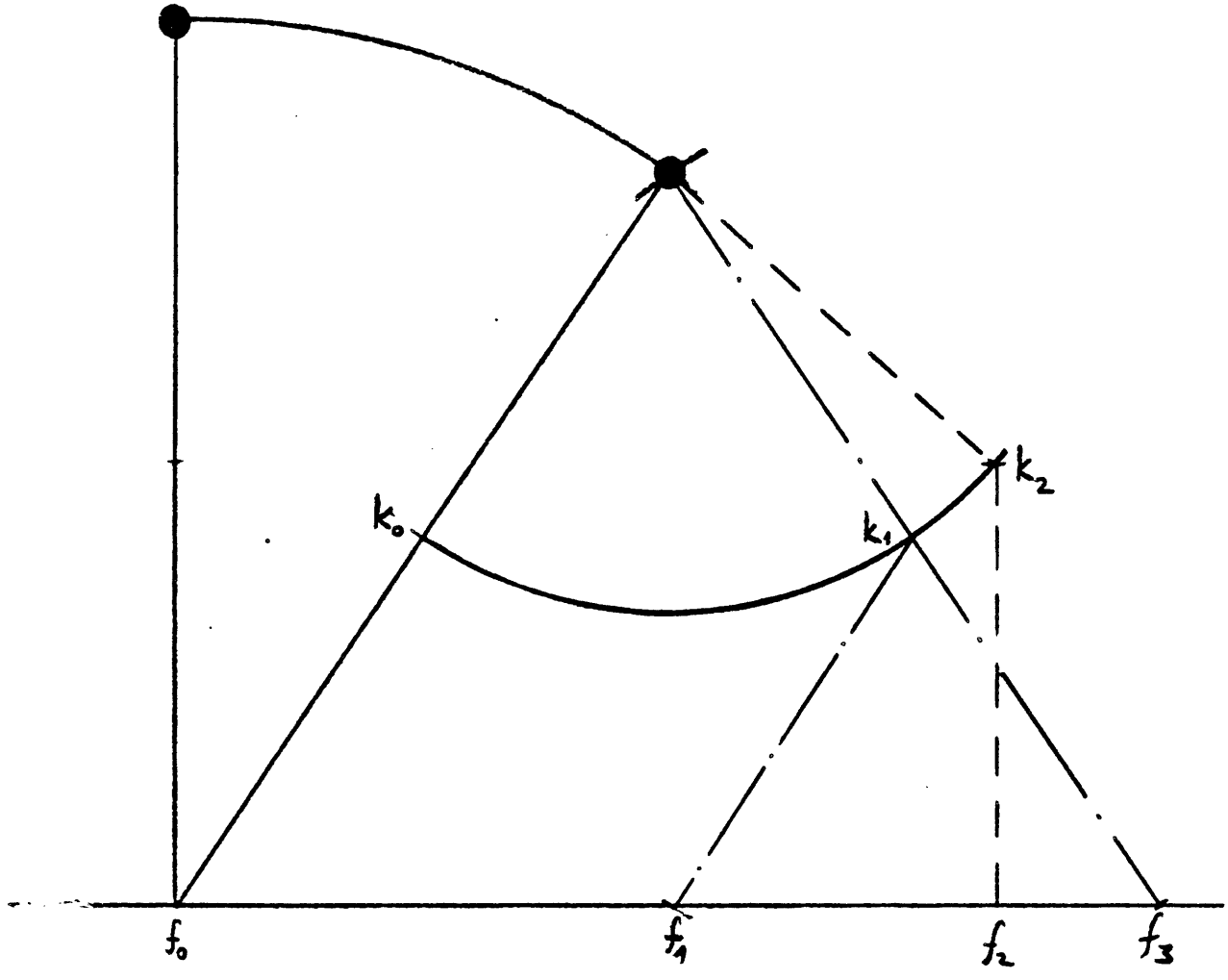

Figure 3-3: Foot-floor contact at low hip position

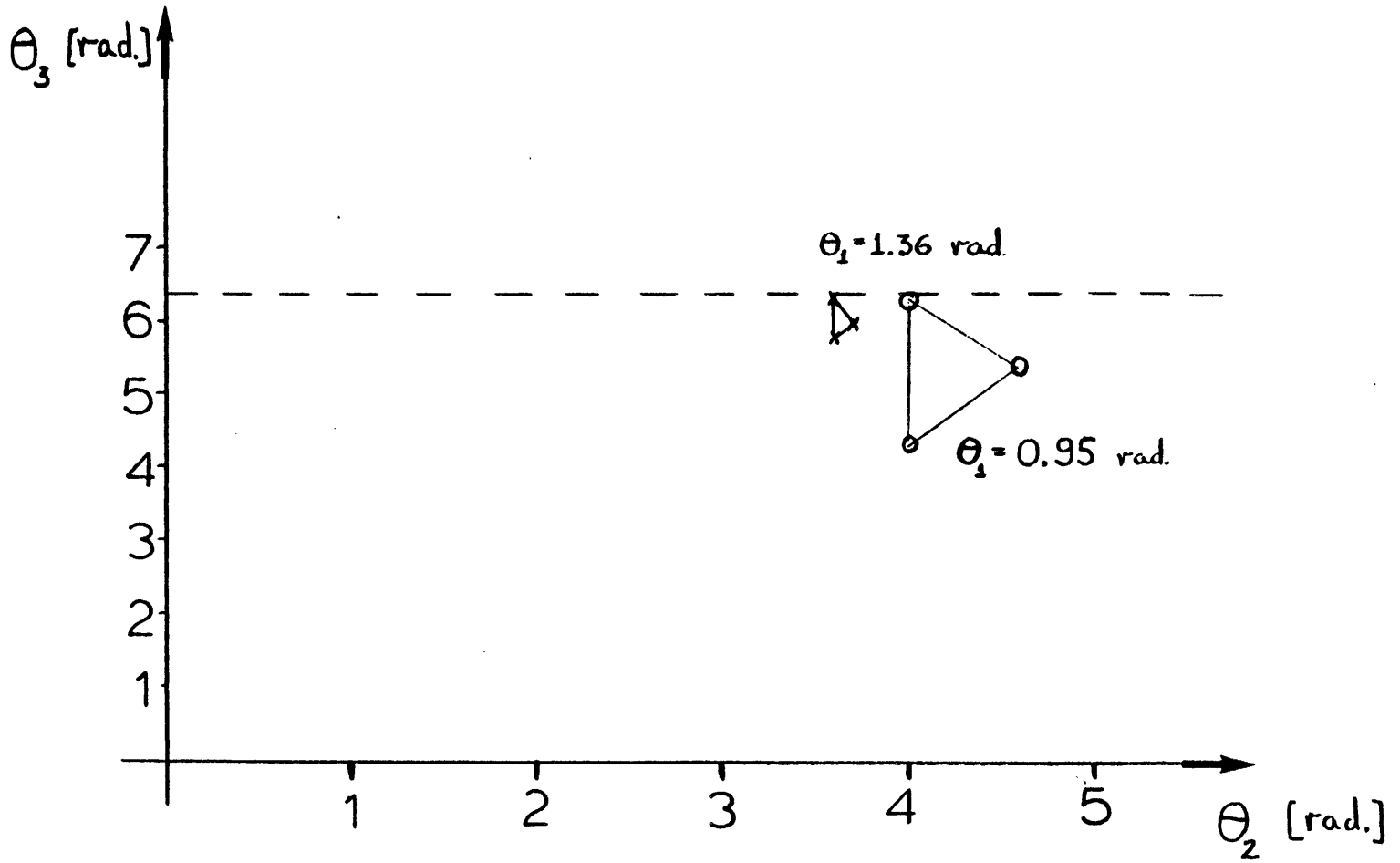

Figure 3-4: Joint space plots of target zones for different hip positions

relathionship between the magnitude of the disturbance and the strength of the available actuators (muscles), which determines whether a recovery from the disturbance is possible. Such a relationship for an electromechanical model is described in the following chapter.

Chapter 4
A Simple Pendulum Analysis

4.1 Problem formulation

The simplest model that has been developed to describe some aspects of the gait process, is the inverted pendulum model ([30], [51], [2]). This model is used here to illustrate some aspects of the gait recovery problem. Gait recovery involves overcoming unpredictable disturbances, so that a regular periodeic movement can resume. As in any other controlled movement, there must exist a relathionship between the magnitude of the disturbance and the strength of the available actuators (muscles), which determines whether a recovery from the disturbance is possible. Such a relationship for an electromechanical model is described in this chapter.

A vertical pendulum, pinned at the bottom to a frictionless-joint, is in a state of non-stable equilibrium. Such a pendulum, being an energy - conserving system, would complete a full revolution - if disturbed from its local state of equilibrium (Fig. 4-1). If such a pendulum is disturbed along its course, in such a way as to reduce its total energy, it no longer can complete a full revolution, and will come to a stop at $\theta < 2\pi$.

In order to have the pendulum successfully complete one revolution, a motor which generates a positive torque - τ at the joint can be applied. If the goal of using the motor is to compensate the system for the disturbance, there should be a relationship between the magnitude of the disturbance, the phase at which the

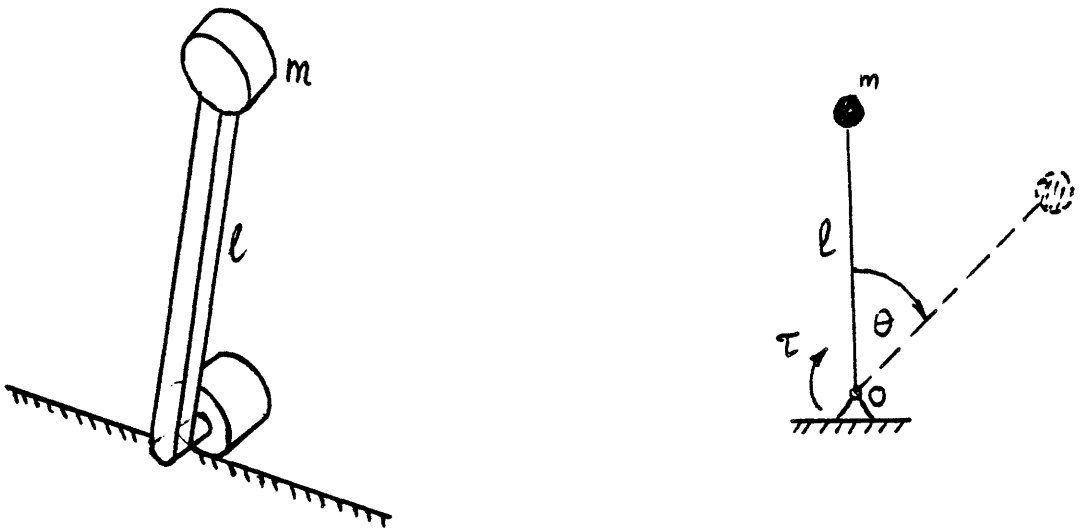

Figure 4-1: The inverted pendulum

disturbance took place, and the minimum actuator strength required to compensate for its effect. The work described in this chapter deals with this relationship.

4.2 Description of the Model

The pendulum's equation of motion can be derived easily, using Newton's laws of motion (see Fig. 4-1 for nomenclature)

$$\Sigma M_0 = I_0 \frac{d^2\theta}{dt^2} \tag{4.1}$$

$$ml^2 \frac{d^2\theta}{dt^2} = \tau + mgl\ sin\theta \tag{4.2}$$

Adding the general characteristics of an electrical motor (see Fig. 4-2)

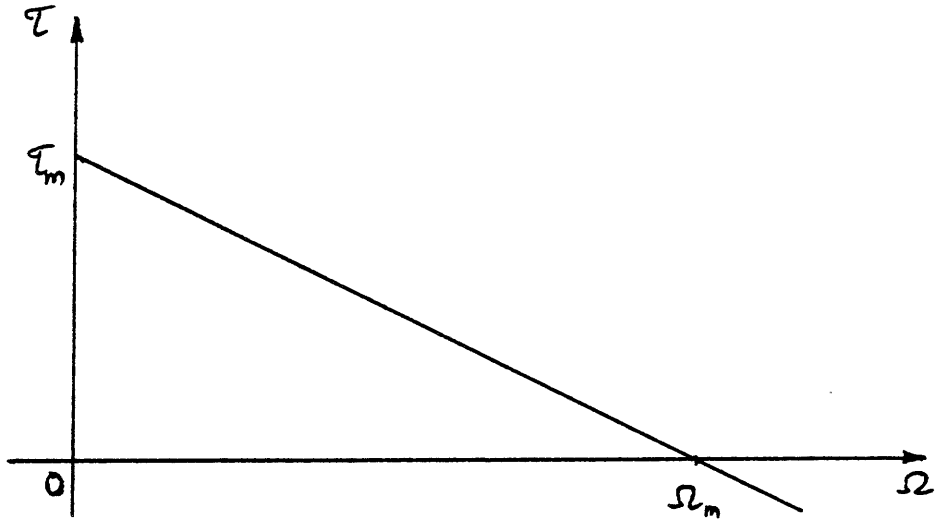

Figure 4-2: Motor characteristics

$$\tau = \tau_m - (\frac{\tau_m}{\omega_m})\,\omega \tag{4.3}$$

The dynamic equation of the pendulum is therefor

$$ml^2 \frac{d^2\theta}{dt^2} = \tau_m + mgl\ sin\theta - (\frac{\tau_m}{\omega_m})\,\omega \tag{4.4}$$

$$\frac{d^2\theta}{dt^2} + \frac{\tau_m}{ml^2\omega_m}\frac{d\theta}{dt} - \frac{g}{l}\,sin\theta = \frac{\tau_m}{ml^2} \tag{4.5}$$

In order to non-dimensionalize Eq. (4.5) a new time scale was chosen

$$t = \sqrt{(\frac{g}{l})}\,t \tag{4.6}$$

hence

$$dt = \sqrt{(\frac{g}{l})}\,dt \tag{4.7}$$

Using Eq. (4.7), all the time derivatives in Eq. (4.5) can now be rewritten in a non-dimensional form:

$$\frac{d\theta}{dt} = \frac{d\theta}{dt}\frac{dt}{dt} = \sqrt{\left(\frac{g}{l}\right)}\frac{d\theta}{dt} \tag{4.8}$$

and similarly

$$\frac{d^2\theta}{dt^2} = \frac{g}{l}\frac{d^2\theta}{dt^2} \tag{4.9}$$

substituting (4.8), (4.9) into (4.5) yields:

$$\frac{d^2\theta}{dt^2} + \frac{\tau_m}{ml^2\omega_m}\sqrt{\left(\frac{g}{l}\right)}\frac{d\theta}{dt} - \frac{g}{l}\sin\theta = \frac{\tau_m}{ml^2} \tag{4.10}$$

and rearranging (4.10):

$$\theta'' + \frac{\tau_m}{mgl}\sqrt{\left(\frac{g}{l}\right)}\frac{1}{\omega_m}\theta' - \sin\theta = \frac{\tau_m}{mgl} \tag{4.11}$$

where

$$\theta' = \frac{d\theta}{dt} \qquad \theta'' = \frac{d^2\theta}{dt^2}$$

The problem may now be stated in the following terms: for a given disturbance (given in terms of $\Delta\theta'$) occuring at an angle θ of a free falling pendulum, what is the minimum value of τ_m (for a given ω_m), required to restore the system's original energy status in a time

$$t = T - t_d$$

(where T is the period of a free swinging pendulum, and t_d is the time the

disturbance took place).

4.3 Method of Solution

In order to describe the solution, two terms should be defined:

1. A - a "stall torque" of a given motor
2. B - a "no-load" velocity for a given motor

A and B are non-dimensional, and are given by the following equations:

$$A = \frac{\tau_m}{mgl}$$

$$B = \omega_m \sqrt{(\frac{\overline{l}}{g})}$$

A computer program which looks for the value of the minimum A for a given B, required to overcome a disturbance of $\Delta\theta'$ at an angle θ within a time

$$t_{final} = T - t_d$$

(T= period; t_d = time of disturbance). Once a value of A_{min} has been found (to within an error of ϵ=0.001 in the total energy in the final time step), the program repeats the search for a new set of values (θ;$\Delta\theta'$). The flow chart of the computer program is given in Fig. 4-3. The program scans the range of phase angles (in radians)

$$0.2 \leq \theta \leq 6.2$$

(in increments of 0.1 radians). The limits of 0.2 and 6.2 radians were chosen as

angles where the angular velocity is small, and yet a change of 0.1 rad/sec in the angular velocity will not cause the pendulum to have negative velocity. For each phase angle θ, it introduces step changes in the angular velocity

$$0 < \Delta\theta' < \theta_{cr}'$$

in increments of 0.1 (θ_{cr}' is the angular velocity of a free-falling pendulum at that angle - θ). The search routine for the minimum values of A has 2 major parts:

1. The integration package
2. The comparison and calculation of A.

The integration routine in this program is the DHPCG subroutine from the SSP library. It uses Hamming's modified predictor-corrector method for the solution of a general, ordinary, first-order, initial value, set of differential equations. Equation (4.11) has been rewritten as two first-order differential equations using the following substitution:

$$Y_1 = \theta$$
$$Y_2 = \theta' \qquad (4.12)$$

Substitution of (4.12), A and B in (4.11) yields:

$$Y_1' = Y_2$$
$$Y_2' = sinY_1 - \frac{A}{B}Y_2 + A \qquad (4.13)$$

The initial conditions for each simulation consist of (Y_1;Y_2) at t=0, which determine an initial state after a step change in θ' took place. The value of A for

any iteration depends on the error (in the final time and energy) obtained at the end of the previous iteration. A simulation terminates if one of the following conditions is satisfied:

1. $Y_1 > 2 \cdot \pi$

   - one full revolution has been completed

2. $Y_2 \leq 0 for Y_1 < 2 \cdot \pi$

   -pendulum stopped before completing a full revolution

Upon the termination of a simulation, the sum of the errors in the energy and time is determined. If the error is larger than the maximum error allowed (ϵ_{max}=0.001), a new value for A is calculated for the next iteration. This value depends on the required change in the total energy of the system: A is increased if the energy needs to be increased (or decreased otherwise).

Convergence of the search algorythm is assured by comparing the error at the end of each iteration to the error in the previous iteration. If the error increased, the change in A calculated at the end of the last iteration is halved, and used as an input for the next iteration. The process is repeated until convergence is achieved.

4.4 Results

Two different actuator characteristics were examined (see Fig. 4-4). The actuators are referred to as actuators I and II, or as case I and II.

Two values of B were examined (see Fig. 4-4 for the definition of B): B=10 and B=1. As the maximum angular velocity of a free - swinging pendulum is

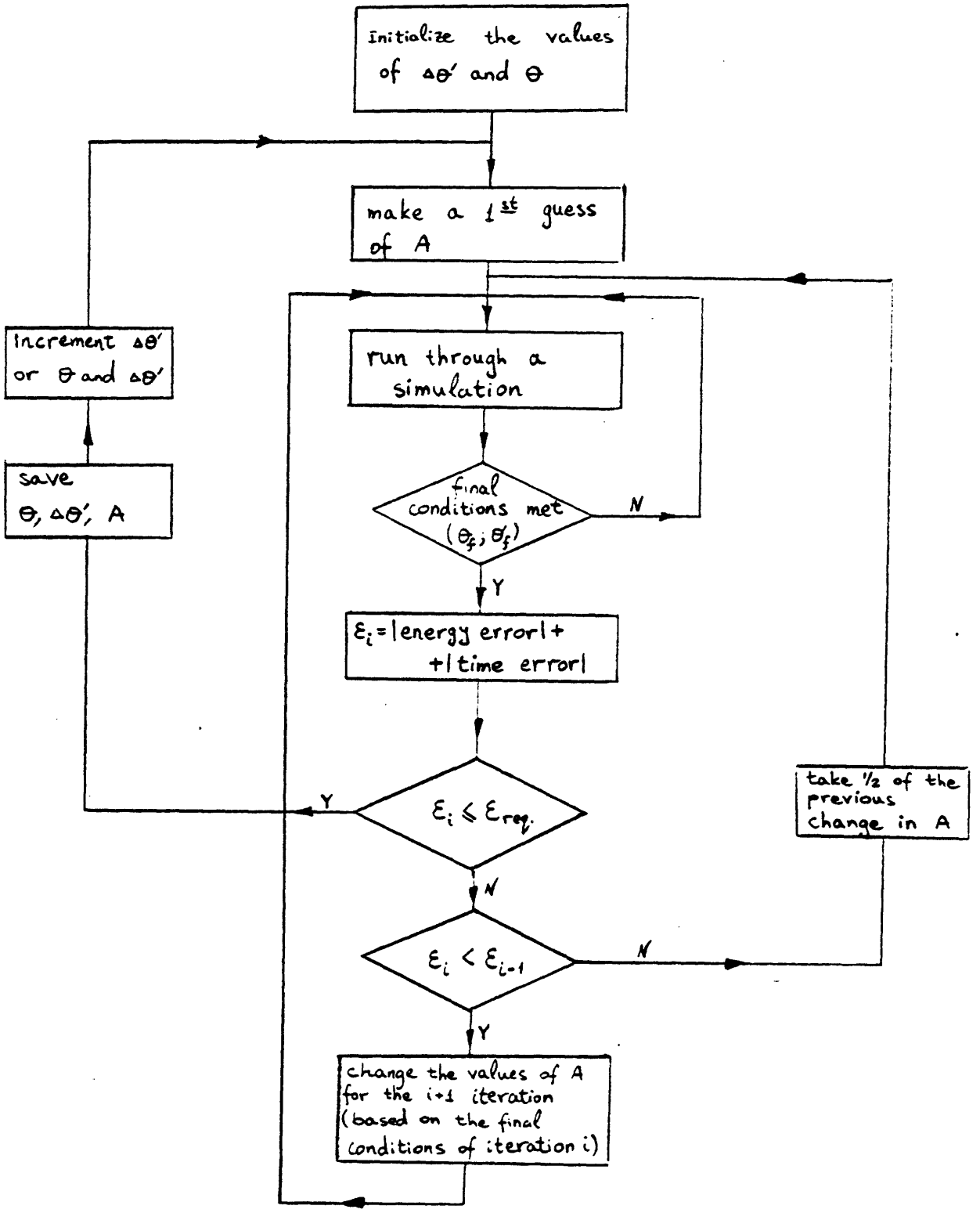

Figure 4-3: Flow chart of the program which calculates A_{min}

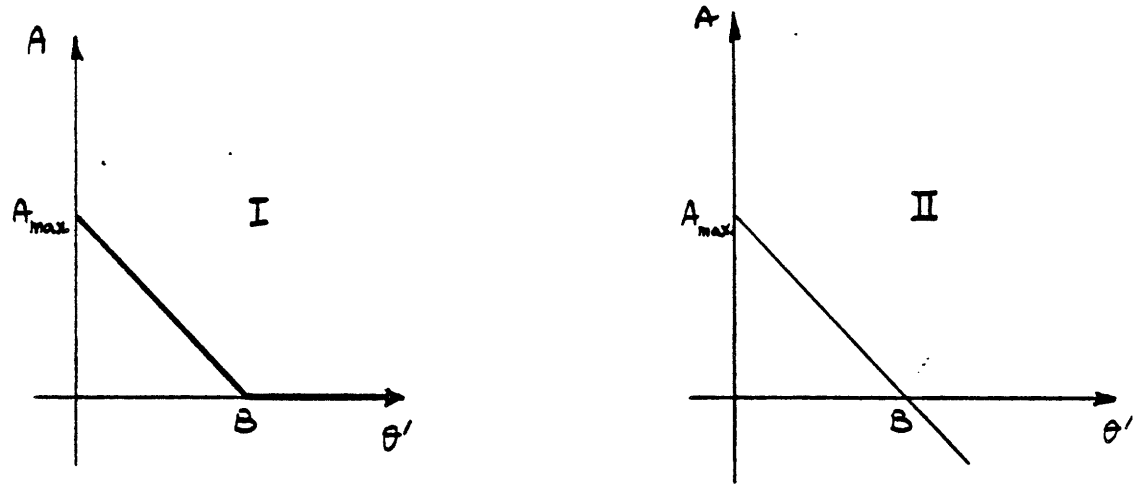

Figure 4-4: Actuator characteristics

$\theta_{crmax}'=2$, an actuator having B=10 will never reach the state of

$$A \leq 0$$

, whereas an actuator with B=1 will reach that state. This means that such an actuator will become an additional load for the pendulum for $\theta'>B$ in case II (i.e. - it will drain energy from the system), whereas in case I it will not change the energetic state of the system (for $\theta'>B$). Both actuators will add energy to the system for $\theta'< B$.

As indicated in the previous section, the disturbances domain which was examined was (in radians)

$$0.2 \leq \theta \leq 6$$

; $0< \Delta\theta'<\theta_{cr}'$. The increments in both θ and $\Delta\theta'$ were 0.1. The values of A_{min} obtained for each disturbance [defined by $(\theta;\Delta\theta')$] can be plotted as a 3-D surface over the disturbances domain. Such a surface for actuator I and for B=10 is

shown in Fig. 4-5. As expected, the value of A_{min} increases monotonically as θ and $\Delta\theta'$ increase. This means that the later in the cycle a disturbance is introduced, and/or the stronger it is - the stronger the actuator that is required to successfully correct the trajectory of the pendulum within a predetermined amount of time. The surface also becomes steeper with increasing θ, meaning that larger increases in A are required (for the same increase in $\Delta\theta'$) for larger values of θ. Figures 4-6 and 4-7 show the stability surface for B=1, actuator types I and II respectively. Fig. 4-6 shows that the surface is monotonic in the $\Delta\theta'$ direction, but has a maximum in the θ direction. This maximum for values of $\Delta\theta'<1$ occurs at $\theta=\pi$, whereas for larger values of $\Delta\theta'$ its location shifts to larger values of θ.

Fig. 4-7 shows that a large value of A_{min} is required to overcome small disturbances at phase angles smaller than 4.5 radians, and that the values of A_{min} change very little for larger disturbances. Still - going in the θ direction - for a fixed $\Delta\theta'$ shows a maximum for A_{min}. The location of the maximum changes almost linearly with $\Delta\theta'$.

Figures 4-8 - 4-10 describe the effect of a time delay on the surfaces of actuators having B=1. The time delay takes place between the introduction of the disturbance and the introduction of the corrective torque. All the surfaces increase monotonically in the $\Delta\theta'$ direction, and have maxima in the θ direction. The locations of the maxima are indicated by the small crosses (or the blackened areas).

4.5 Discussion

The $(\theta;\Delta\theta')$ plane spans the combinations of phase angle and step change in velocities, which constitute the physical disturbances to the system. Only part of this plane, though, is of interest for the analysis presented in this work; this is the

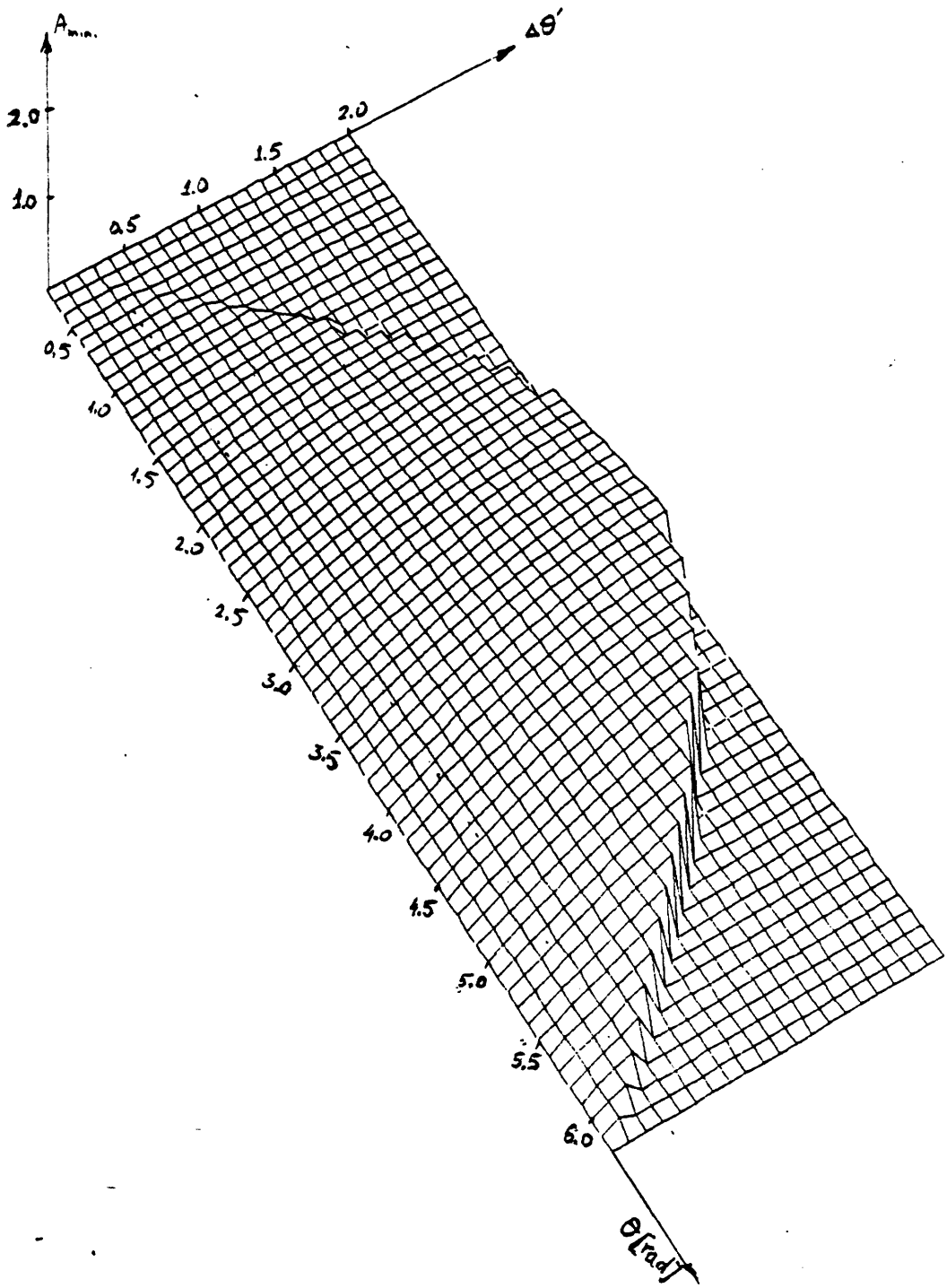

Figure 4-5: Stability surface for actuator I, B=10

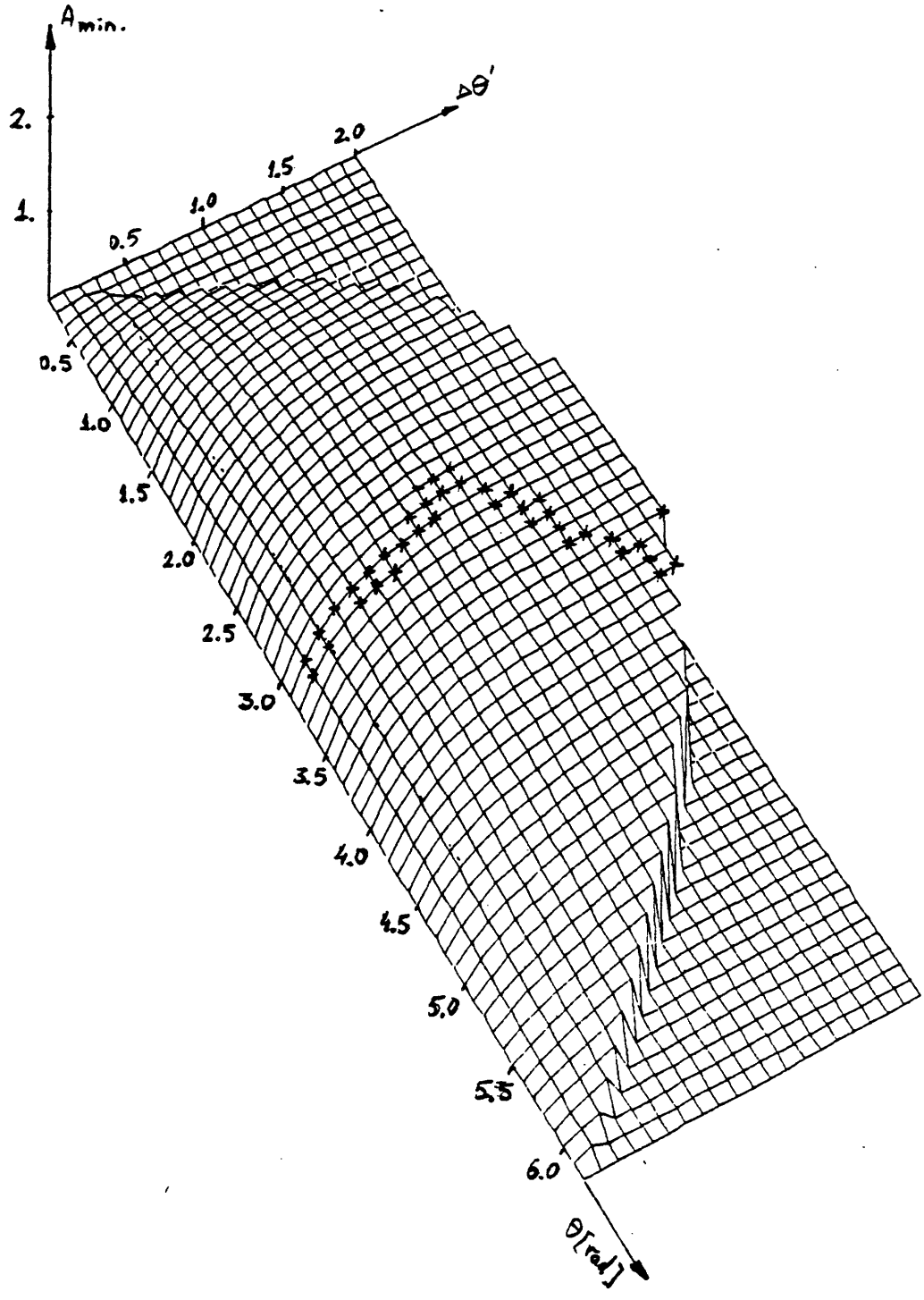

Figure 4-6: Stability surface for actuator I, B=1

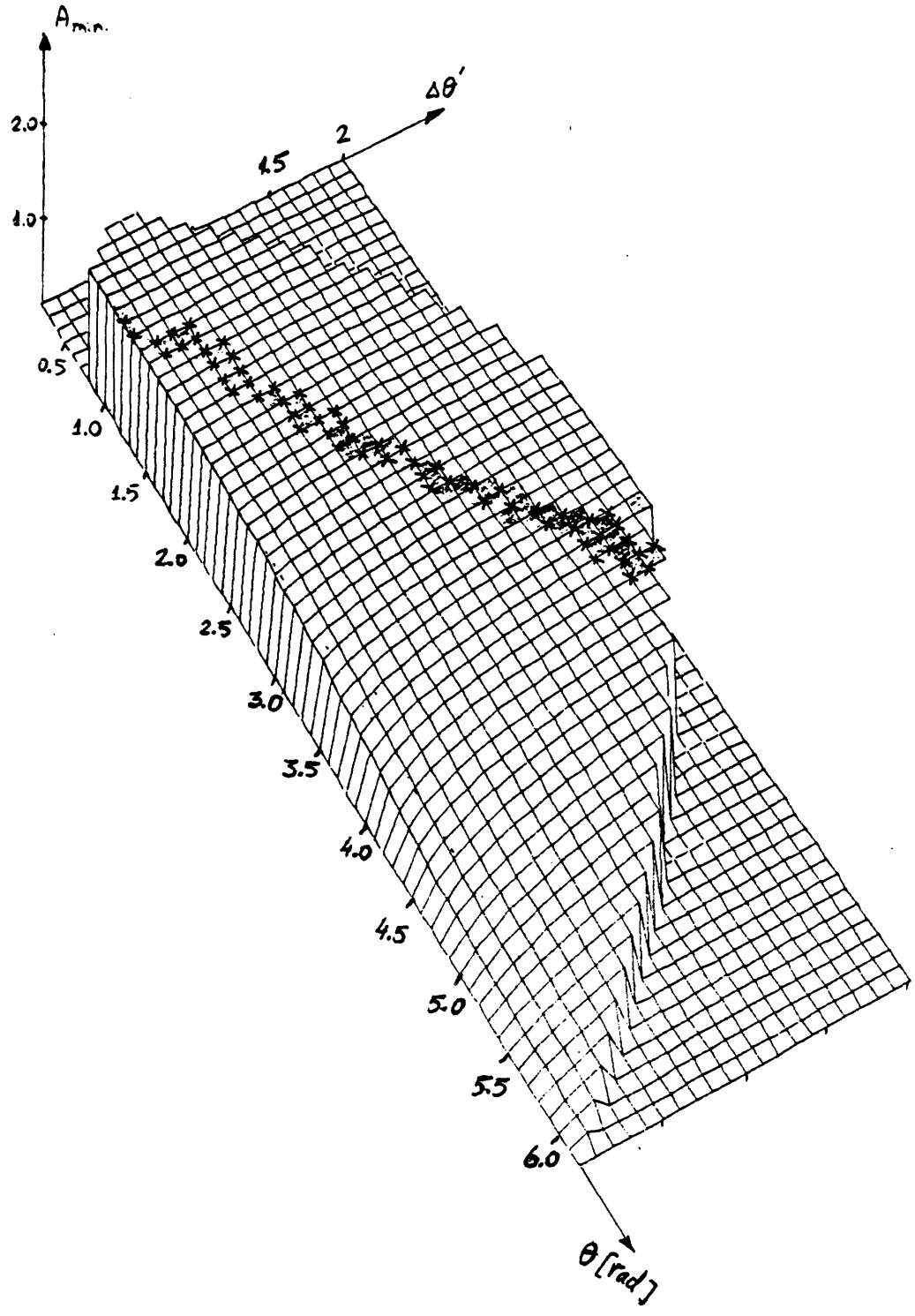

Figure 4-7: Stability surface for actuator II, B=1

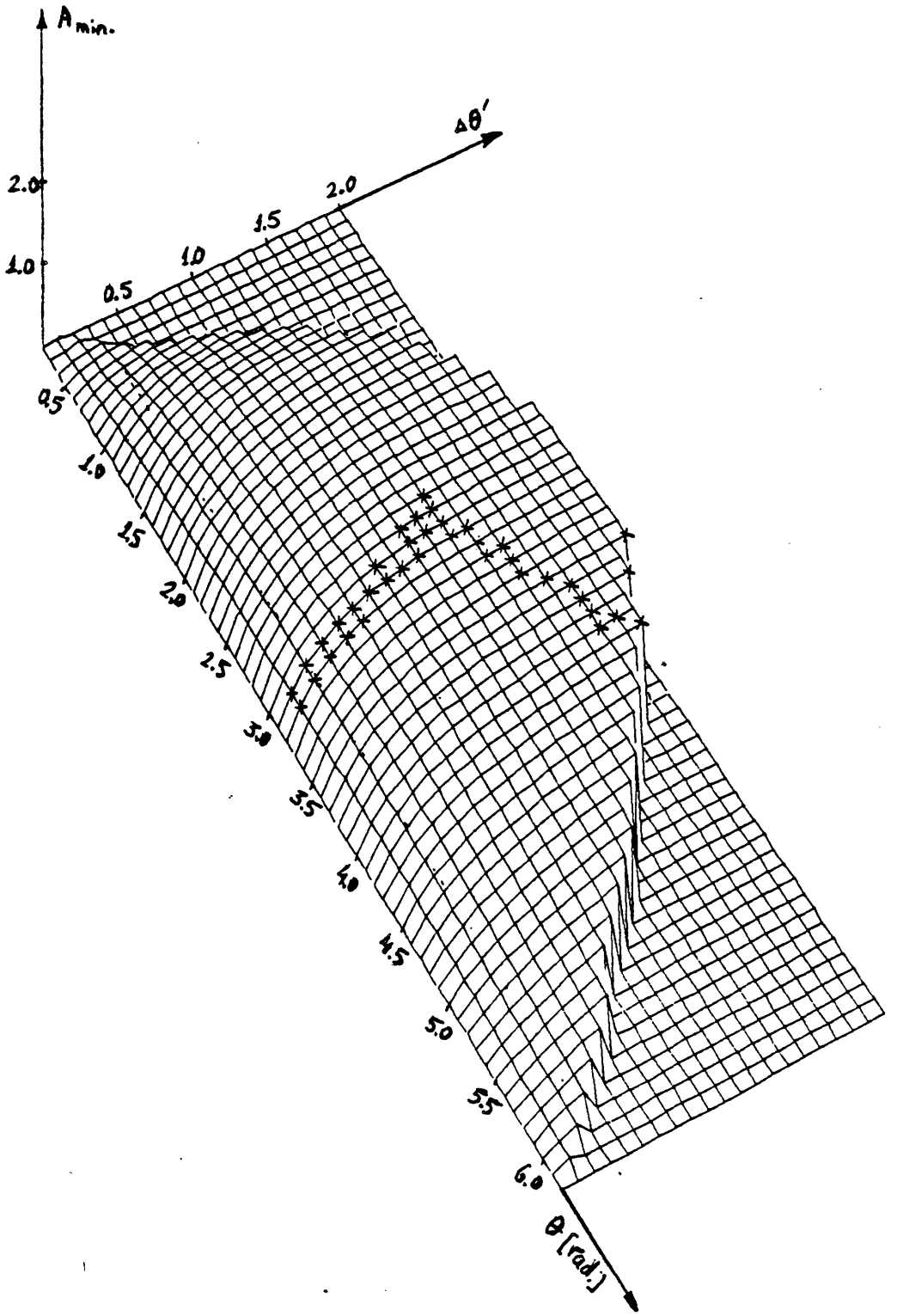

Figure 4-8: The effect of time delay Δt=0.1 on the stability surface of actuator I, B=1

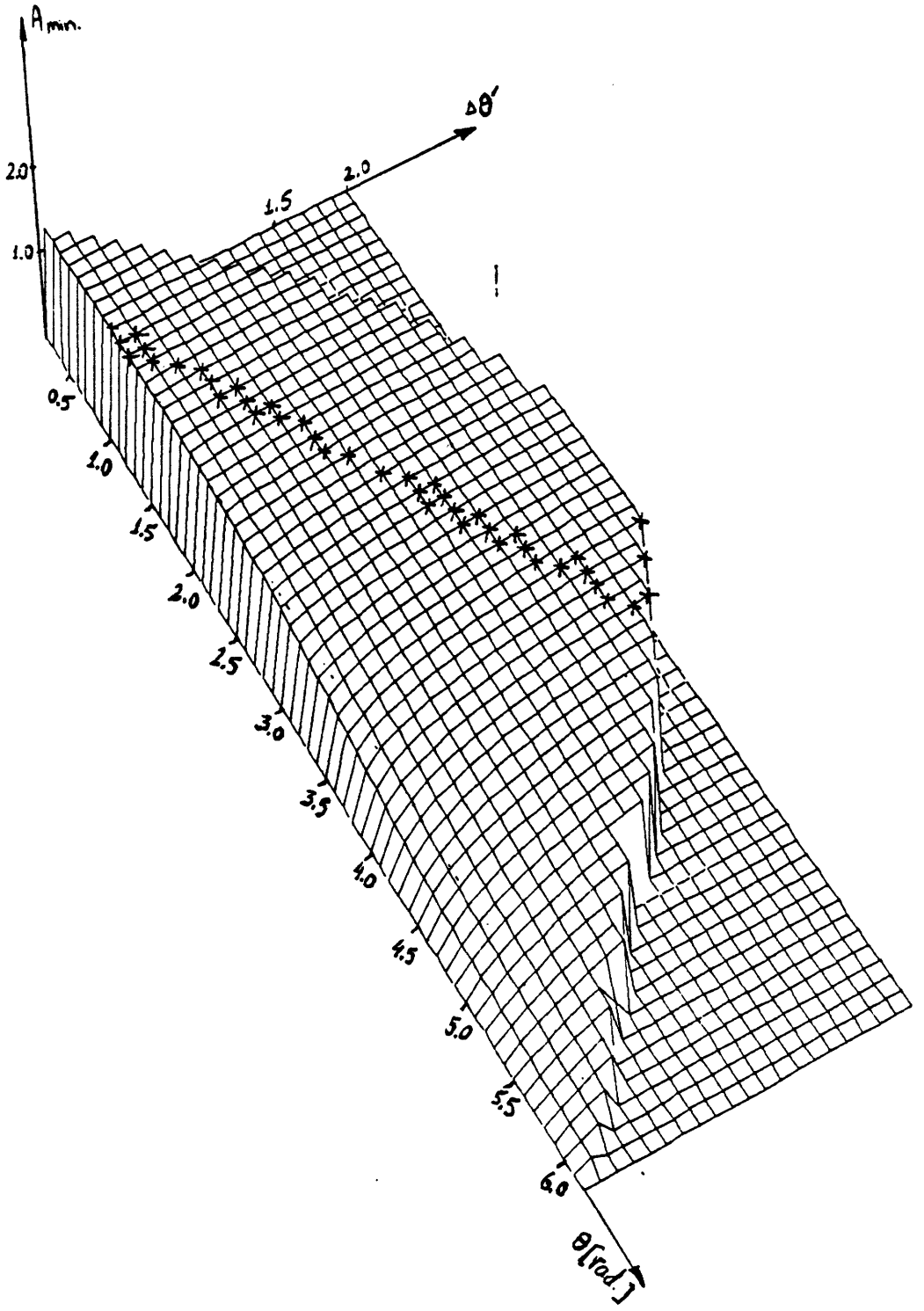

Figure 4-9: The effect of time delay $\Delta t=0.1$ on the stability surface of actuator II, B=1

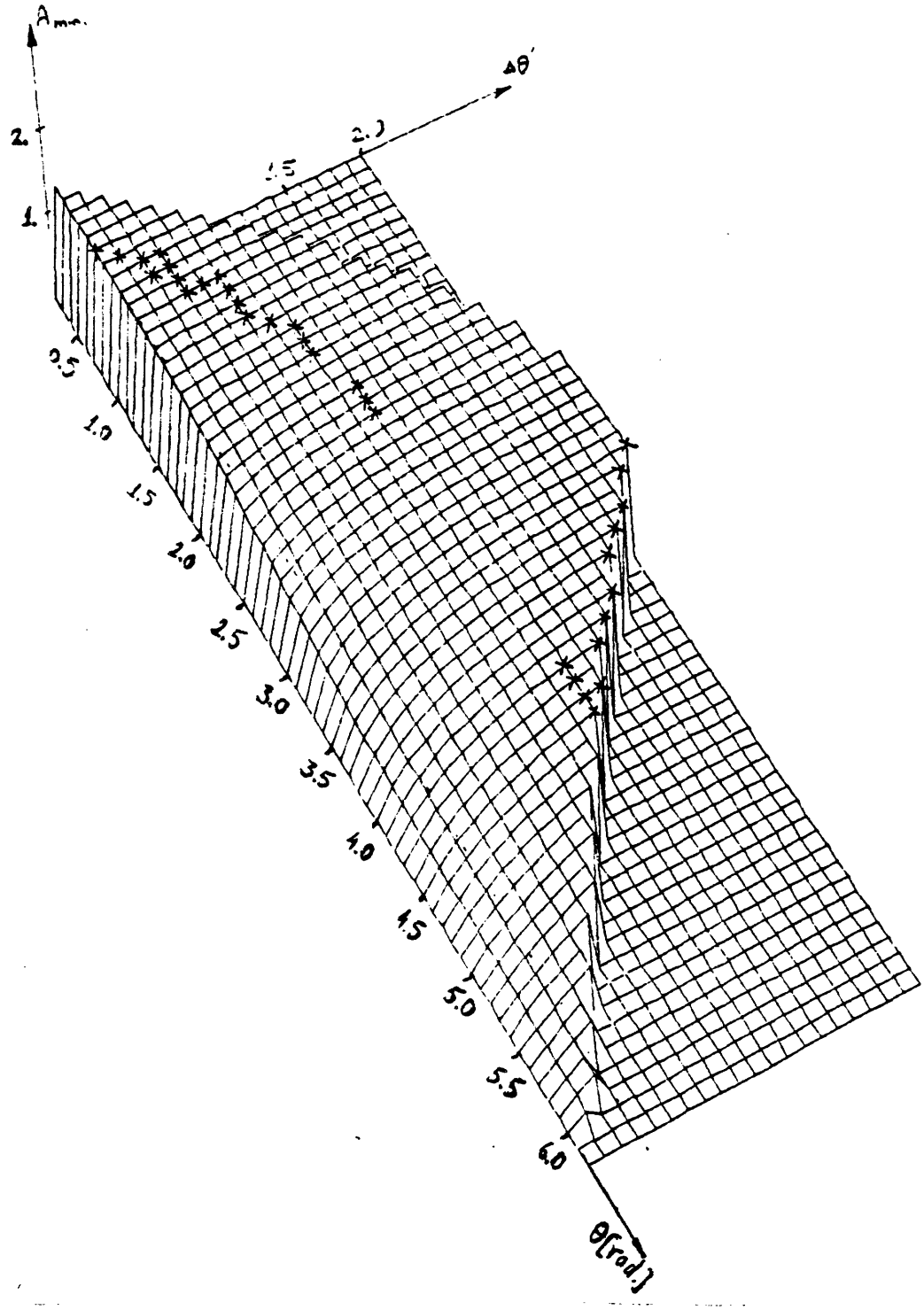

Figure 4-10: The effect of time delay $\Delta t=0.5$ on the stability surface of actuator II, B=1

sub-domain bound by the state-space relationship between θ and θ_{cr}', which is the angular velocity of a free falling pendulum. This relationship can be solved analytically, and is given in eq. (4.14)

$$\theta_{cr}' = \sqrt{(2\,(1 - cos\theta))} \tag{4.14}$$

Hence - the disturbances domain is given by eq. (4.15):

$$\Delta\theta' < \sqrt{2\,(1 - cos\theta)} \tag{4.15}$$

Therefore, the stability surfaces (figures 4-5 - 4-10) constitute the limiting disturbances allowed for systems under the effect of a given family of actuators (chracterized by the values of B) and a time delay Δt.

As an example one can look at cross-sections of the stability surfaces at given "heights" (i.e. constant values of A_{min}). Such curves can be termed Iso (or Equi) - actuator curves, since those are the $(\theta;\Delta\theta')$ combinations which require the same values of A_{min}. Fig. 4-11 describes iso-actuator curves for actuator II with B=10. Since the range of θ' is so far from the value of B, it is expected that there will be no difference between the stability surfaces for actuators I and II. This indeed is the case.

Fig. 4-11 can be used as a reference for a motor + pendulum system having B=10: for a given disturbance (characterized by the values of $(\theta;\Delta\theta')$), the value of A_{min} can be obtained. Point 1 in Fig. 4-11 specifies that the minimum value of A_{max} in Fig. 4-4 required to recover from a disturbance of $\Delta\theta'$=1 which took place at θ=3.2 radians is A_{max}=0.6. If the actuator of the system at hand has a smaller value of A_{max} - the system is going to fail (i.e. the pendulum will stop before completing a full revolution)

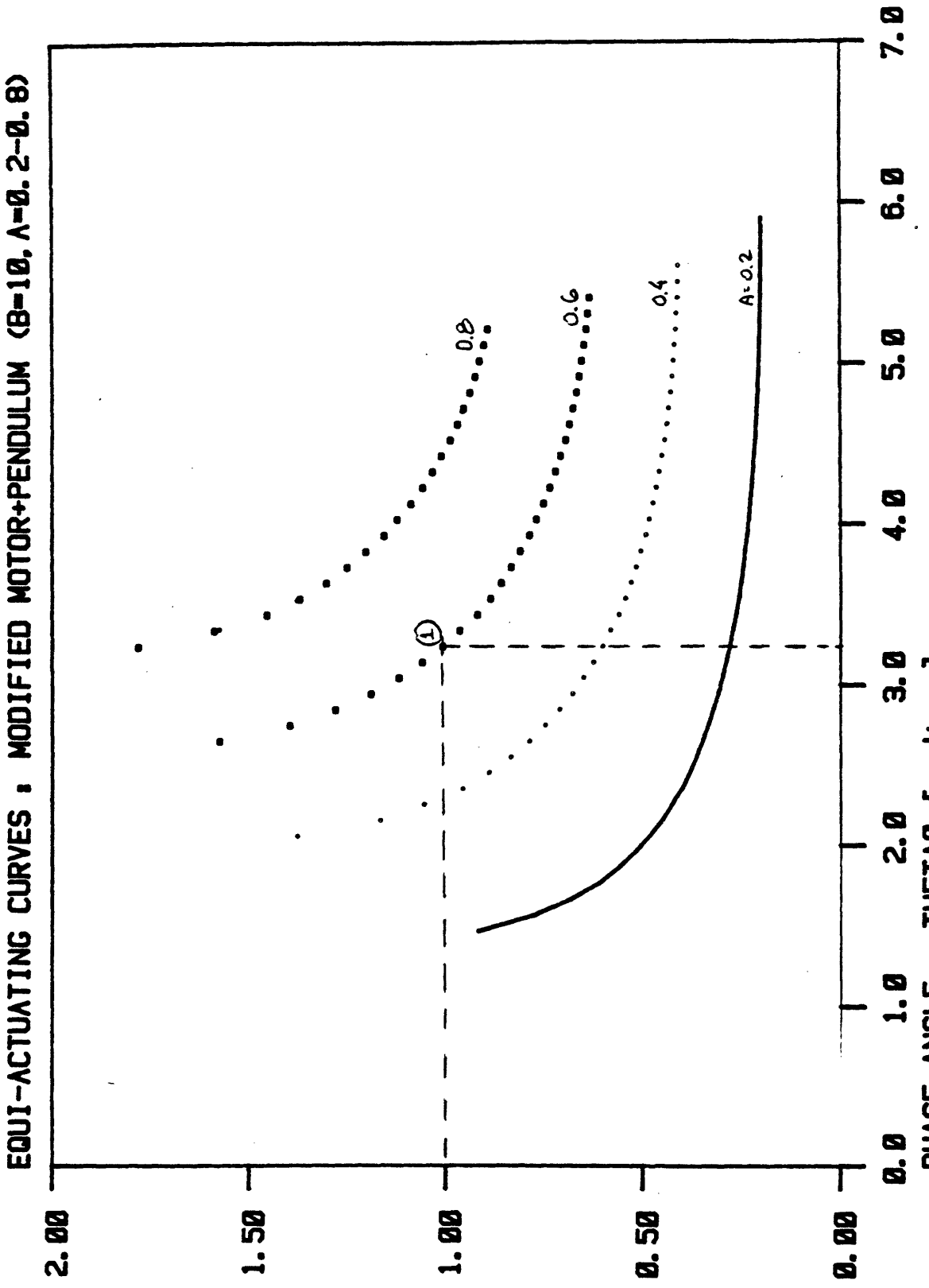

Figure 4-11: Iso - actuator curves for actuator II with B=10

A different perspective can be obtained by characterizing the range of disturbances "allowed" for a given actuator. From the shape of the curves in Fig. 4-11 it is clear that they have been derived from a monotonic surface: the same velocity disturbances occuring later in the cycle require stronger actuators, or vice versa - the ability of a given actuator to successfully overcome a disturbance decreases as the phase at which the disturbance takes place - increases.

This, however, is not true for the actuator I B=1 case (see Fig. 4-12). In this case the maximum velocity at which the motor can add energy to the system is equal to half the maximum angular velocity of a free - swinging pendulum. The field of gravity produces here the "paradoxical" result of increasing the range of allowed disturbances for $\theta > \pi$. In this part of the cycle the gravitational deceleration, coupled with the disturbance (which also reduces the angular velocity), cause the pendulum to spend more time in velocities which are smaller than B, and hence - enable the actuator to add energy to the system. This is also the reason why the curves have minima for smaller values of $\Delta\theta'$ (the pendulum spends larger portions of the cycle at velocities larger than B).

The effect of gravity is accentuated for actuator II with B=1 (see Fig. 4-13). As this actuator drains energy from the system for $\theta' > B$ it will require the largest actuators for a given disturbance. From Fig. 4-7 it is also clear that there is a "threshold phenomenon" for disturbances occuring up to $\theta = 4$ radians: large values of A are required to recover from small disturbances, and only small increments to those values are required to cover the whole range of allowed disturbances. This is due to the fact that small disturbances in the beginning of the cycle cause the system to spend a large portion of the cycle at velocities higher than B, and hence - lose a large portion of the original energy.

It is interesting to note that the increasing portions of Fig. 4-13 converge to

the appropriate portions of Fig. 4-12, confirming the observation that under those disturbances the system will always have angular velocities smaller than B. The iso - actuator curves of figures 4-11 - 4-13 converge at the right limit of the allowed disturbance - domain, as the absolute value of the velocity gets very small, and the problem becomes a quasi - static one, requiring a given value of A. This observation is illustrated in Fig. 4-14.

4.5.1 The effect of a time delay

One can generally expect a time delay, which exists between the introduction of the disturbance and the application of a corrective torque, to affect the system in two ways. It can decrease the disturbances domain (as no actuator can recover a system which stops within the time delay, an event which is considered a failure), and increase the actuator values required to recover from a certain disturbance.

A comparison of figures 4-6 and 4-8 shows that a time delay of 0.1 (while the period T=10.5) reduces the right limit of the allowed disturbance domain, while only changing slightly the general shape of the surface. The numerical values change very little in most of the domain, as shown in Fig. 4-15. The effect of the delay increases for high values of $\Delta\theta'$.

A more pronounced effect can be shown by increasing the time delay to 0.5 (see figures 4-7 - 4-10). The absolute values of A_{min} for a certain disturbance are still very similar, but the right limit of the disturbances domain is changed as to substantially reduce the allowed domain. The shape of the stability surface also changes, and it can be viewed as a combination of the monotonic surface from Fig. 4-5 (for $\theta>2.5$), and the original surface from Fig. 4-7. The reason is that the time delay will prevent engaging the motor too early (while the pendulum is

accelerating) at velocities larger than B; it also causes the system to reach much lower velocities (before the motor is turned on) and the variation in the actuator torque is therefor small. Hence the system will resemble the pendulum with the actuator having B=10. Another way to look at the iso - actuating curves is by transforming the velocity disturbance into energy disturbance. As the disturbance occurs instantaneously, one can assume that the only change in energy happens due to a decrease in the kinetic energy. The change in energy is given by Eq. (4.16):

$$\Delta E = \tfrac{1}{2}\,\theta_{cr}'^2 - \tfrac{1}{2}\,\theta_0'^2 \tag{4.16}$$

- θ_{cr}' - angular velocity prior to the disturbance

- θ_0' - angular velocity after the disturbance

Using the relationship

$$\theta_0' = \theta_{cr}' - \Delta\theta' \tag{4.17}$$

$$\Delta E = \tfrac{1}{2}\,\Delta\theta'\,(\theta_0' + \theta_{cr}')$$

$$\Delta E = \tfrac{1}{2}\,\Delta\theta'\,(2\theta_{cr}' - \Delta\theta') \tag{4.18}$$

Eq. (4.18) was used to transform the iso - actuating curves of figures 4-11 - 4-13 into figures 4-16 - 4-18 respectively. The almost linear relationship in Fig. 4-16 suggests that such a system can be treated as if it has a constant actuator; the ability of the actuator to recover energy depends only on the time the disturbance occurred, and is inversely proportional to the distance between that angle and the target $\theta=2\pi$. Figures 4-17, 4-18 illustrate the non-linear aspects of using an actuator with B=1; Fig. 4-18 especially stresses the increase in the actuator's

ability to negotiate increased disturbances later in the cycle.

4.6 Conclusions

An analysis of the relationship between velocity disturbances, the phase angle at which they occurred in a periodic system, and the minimum acuator required to recover from such a disturbance has been made. The results have been described in terms of stability surfaces and iso-actuator curves. The stability surfaces have been shown to be a useful tool in identifying the requirements for stability under disturbances at different points in the periodic cycle.

The iso - actuator curves could be used as a reference for identifying the allowed disturbances domain of a given system. The effect of a time delay seems to be a decrease in the size of the allowed disturbances domain, and have a rather limited effect on the numerical values of the minimum actuator required to recover from a given disturbance.

Actuators which are allowed to drain energy out of the system (i.e. type II actuators) will be more beneficial if they are turned on only in certain parts of the cycle (which would minimize energy drain out of the system). Hence the stability surfaces can be used not only to characterize the stability range (i.e. the allowed disturbances domain) of a given system, but also as a design tool for theoretically examining the effect of different control strategies on the shape and size of these surfaces. Even from this simple model it is easy to see how the recommendation to use high values of B is quantitatively based on the appropriate stability surfaces.

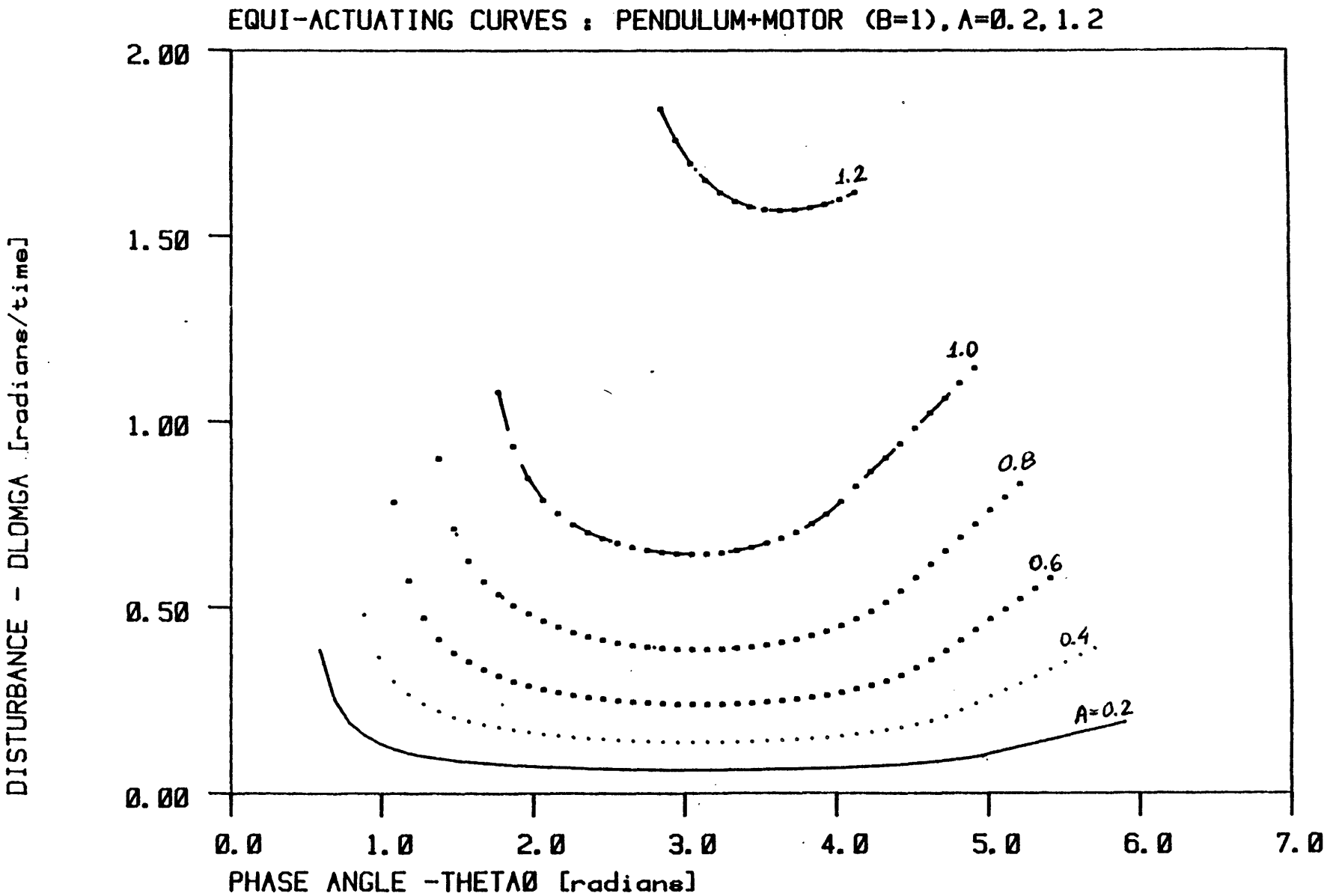

Figure 4-12: Iso - actuator curves for actuator I with B=1

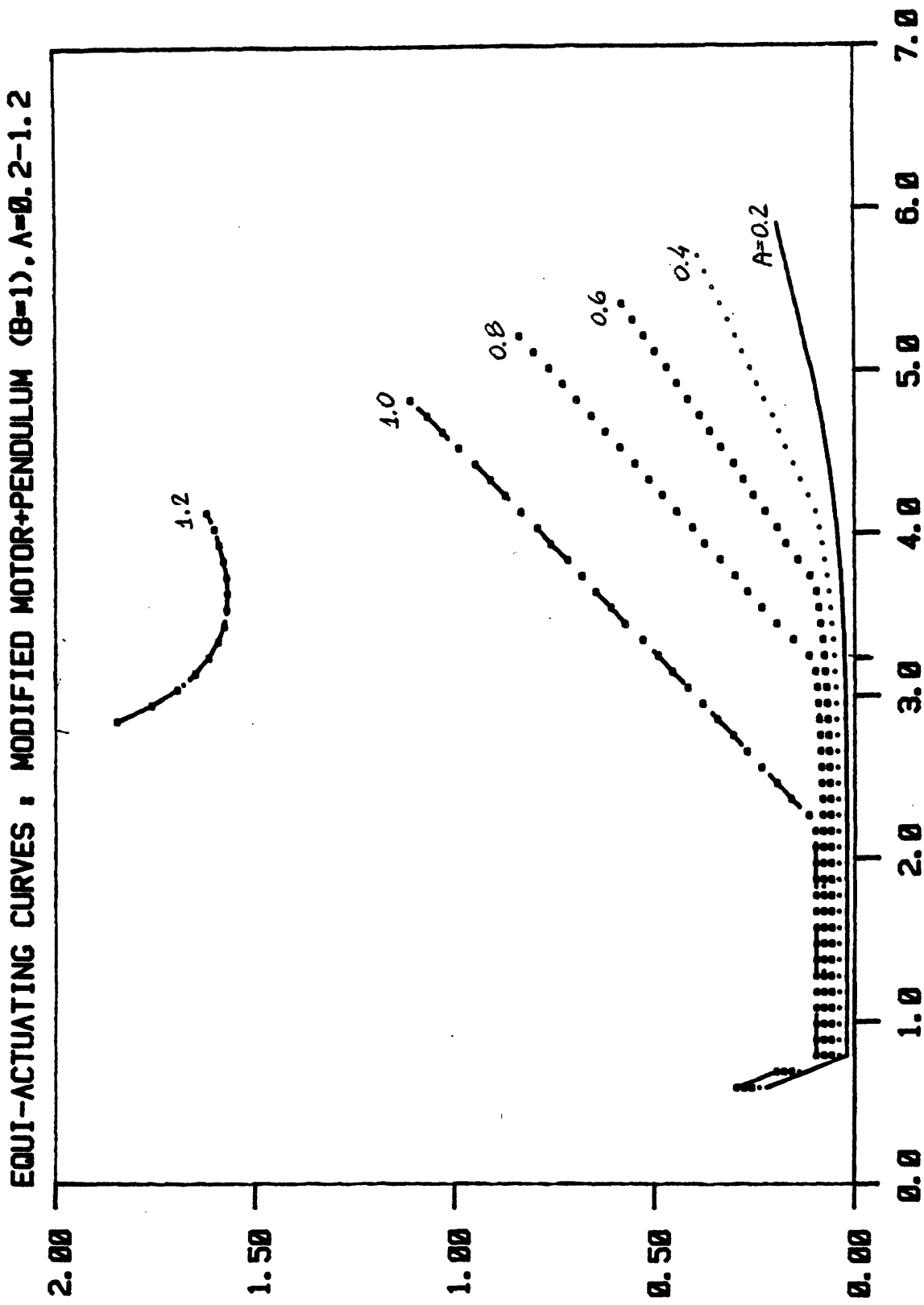

Figure 4-13: Iso - actuator curves for actuator II with B=1

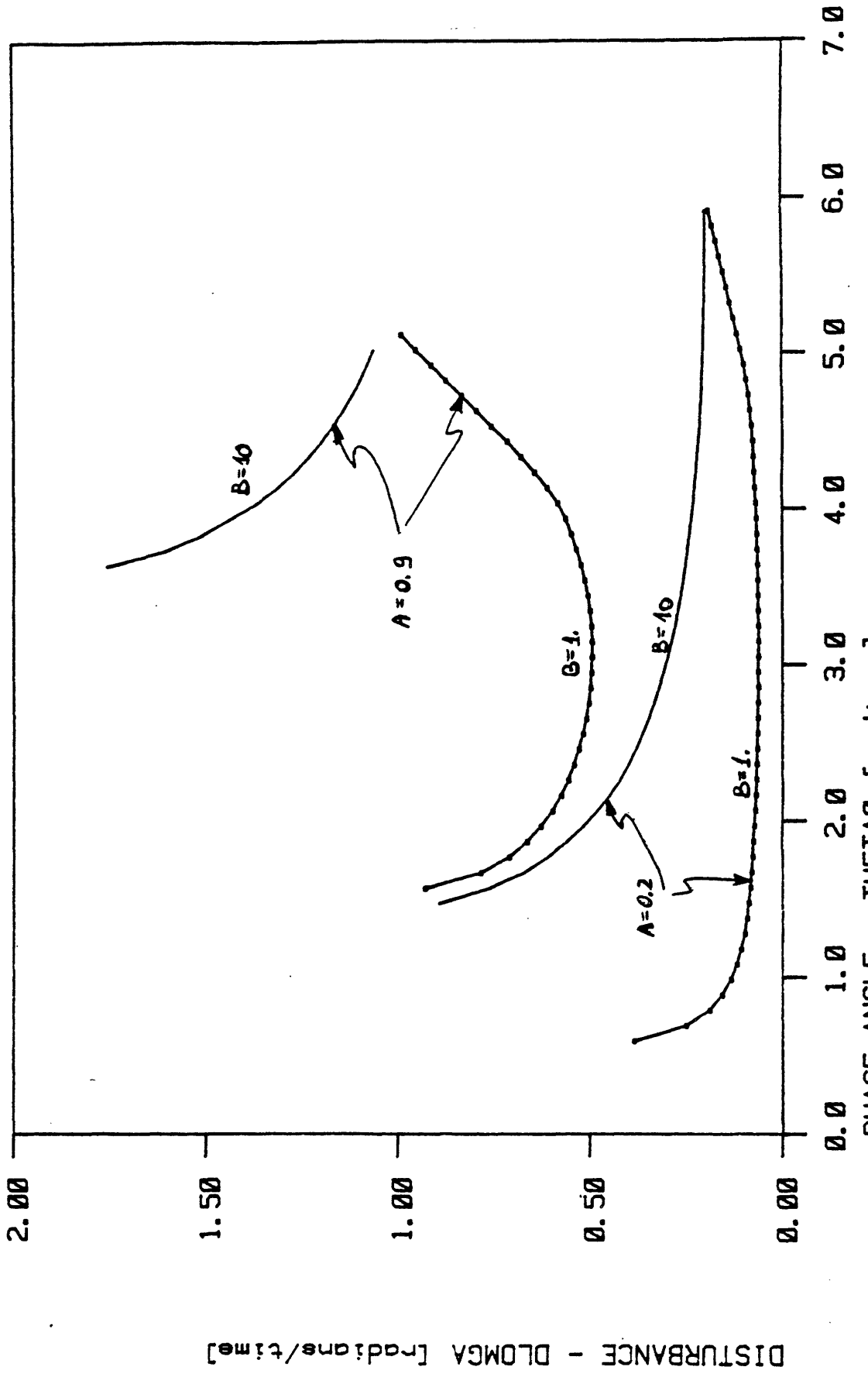

Figure 4-14: Iso - actuator curves for type I actuators (B=1,10)

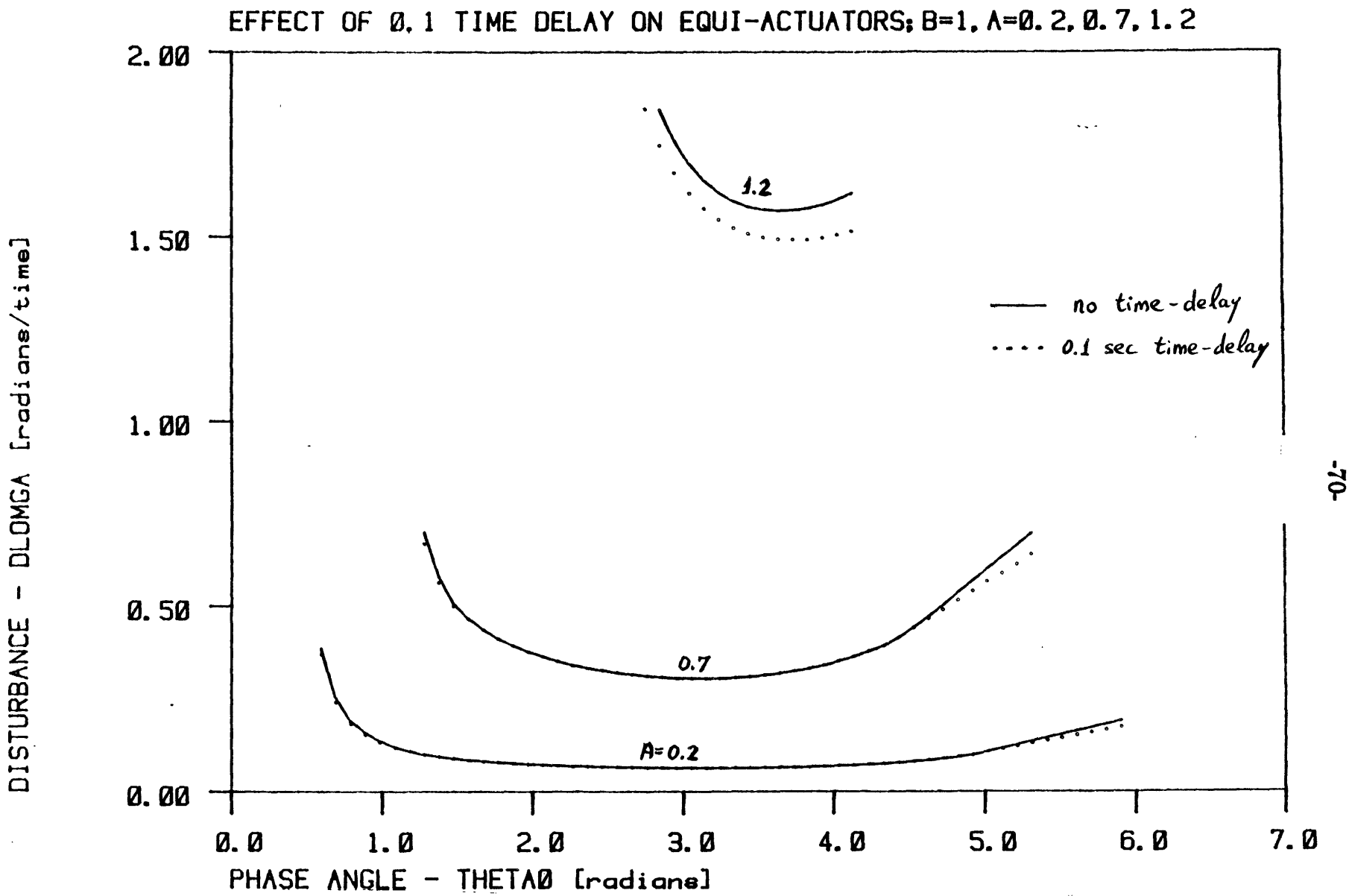

Figure 4-15: The effect of a time delay of 0.1 on the iso - actuator curves of actuator I with B=1

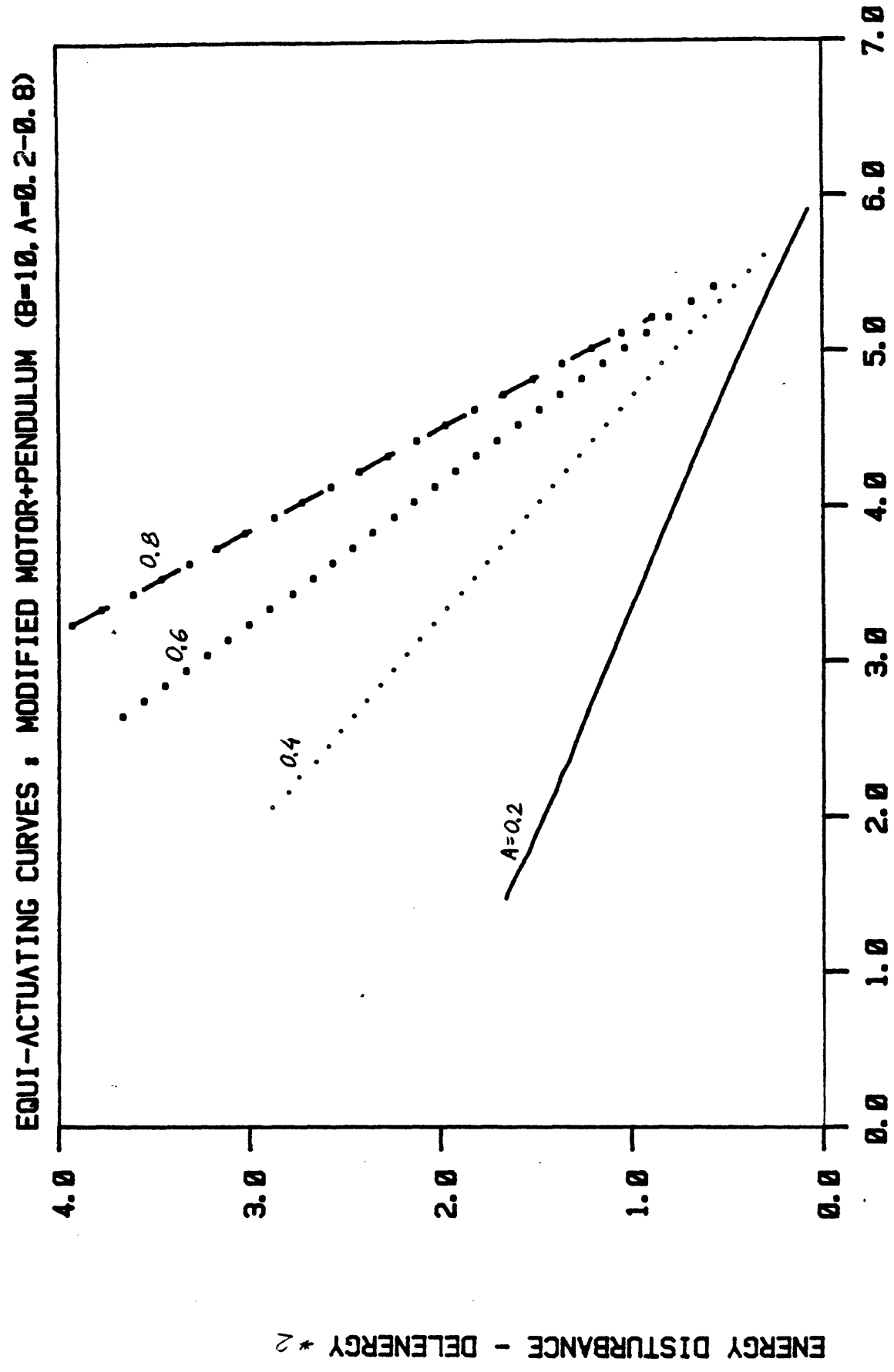

Figure 4-16: Iso - actuator curves (actuator II, B=10) for energy disturbances

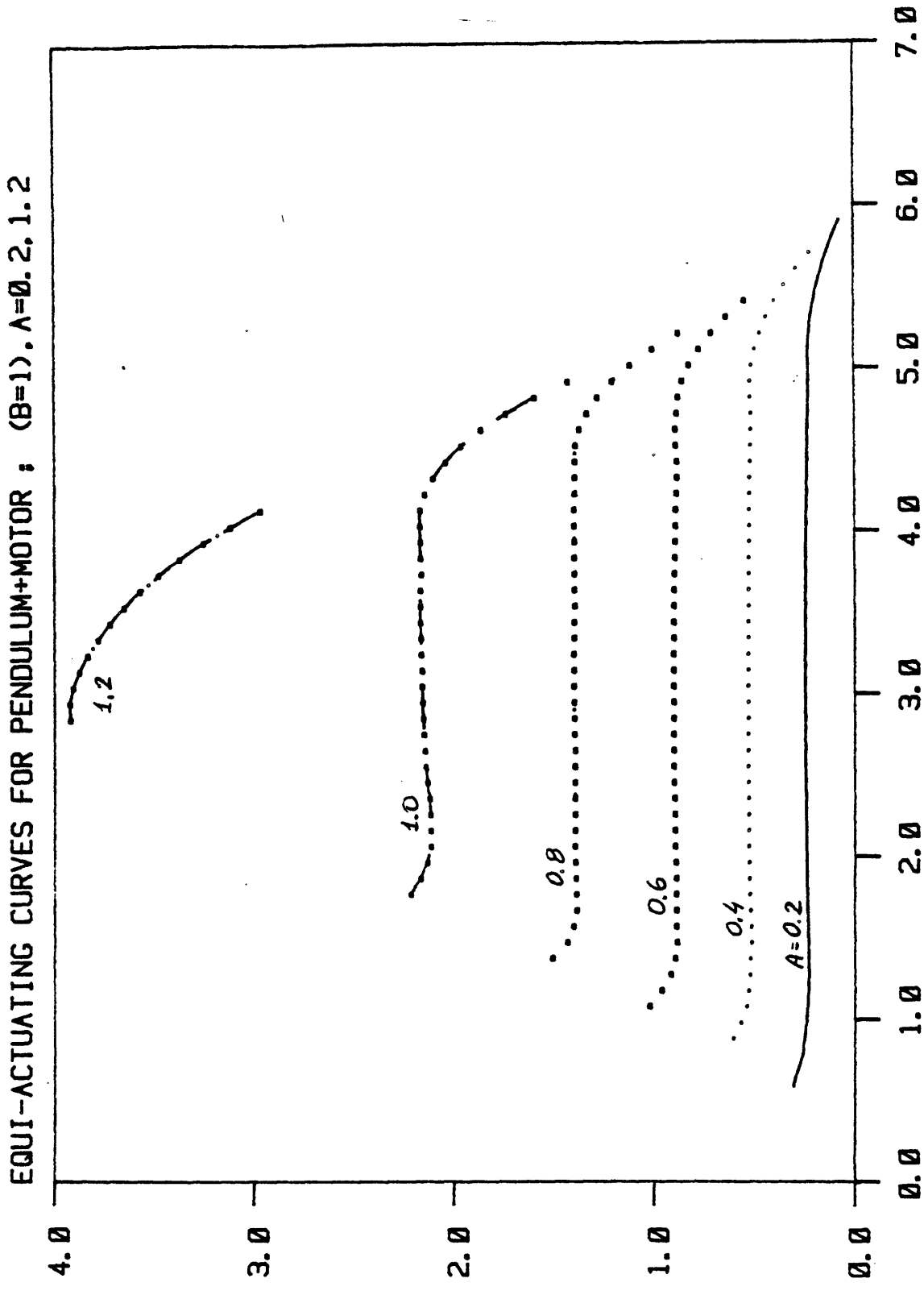

Figure 4-17: Iso - actuator curves (actuator I, B=1) for energy disturbances

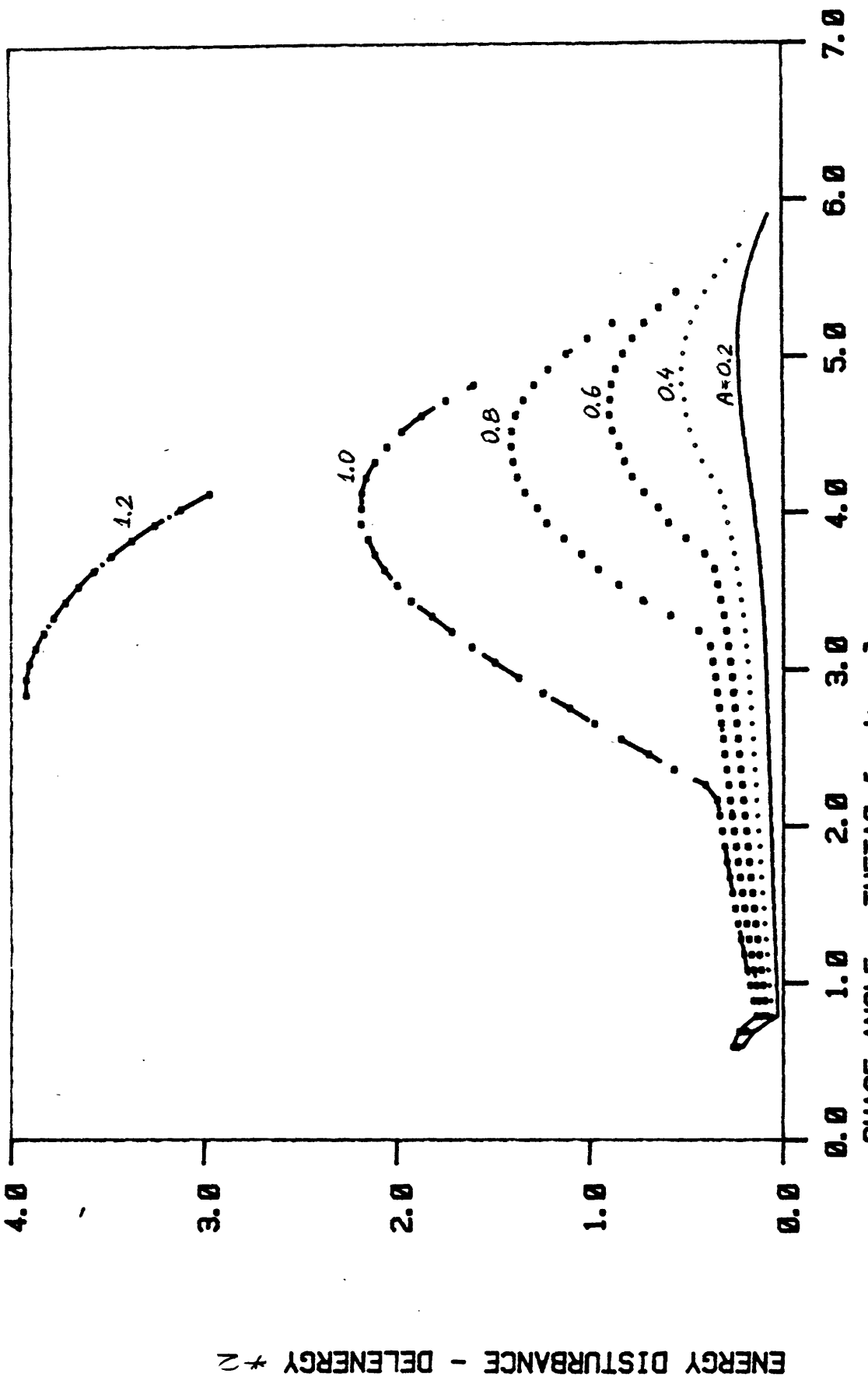

Figure 4-18: Iso - actuating curves (actuator II, B=1) for energy disturbances

4.7 Limitations

The solution of the two-point-boundary-value-problem supplies a wealth of information on the relationships of given disturbances, states where those disturbances take place and the actuators available to correct them. The major problem for such an approach is the necessity to solve the problem again for any new disturbances. If for example, the disturbances were position disturbances rather than velocity disturbances, the whole process of generating the iso-actuator surfaces will have to be repeated.

The problem is even more compounded if the system has more than one degree of freedom. The number of combinations of states and disturbances that will have to be solved for becomes very quickly prohibitive. Hence,there exists a need to develop a new formulation, which will be effective in dealing with a larger number of degrees of freedom, even at the expense of getting a more general information, and a less detailed one.

Such a formulation, which uses sets to describe families of possible disturbances, will be illustrated in the following section and further explained in Chapter 5. Its application to multi-linkage systems in general, and to gait-models in particular will be discussed in chapters 6 and 7.

4.8 An Illusration of Set-Theoretic Analysis Capabilities

In any attempt to develop a mathematical formulation of events such as disturbances and recovery mechanisms, a researcher encounters the problem of how to describe the disturbances. One could assume the deviations in the positions and angular velocities of the different joints from the nominal trajectories, and using a

model of the system then try to predict the future propagation and correction of such disturbances. Such an approach is hampered by the large number of state variables and by the necessity to simulate simultaneous disturbances to all the state variables.

Stumbling is a typical example of a disturbance that can be encountered. It usually takes place due to an interference of the environment with the movement of the swinging leg. Such a disturbance will affect all the links of the swinging leg, but its propagation to the leg in stance may be quite limited, due to the large mass difference between the swinging leg and the rest of the body (as a 1^{st} order approximation one can assume that the mass of the rest of the body is located at the center of mass, which is approximately in the pelvis). Hence, in order to study the effect of such disturbances, one should simulate simultaneous changes in the values of all the state variables of the swinging leg. Due to the large number of state variables, a large number of simulations may be required in order to learn about the internal characteristics of the system, and one runs the risk of losing the forest for the trees.

It is exactly this point which is the strongest attribute of Set-Theoretic analysis. One does not need to know the exact magnitude of each of the disturbances, and there is no need to try and isolate artificially introduced disturbances. As long as the upper bound of the disturbances is known, they can all be treated in the same manner, namely - by studying the propagation of the boundaries of the disturbances (rather than the actual disturbances themselves).

A simple example is in order here. Fig. 4-19 describes a simple pendulum which is released from rest at point A. If there is no friction in the joint, the pendulum will oscillate and come to momentary rest at point B. If the pendulum experiences an initial disturbance which causes it to begin its movement at A'

rather than at A, the highest position on the other side will appropriately be B'. If the disturbance at A is a velocity disturbance rather than a position disturbance, a new simulation needs to be performed in order to study the effect of this disturbance.

Hence, it is clear that in order to study the range of possible amplitudes obtained from combinations of position and velocity disturbances taking place at A, one needs to perform an enormous number of simulations. Set-Theoretic analysis is a mathematical tool which enables the study of the propagation of uncertainties (or disturbances) in a dynamic system. Rather than looking at the propagation of one disturbance, it enables predicting the propagation of a set of bounded disturbances through the system.

An illustration of Set-Theoretic analysis capabilities can be described by the following problems (applied to the above pendulum). .

1. For an initial uncertainty in the pendulum position of 5^0, and an initial uncertainty of 1^0/sec, what are the bounds on the position and velocity of the pendulum at t=0.5 sec.

2. For a pendulum driven by a motor whose output torque is subject to uncertainty of 1 Nt-m, what will the resulting uncertainty in the position and velocity of the pendulum at t=0.5 sec.

Without the use of Set-Theoretic analysis, a large number of simulations would be required in order to try and solve problem 1, but it is almost certain that the large number of simulations needed to address problem 2 is going to be prohibitive.

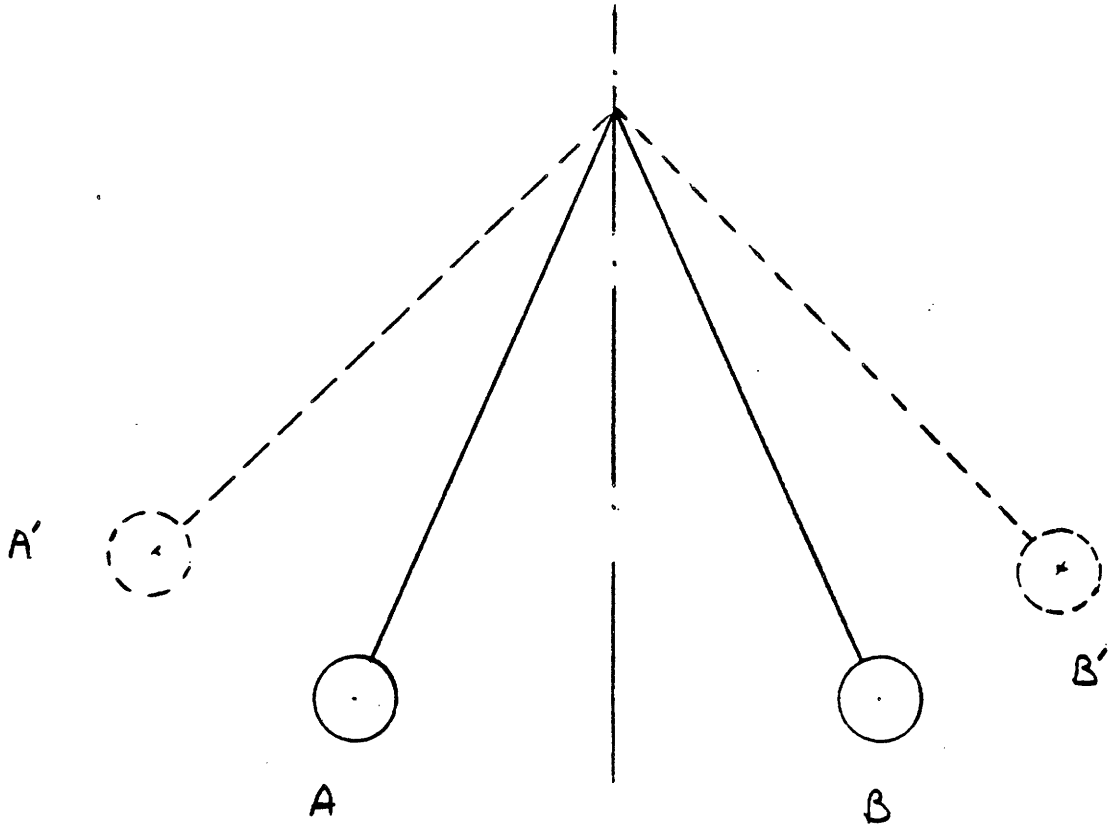

Figure 4-19: A simple free swinging pendulum

Chapter 5
Set-Theoretic Analysis of Multi-Linkage Systems

5.1 The Unknown-but-Bounded Class of Problems

Dynamic systems can in general be divided into deterministic and non-deterministic systems. Deterministic systems can be fully characterized at any given time (i.e. their states, outputs and inputs can be described as explicit functions of time). Non-deterministic systems can generally be divided into systems where either some statistical properties of the system variables are known or the bounds on the variables are known. Stochastic processes are an example of the former, and Set- Theoretic analysis is an example of the latter.

Set-Theoretic models (which are also called unknown-but-bounded) describe systems where the only information available about any of the system's states is its bounds. No information is given about the likelihood of a state within the bounds, but a state could not exist outside the bounds. As the bounds change with time, a tube which bounds all the possible states is formed. Hence the talk about the "state-in-the-tube" problem.

The underlying assumption of Set-Theoretic analysis is that there is a relationship between bounded sets of inputs, disturbances and outputs of a given system. This relationship can mathematically be described by the propagation of the bounds of those sets.

Fig. 5-1 describes a planar set bounded by a polygon and its approximation

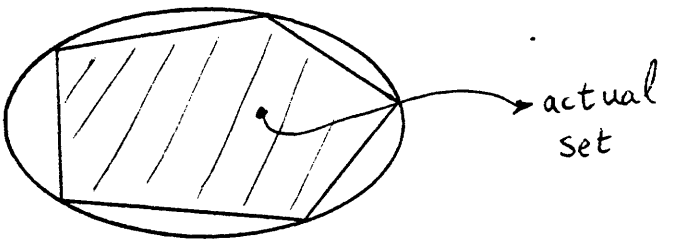

Figure 5-1: An actual set bounded by a polygon and its approximation by an ellipse

by an ellipse. Describing the set as being bounded by the polygon is mathematically more complex and results in a smaller bound on the set. Using the ellipse to describe the set is mathematically easier, but results in a larger bound (i.e more points which were originally outside the set are now included in the set bounded by the ellipse). This example illustrates the inherent trade-off between mathematical complexity and geometric accuracy. The route that has been taken in this work is the route of mathematical simplicity, hence all the sets will be described by ellipsoids or transformations of ellipsoids (in the two dimensional space, the ellipsoids degenerate into ellipses).

5.2 The Historical Development of Set-Theoretic Analysis and Control

The two major aspects in applying Set-Theoretic to the study of dynamic systems are Set-Theoretic analysis and Set-Theoretic synthesis. As an analytic tool, Set-Theoretic could be used for the study of the interrelations between bounded sets of actuators, states and disturbances. In the synthesis mode it can be used to design acceptable or optimal controllers, such that the constraints on the actuators or outputs will not be violated as long as the disturbances are bounded.

The first discrete time formulation of Set-Theoretic analysis using ellipsoids to describe convex sets was done by Schweppe [46], in the context of estimation theory (see also Schweppe and Knudsen [45]). Schweppe [47] traces some of the ideas to the work of Kahan [21] who described the geometry of intersecting ellipsoids, and to the works by Witsenhausen [62], [63] and [64], who used support functions and Dynamic Programming to describe the "state in the tube" problem, as well as to design controllers to satisfy the "target tube" constraints, while optimizing a cost function. Schlaepfer [43] and Schlaepfer and Schweppe [42] extended the analysis to include continuous time domain formulation. The geometric shapes of the bounded sets that have been studied include ellipsoids and polyhedra([20], [50]).

The use of Set-Theoretic formulation as a practical control design tool has been demonstrated in the applications for electrical power plants ([13] and [12]), and nuclear power plants [31]. Some of the latest advances in Set-Theoretic applications include the works of Sira-Ramirez [50] on the control of lagre scale systems, and Usoro [56] who developed a control algorithm to optimize the value of the feedback gains for maximum disturbance tolerance. Usoro also showed that for a linear time invariant system the Set-Theoretic approach produces an operating point for the system where the control and output constraints "meet".

5.3 Mathematical Formulation

It is interesting to consider the unknown-but-bounded case as an extension of the stochastic class of control problems (which include both input and observation disturbances). The stocahstic case can be characterized by the following equations:

$$\frac{d\vec{x}(t)}{dt} = F(t)\vec{x}(t) + G(t)\vec{w}(t)$$

$$E\{\vec{x}(0)\} = 0$$

$$E\{\vec{w}(0)\} = 0$$

$$E\{\vec{x}(0)\,\vec{w}'(t)\} = 0$$

$$E\{\vec{x}(0)\,\vec{x}\,'(0)\} = \Psi$$

- $\vec{x}(t)$ - is the state vector
- $\vec{w}(t)$ - is the input disturbance
- $F(t)$, $G(t)$ - are matrices
- $\vec{x}(0)$, $\vec{w}(0)$ - are the initial state variable and disturbance respectively

If $\Gamma(t)$ is defined as the covariance matrix of $\vec{x}$

$$\Gamma(t) = E\{\vec{x}(t)\,\vec{x}\,'(t)\}$$

From [6] - the covariance matrix of two variables x and y is defined as:

$$C_{xy} = \int\int_{-\infty}^{\infty} (x-\mu_x)(y-\mu_y)p(x,y)dxdy$$

where μ_x and μ_y are the mean values of x and y respectively, and p(x,y) is the joint

probability density function of x and y).

The differential equation for $\Gamma(t)$ is:

$$\frac{d\Gamma(t)}{dt} = F(t)\Gamma(t) + \Gamma(t)F'(t) + G(t)Q(t)G'(t)$$

$$\Gamma(0) = \Psi$$

where Q(t) is related to the correlation function of

$$\vec{w}(t)$$

by:

$$E\{\vec{w}(t_1)\,\vec{w}'(t_2)\} = \delta(t_1 - t_2)Q(t_1)$$

As $\Gamma(t)$ is the covariance matrix of $\vec{x}$, then if it is positive definite it can be geometrically described in the state space as an ellipsoid, whose axes are along the directions of the eigenvectors of the covariance matrix, and the lengths of the axes are equal to the square roots of the eigenvalues.

The geometric interpretation can be illustrated by the following example: a dynamic system is described by two decoupled state equations, with two independent state variables (x_1, x_2). If the state variables are random, the covariance matrix in this case becomes a diagonal matrix

$$\Gamma = \begin{vmatrix} a_1 & 0 \\ 0 & a_2 \end{vmatrix}$$

where a_1 and a_2 are the variance values of x_1 and x_2 respectively. If Γ is positive definite then it can be described as an ellipse whose semi-axes are along x_1 and x_2 in the state space, and whose lengths are the square roots of a_1 and a_2 respectively.

The mathematical formulation and the geometric interpretation can be extended to the unknown-but-bounded case (a detailed explanation can be found in Scweppe [47]). For a linear system described by

$$\frac{d\vec{x}(t)}{dt} = F(t)\vec{x}(t) + G(t)\vec{w}(t)$$

where

$$\vec{x}(0) \in \Omega_x(0) = \{\vec{x}: \vec{x}'\Psi^{-1}\vec{x} \leq 1\}$$

and

$$\vec{w}(t) \in \Omega_w(t) = \{\vec{w}: \vec{w}'Q^{-1}(t)\vec{w} \leq 1\}$$

The initial state uncertainty - $\vec{x}(0)$ is bounded by the ellipsoid Ψ in the state space, and the input disturbance uncertainty - $\vec{w}(t)$ is bounded by the time varying ellipsoid Q.

The time propagation of the ellipsoids which describe the state uncertainty is given by the following differential equation [47]:

$$\frac{d\Gamma(t)}{dt} = F(t)\Gamma(t) + \Gamma(t)F(t)' + \beta(t)\Gamma(t) + \frac{1}{\beta}G(t)Q(t)G(t)'$$

where

$\Gamma(0)=\Psi$

and

$$0 \leq \beta(t) \leq \infty$$

β(t) is a free parameter which is optimized to minimize the size of the Γ ellipsoids. Note that small values of β tend to amplify the effect of the input noise, while large values will tend to drive the system into instability (as their effect is similar to that of large gains in linear feedback systems).

This equation can be simplified when the propagation of only initial uncertainties is studied, and the system is free of any continuous or discrete input noise at any time after t=0. In this case Q=0 and the size of the ellipse can be minimized by choosing β(t)=0.

To summarize - there is an equivalence between the differential equations and the geometric interpretation between the covariance matrix in the stochastic case, and the state bounding ellipsoids in the Unknown- but-Bounded case.

5.4 The Mathematical Linearization

The linearization of the non-linear state equations is carried out as an extension of the "operating point" linearization, suggested by Schultz and Melsa [44]. For a non-linear system whose state equations are given by :

$$\frac{d\vec{x}}{dt} = \overline{F}(\vec{x},\vec{u})$$

and for

$$\overline{F}(\vec{x},\vec{u})$$

which is continuously differentiable, a linearization can be done around any state

$$\vec{x}$$

and input

$$\vec{u}$$

which are the solution to the state equation.

Using a Taylor expansion around that point (and neglecting higher order terms

$$\frac{d}{dt}(\vec{x}+\delta\vec{x}) = \overline{F}(\vec{x},\vec{u}) + \frac{\partial\overline{F}}{\partial\vec{x}}\,\delta\vec{x} + \frac{\partial\overline{F}}{\partial\vec{u}}\,\delta\vec{u} + \textit{higher order terms}$$

By substituting the state equations into the Taylor expansion (and neglecting higher order terms) the final result is obtained:

$$\frac{d}{dt}(\delta\vec{x}) = F\,\delta\vec{x} + B\,\delta\vec{u}$$

Where

$$F = \frac{\partial\overline{F}}{\partial\vec{x}}$$

$$B = \frac{\partial\overline{F}}{\partial\vec{u}}$$

5.5 The Dynamic Equation Generator

As we have seen in the previous sections, Set-Theoretic Analysis has been successfully applied to linear systems described by state equations. This fact prompted the search for a procedure that could automatically produce linearized state equations for a multi-linkage system. The procedure that has been developed involves three major steps:

1. Generating the dynamic equations
2. Generating the state equations
3. Linearizing the state equations

The following sections describe the details of that procedure.

There are generally two different methods for developing the dynamic equations of a multi-linkage system: the Lagrangian approach and the Newtonian approach. The Lagrangian approach derives the dynamic equations from the expressions for the kinetic and potential energy of the system, whereas the

Newtonian approach derives the dynamic equations for each link and adds the geometric constraints to those equations.

Paul [40] descibes an algorithm (based on the Lagrangian approach) for deriving the dynamic equations of a multi-linkage system with revolute or prismatic joints. This algorithm has been chosen for its recursive nature and ease of implementation on a symbolic language manipulator (like Macsyma). The algorithm requires the user to submit two kinds of input for each link:

1. The A matrix

2. The inertial properties

5.5.1 The A matrix

A convenient way to describe the kinematics of a rigid link is to attach a coordinate system to that link. The A matrix describes the homogeneous transformation [9] between the coordinate systems of two adjacent links. This transformation enables one to calculate the kinematics of each of the links relative to another link, or to an inertial reference system. For a general revolute joint, the A matrix represents two translations and two rotations, but in the planar model that is being analyzed in this work, each transformation involves one translation and one rotation.

The homogeneous transformation for a planar revolute linkage is shown in Fig. 5-2. Link OO_2 rotates around point O relative to the inertial reference frame. The next link is pinned at point O_1. The A matrix for the transformation of a link is given by the following 4x4 matrix:

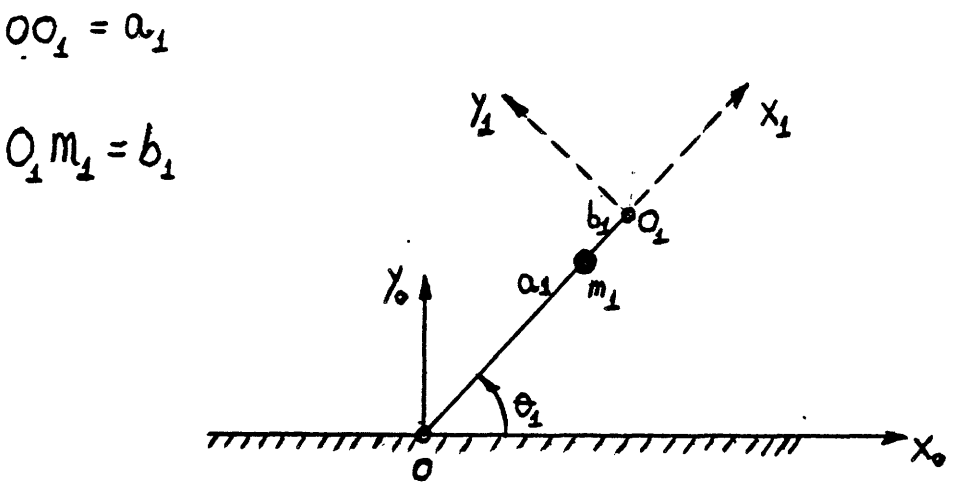

Figure 5-2: The A transformation for a revolute linkage

$$A = \begin{vmatrix} \cos\theta & -\sin\theta\cos\alpha & \sin\theta\sin\alpha & a*\cos\theta \\ \sin\theta & \cos\theta\cos\alpha & -\cos\theta\sin\alpha & a*\sin\theta \\ 0 & \sin\alpha & \cos\alpha & d \\ 0 & 0 & 0 & 1 \end{vmatrix}$$

The four parameters which characterize the transformation are:

- θ - rotation around the joint axis (the generalized coordinates)
- a - the distance between the joint axes
- α - the twist of the link (in a plane perpendicular to a)
- d - the relative translation of the coordinate systems (along the joint axis)

For a planar model α=0 and d=0.

The three link model which has been analyzed in this study is described in Fig. 5-3. The parameters for the A matrices of the three links are given in table 5-I.

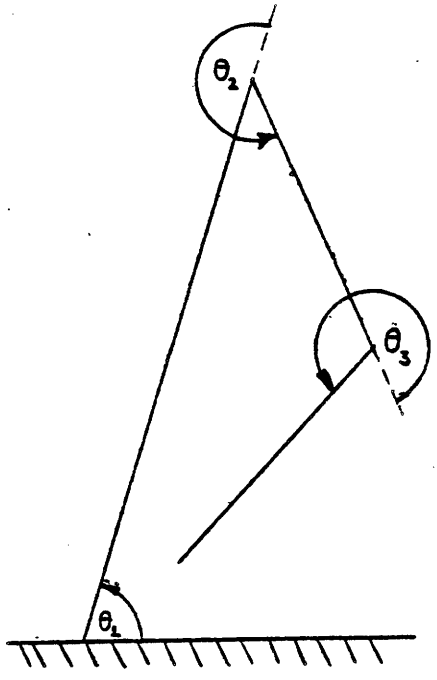

Figure 5-3: The three link model

link	θ	a
1	θ_1	l_1
2	θ_2	l_2
3	θ_3	l_3

Table 5-I: Parameters for the three link model

Substitution of the parameters into the A matrix results in the A matrices for the three links in the model.

5.5.2 The inertial properties

The second set of inputs that is required from the user is the inertial properties of each of the links. These include the distribution of the mass and the moments of inertia for each link, in the coordinate system that is attached to the link. This information is included in the J matrix (which again has to be given for every link).

The general format of the J matrix is as follows:

$$\begin{bmatrix} \frac{-I_{xx}+I_{yy}+I_{zz}}{2} & I_{xy} & I_{xz} & m_i\bar{x}_i \\ I_{xy} & \frac{I_{xx}-I_{yy}+I_{zz}}{2} & I_{yz} & m_i\bar{y}_i \\ I_{xz} & I_{yz} & \frac{I_{xx}+I_{yy}-I_{zz}}{2} & m_i z_i \\ m_i\bar{x}_i & m_i\bar{y}_i & m_i\bar{z}_i & m_i \end{bmatrix}$$

The parameters which characterize the J_i matrix are:

- m_i - the mass of the link
- x_i, y_i, z_i - the coordinates of the center of gravity
- I_{ixx}, I_{iyy}, I_{izz} - principal moments of inertia

- I_{ixy}, I_{ixz}, I_{iyz} - cross moments of inertia

As the planar model described above contains only point masses, the J_i matrices become:

$$\begin{vmatrix} m_i b_i^2 & 0 & 0 & -\frac{1}{2} m_i b_i \\ 0 & 0 & 0 & 0 \\ 0 & 0 & 0 & 0 \\ -\frac{1}{2} m_i b_i & 0 & 0 & m_i \end{vmatrix}$$

5.5.3 The T transformation and the dynamic equations

In order to describe the position and orientation of the links in an inertial reference frame, a new transformation is needed. This transformation is called the T transformation, and it can be derived for each of the links by concatenating the A transformations from the first link (which is expressed relative to an inertial reference system), up to the link of interest. Hence the T transformation of the i^{th} link can be obtained by

$$T_i = A_1 \cdot A_2 \cdot \cdots \cdot A_i \tag{5.1}$$

Once the T transformations for all the links have been obtained, three groups of terms have to be derived. Those terms are D_i, D_{ij} and D_{ijk}.

$$D_i = \sum_{p=i}^{N} -m_p \vec{g}' \frac{\partial T_p}{\partial q_i} r_p^p \tag{5.2}$$

$$D_{ij} = \sum_{p=\max(i,j)}^{N} \text{trace} \left(\frac{\partial T_p}{\partial q_j} J_p \frac{\partial T_p'}{\partial q_i} \right) \tag{5.3}$$

$$D_{ijk} = \sum_{p=\max(i,j,k)}^{N} \text{trace} \left(\frac{\partial^2 T_p}{\partial q_j \partial q_k} J_p \frac{\partial T_p'}{\partial q_i} \right) \tag{5.4}$$

After the terms in equations (5.2) - (5.4) have been derived for all the N links

in the model, they can be substituted into the following equation, to generate the dynamic equations of the system:

$$F_i = \sum_{j=1}^{N} D_{ij} \frac{d^2 q_j}{dt^2} + \sum_{j=1}^{N} \sum_{k=1}^{N} D_{ijk} \frac{dq_j}{dt} \frac{dq_k}{dt} + D_i \qquad (5.5)$$

5.5.4 The automatic generation of linearized state equations

It is quite clear from the description of Paul's algorythm, that any implementation of it for more than one link, will involve a tremendous computational burden. Due to the large size of the terms that are being generated, the probability of making algebraic errors increases tremendously. This was the primary reason for trying to automate the process. This goal has been successfully completed by the use of the symbolic language manipulator Macsyma, which is a software package capable of manipulating mathematical symbols as well as numbers.

The process of generating the linearized state equations using Macsyma, involves the following steps:

1. Input the A matrices for all the links
2. Input the links' centers of mass (in the links' coordinate system)
3. Input the J matrices for all the links
4. Input the $\vec{g}$ vector (the gravitational acceleration) in the inertial reference system
5. Calculate the T transformations for all the links
6. Calculate the 1^{st} and 2^{nd} partial derivatives of T with respect to the generalized coordinates q_i

7. Calculate the D_i, D_{ij} and D_{ijk} terms

8. Substitute those values into Eq. (5.5), to obtain the dynamic equations.

9. Transform the dynamic equations into the state equations

10. Linearize the state equations

11. Produce the FORTRAN code for the state equations and the linearized state equations.

The above procedure has successfully generated the linearized state equations of a model comprised of two links. The most general case analyzed was a three link model with a prescribed kinematics of the first link. The results based on this model will be presented in the following chapters.

5.6 The Application of Set-Theoretic Analysis to Multi-Linkage Systems

Applying Set-Theoretic analysis to multi-linkage systems required an extensive programming effort. In order to facilitate the debugging process and future expansion of the algorithms, a set of modular programs have been developed. The major components of the set of programs are:

- integration of the state equations
- time propagation of the elllipsoids of uncertainty
- extraction of geometric information from the ellipsoids
- transformation and graphics display programs

The results of the interim calculations were saved on disk files.

5.6.1 The integration of the state equations

The state equations (that had been previously generated by MACSYMA) were integrated using the DVERK routine of the IMSL library(IMSL, Houston, TX). This routine uses Runge-Kutta formulas of orders 5 and 6 for the integration algorithm. The parameters of each simulation were written into the header of the output file, and the values of the state variables for each time step were written sequentially into the file.

The sensitivity to the time step size was tested. For values smaller than 0.05 second there were no significant changes in the values of the state variables, the values of $\Gamma(t)$ or the eigenvalues and the eigenvectors of the linearized state equations (the F matrix). Hence - a value of 0.01 second for the time step size was selected.

5.6.2 The propagation of the ellipsoids of uncertainty

The propagation of the ellipsoids of uncertainty is given by the solution to the differential equations for $\Gamma(t)$. This program uses the DVERK integration package too. The three elements of the program are:

1. Calculation of the linearized terms in the state equations.
2. Integration of the differential equations for $\Gamma(t)$.
3. Calculation of the eigenvalues and eigenvectors of $\Gamma(t)$.
4. Storage of the results.

It is important to note that the above sequence of calculations is repeated for each time step, hence the linearization is being done continuously around the nominal trajectory. The initial conditions and the momentary values of the

actuators and the state variables were read from the output file of the previous stage (the state equations integration).

5.6.3 Extraction of geometric features

The differential equation for $\Pi(t)$ yields a time-variable ellipsoid in the four-dimensional state space. In order to graphically display that information, a question arises as to what the real uncertainty in the different state variables is. To illustrate this point a two-dimensional example is examined first.

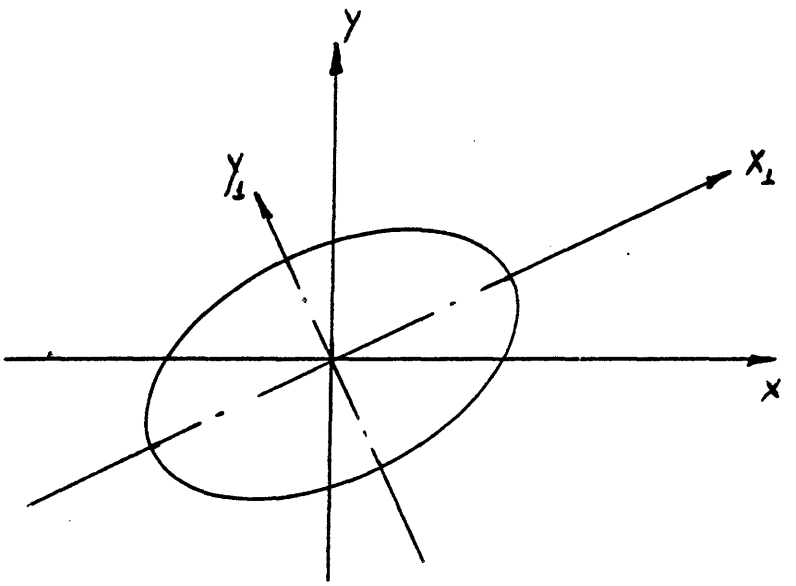

Figure 5-4: A planar region bounded by an ellipse

The bounded planar region described in Fig. 5-4 shows a range of possible values (x;y) for a point located inside the ellipse. The actual uncertainty in the value of x is obtained by taking the projection of the large axis (along the x_1 direction) upon the x axis. This is different than the range of x values obtained

from the intersection of the ellipse by the x axis. Hence, the uncertainty is not simply determined by the intersection of the ellipse with the axes, but by the projection of the ellipse upon the axes.

The generalization of the above example to the four-dimensional space, involves the projection of a four-dimensional ellipsoid on a two-dimensional plane. Such a projection produces an ellipse, and is mathematically described by a 2x2 positive definite matrix. This matrix is extracted from the 4x4 Γ matrix which describes the ellipsoid. The elements that are being extracted are the row and column elements which correspond to the state variables that span the plane.

The emphasis in this work was on studying the uncertainties in the geometric space, hence - the uncertainties in (θ_2 and θ_3) were of interest. These uncertainties were generated by extracting the [1,1], [1,2], [2,1] and [2,2] terms in the matrix Γ.

5.6.4 Geometric transformations and the graphic display

The 2x2 matrix that was extracted from Γ(t) describes an ellipse in the (θ_2,θ_3) plane. The ellipse describes the bounded set of possible locations of the model in the two-dimensional joint space. This set can be transformed into the geometric (physical) space by two possible transformations:

1. A linear transformation

2. A nonlinear geometric transformation

5.6.4.1 The linear transformation

The linear transformation maps an ellipse in one space into an ellipse in a different space. If T describes a linear transformation from the joint space described by $\vec{\theta}$, to the geometric space described by $\vec{x}$:

$$\vec{x}=T\vec{\theta}$$

Then the equation for the ellipse in the joint space:

$$(\vec{\theta}-\vec{\theta}_0)' \Gamma^{-1} (\vec{\theta}-\vec{\theta}_0) = 1$$

Results in the following ellipse in the $\vec{x}$ space:

$$(\vec{x}-\vec{x}_0)' (T \Gamma T')^{-1} (\vec{x}-\vec{x}_0) = 1$$

where

$$\vec{x}_0 = T\vec{\theta}_0$$

The eigenvalues and eigenvectors of ($T\Gamma T'$) describe the direction and the magnitude of the axes of the ellipse in the geometric space. It should be noted that since T is constant for a given transformation (it is evaluated at the center of the ellipse in the joint space), the only point in the original ellipse that is accurately mapped from one space to another is the center of the ellipse. The linear transformation will deviate from an accurate mapping of points, and generally - the farther a point is from the ellipse's center - the larger is the error in its mapping from one space to another. Hence, in order to improve the position estimates in the geometric space, a geometric transformation was chosen. The mathematical formulation of that transformation is described in the next section.

5.6.4.2 The geometric transformation

The joint angles uniquely define the position and orientation of the three-link model in the geometric space.

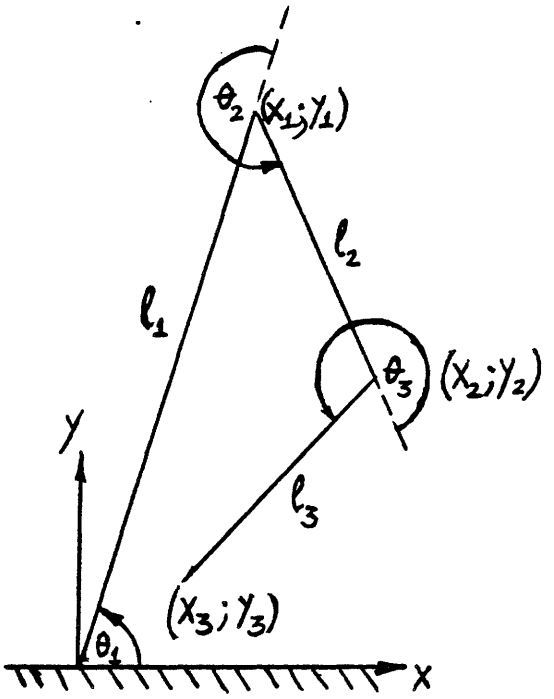

Figure 5-5: The three link model - coordinates in the joint and geometric spaces

Fig. 5-5 describes the three-link model with the following nomenclature:

- $x_1;y_1$ - hip location
- $x_2;y_2$ - knee location
- $x_3;y_3$ - foot location

The geometric transformation from the joint space to the geometric space is given by the following equations.

For the hip:

$$x_1 = l_1 \cdot cos\theta_1$$
$$y_1 = l_1 \cdot sin\theta_1$$

For the knee:

$$x_2 = x_1 - l_2 \cdot sin\theta_2$$
$$y_2 = y_1 + l_2 \cdot cos\theta_2$$

For the foot:

$$x_3 = x_2 - l_3 \cdot sin(\theta_2 + \theta_3)$$
$$y_3 = y_2 + l_3 \cdot cos(\theta_2 + \theta_3)$$

As no uncertainty is assumed in the hip position, it is clear from the above equations that the ellipse in the joint space $(\theta_2;\theta_3)$ will transform into a circular arc in the knee position, and into a closed geometric shape in the foot position. The implementation of the geometric transformation involved the following steps.

1. Extracting the orientation and magnitude of the ellipses' axes in the joint angle space.

2. Constructing a nominal stick figure from the nominal values of θ_1, θ_2 and θ_3 (from the solution of the state equations)

3. Using the geometric transformation to map the joint-space ellipse (discretized to 200 points), into the geometric space.

The completion of the steps described above maps the ellipse from the joint space into the geometric space. One of the interesting features of this transformation lies in its ability to conserve some of the characteristic properties of a multi-linkage system. Due to the geometric constraints introduced by the linkages, the bounded uncertainties in the joint-space translate into line uncertainties in the geometric space near the singularity positions of the system. This can be illustrated by describing the effect of small angular changes in the hip and knee positions when the knee is fully extended vs. when the knee is flexed (Fig. 5-6).

Fig. 5-6 describes the effect of singularity on the coordinate transformation.

Figure 5-6: The effect of singularity on transformations

An ellipse centered around the flexed knee position, will translate into a bounded geometric shape. The same ellipse, centered around the fully extended knee will transform into a collapsed shape which is very close to a curved line. This result is further demonstrated in Chapter 6.

Chapter 6
Propagation of Bounded Disturbances in Multi-Linkage Systems

6.1 The Verification of the Mathematical Formulation

There are three major groups of equations in the stream of programs described in section 3.3:

1. the dynamic equations
2. the linearized state equations
3. the equations describing the propagation of disturbances

Even though all the equations have been automatically generated, it was important to verify those equations to some extent, if only to calm the FORTRAN programmer's inherent distrust toward computerized symbolic language manipulators. The verification procedure was used to isolate the different groups and verify each one of them seperately.

6.1.1 Verifying the dynamic equations

As was shown in chapter 3, the dynamic equations are generated by summing the D_i, D_{ij} and D_{ijk} terms. Paul [40] derives those terms and the dynamic equations for a double pendulum, with point masses at the ends of the two links, in the field of gravity. Hence, the first test was to transform the 3-link model into a double pendulum, by eliminating one of the links. When the terms were compared,

3 terms (D_{211}, D_{212} and D_{221}) were found to be different.

In order to resolve the conflict, the dynamic equations were compared to the dynamic equations of a 2-link mechanism in Shiller [48]. Shiller had used a different algorithm for the generation of the dynamic equations, and those equations were found to be exactly the same as the equations derived in this work.

Since the state equations are just a transformation of the dynamic equations, once the dynamic equations have been verified, the next step was to verify the linearized state equations.

6.1.2 Verification of the linearized terms

The 3-link 2 degree of freedom model includes four state variables. Fig. 5-3 and the definitions of the state variables are repeated here:

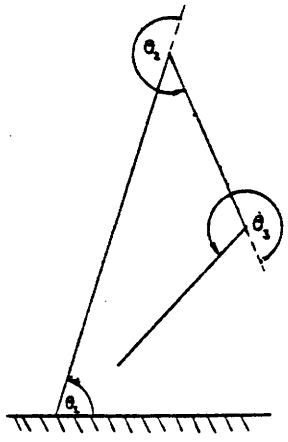

$$\omega_i = \frac{d\theta_i}{dt}$$

$$\alpha_i = \frac{d^2\theta_i}{dt^2}$$

The state variables are:

$x_1=\theta_2$

$x_2=\theta_3$

$x_3=\omega_2$

$x_4=\omega_3$

The linearized state matrix is:

$$F = \begin{vmatrix} 0 & 0 & 1 & 0 \\ 0 & 0 & 0 & 1 \\ f_{3,1} & f_{3,2} & f_{3,3} & f_{3,4} \\ f_{4,1} & f_{4,2} & f_{4,3} & f_{4,4} \end{vmatrix}$$

From the format of the F matrix it is clear that only the 3rd, and 4th rows need to be checked. The verification of those terms was based on the reduction of the 3-link model to a simple pendulum, by making the appropriate mass and length substitutions. In such a reduction only the partial derivatives of the angular acceleration with respect to the angular velocity and angular position of that degree of freedom exist. Hence the only terms that could be tested were $f_{3,1}$, $f_{3,3}$, $f_{4,2}$ and $f_{4,4}$, as the others do not exist for such a reduction.

The verification was done on two levels: substituting the values of the parameters and using MACSYMA to evaluate the original terms; and substituting the numerical values to the FORTRAN code and testing the numerical results.

It is interesting to note that the only error that was found stemmed from the human intervention. The long linearized terms generated by MACSYMA were broken into hundreds of short terms so that they could be handled by the

FORTRAN compiler. The default numbering assignment by MACSYMA was not compatible with the program requirements, hence - the serial numbers of the short terms had to be assigned manually. It is in this assignment that the error took place.

After the error had been corrected, both the symbolic results from MACSYMA and the numerical results from the FORTRAN code corresponded to the theoretical values for a single pendulum.

6.1.3 The differential equations for Γ(t)

The differential equation for the propagation of initial discrete disturbances is

$$\frac{d\Gamma}{dt}=F\Gamma+\Gamma F^{t} \tag{6.1}$$

Schweppe [47] describes a solution to the general class of linear matrix equations

$$\frac{dX(t)}{dt}=F_1X+XF_2+U \tag{6.2}$$

where X, F_1, F_2 and U are time - varying matrices, and X(0) is the initial condition. By defining two functions $\Theta_1(t,t_0)$ and $\Theta_2(t,t_0)$ which satisfy the following equations:

$$\frac{d\Theta_1(t,t_0)}{dt} = F_1(t)\Theta_1(t,t_0)$$

$$\frac{d\Theta_2(t,t_0)}{dt} = \Theta_2(t,t_0)F_2(t)$$

$$\Theta_1(t,t)=\Theta_2(t,t)=I$$

where I is the identity matrix.

It can be shown ([47] page 504) that

$$X(t) = \Theta_1(t,0)\ \{X(0) + \int_0^t \Theta_1{}^{-1}(\tau,0)U(\tau)\Theta_2{}^{-1}(\tau,0)d\tau\}\ \Theta_2(t,0) \tag{6.3}$$

From Eq. (6.1):

$$\begin{aligned} F_1&=F \\ F_2&=A' \\ U&=0 \\ X&=\Gamma \end{aligned} \tag{6.4}$$

Hence, by substituting (6.4) into (6.3) the following equation is obtained:

$$\Theta(t) = \Theta\text{–}(1)(t,0)\Gamma(0)\Theta\text{–}(2)(t,0) \tag{6.5}$$

Θ_1(t,0) and Θ_2(t,0) are the solutions to the equations:

$$\frac{d\Theta_1}{dt} = F\Theta_1$$

$$\frac{d\Theta_2}{dt} = \Theta_2 F' \tag{6.6}$$

With the initial conditions:

$$\Theta_1(0) = I$$

$$\Theta_2(0) = I$$

The solutions to (6.6) were substituted into (6.5) and compared to the results of the direct integration of Eq. (6.1). The results showed that with a coarse time step (Δ(t)=0.1 sec), the results were equal to within 0.1%. Reducing the time step to 0.01 sec. reduced the differences to between 10^{-5} and 10^{-6}%.

6.2 The General Properties of Joint Space Trajectories and Ellipses

As a major portion of the results is going to be described in the joint space, some of the properties of that space will be illustrated in the following section.

Fig. 6-1 describes an imaginary trajectory in the joint-space. As was illustrated earlier, each point in this space defines a unique configuration in the geometric space (i.e. there exists a one-to-one mapping from the joint space into the geometric space; the inverse mapping is generally not uniquely defined, and does not always exist). The joint-space trajectory carries important information not only on the geometric mapping, but on the angular velocities as well. Points on the trajectory which have tangents that are parallel to one of the axes, correspond to

states where one of the angular velocities is zero (ω_3=0 at points A and B, and ω_2=0 at points C and D).

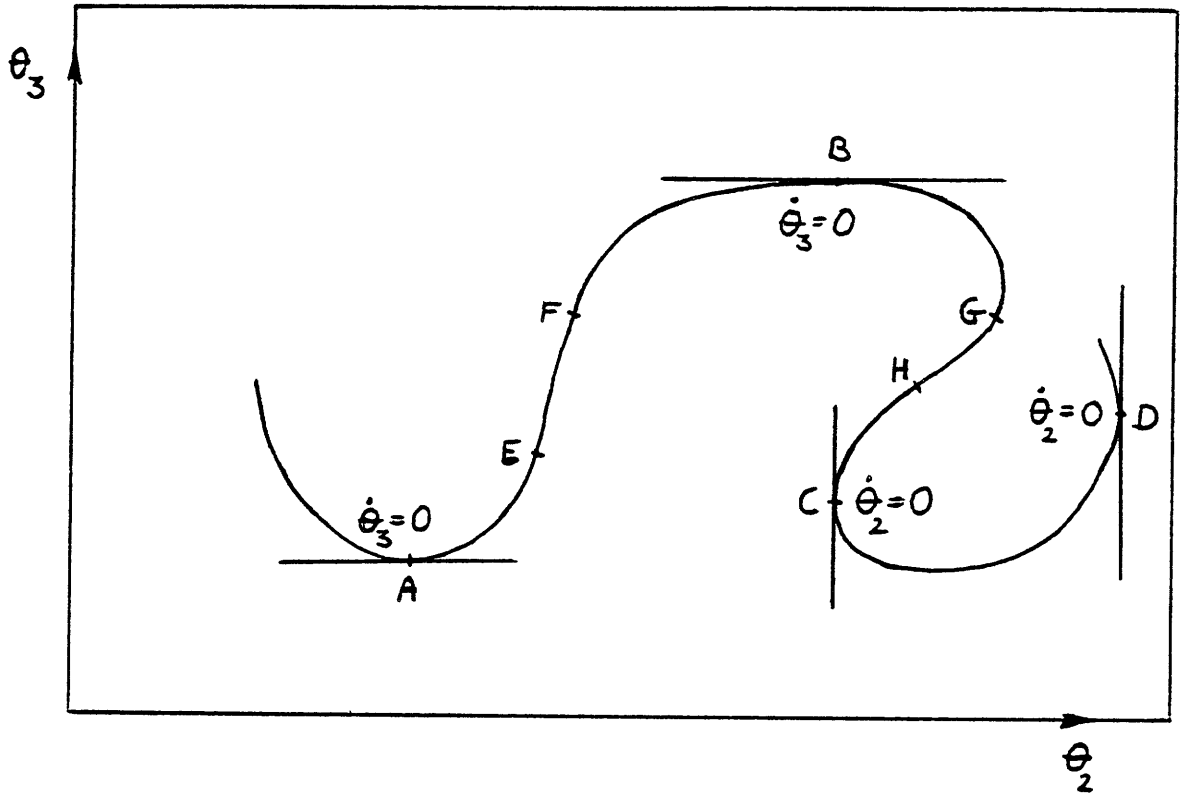

Figure 6-1: A general joint space trajectory

The second interesting property of the joint-space trajectory involves the slope of the trajectory. A positive slope (like the E-F section) means that the two links rotate in the same directions, and a negative slope (section G-H) means that the two links rotate in opposite directions.

Fig. 6-2 describes the time propagation of an initial ellipse of uncertainty. Three features of the ellipses convey important information:

1. the aspect ratio of the axes of symmetry
2. the orientation of the ellipses
3. the size of the ellipses

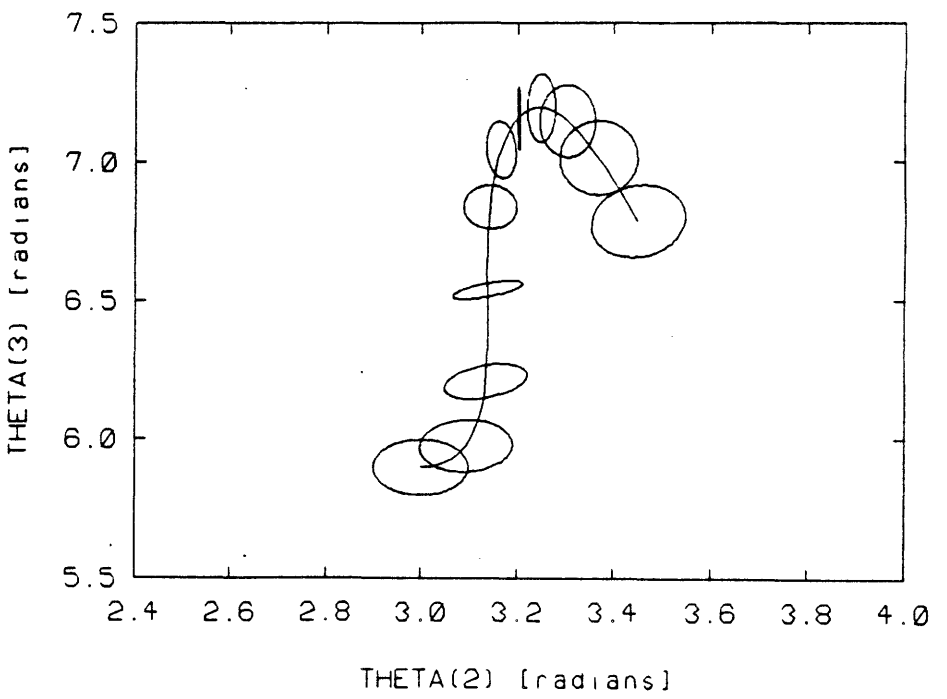

Figure 6-2: The propagation of an initial uncertainty in the joint - space

The aspect ratio of the ellipse's axes indicates the relative uncertainty in the value of the joint angles. If one of the axes shrinks down to zero, the uncertainty in the value of that angle diminishes, and the value of the angle converges to its nominal value. The significance of the relative uncertainty in the values of the two joint angles for the determination of the foot (or the tip of the multi-linkage system in the general case) is illustrated in Fig. 6-3

If the uncertainty in θ_3 is zero (Fig. 6-3a), the uncertainty in θ_2 translates into two circular arcs in the geometric space (for the knee and foot location). Both arcs are centered at the hip. If the uncertainty in θ_2 is zero (Fig. 6-3b), there is no uncertainty in the knee position, and the uncertainty in the foot position is a circular arc centered at the knee.

The orientation of the ellipses describes the directions along which the

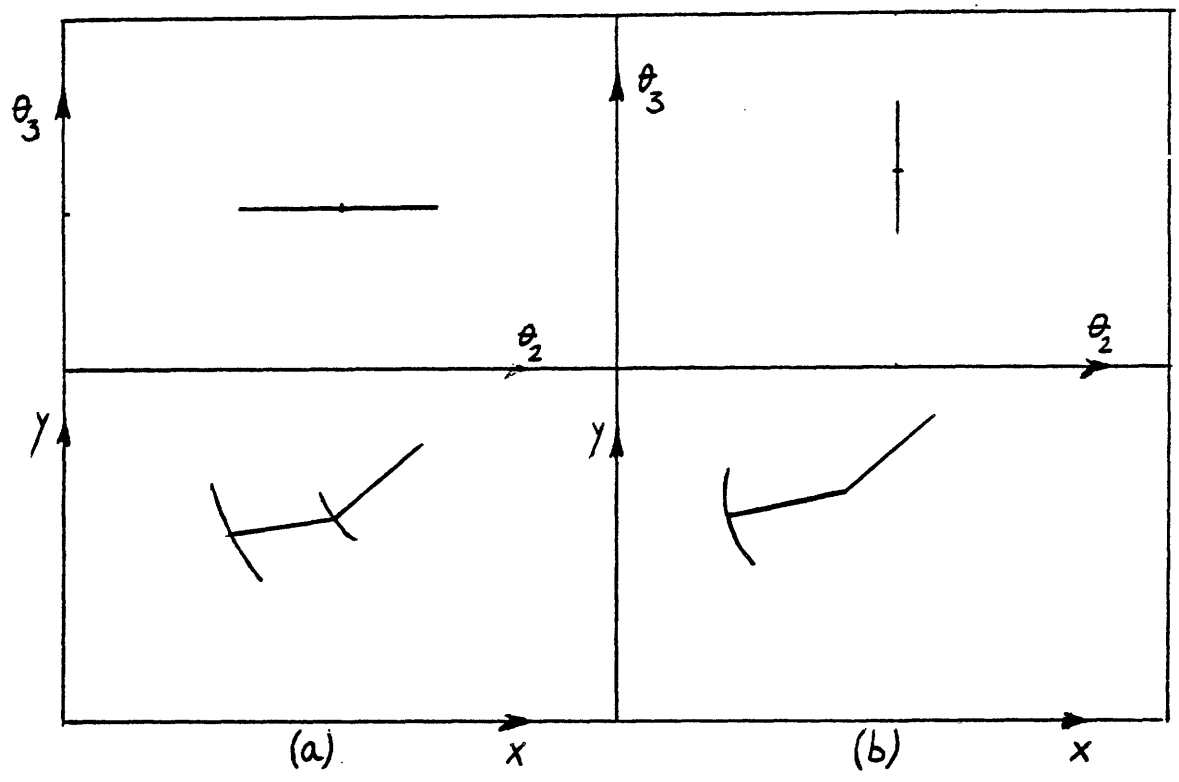

Figure 6-3: The geometric interpretation of line uncertainties

smallest and the largest uncertainties exist. Fig. 6-4 illustrates that point: the uncertainties in θ_2 and θ_3 are indicated by $\Delta\theta_2$ and $\Delta\theta_3$ respectively. As the ellipse's axes of symmetry are in the directions of ϕ_2 and ϕ_3 (the directions of the eigenvectors of the ellipse), the largest and the smallest uncertainties are in those directions, and they have the values of $\Delta\phi_2$ and $\Delta\phi_3$ respectively. The significance of this result in the geometric space is that the uncertainties in the positions of both the knee and the foot may be described by sections of curves (rather than bounded areas).

The size of the ellipses in the joint space is related to the overall sensitivity of the system. If the size of the ellipses decreases, that means that the uncertainty in the position goes down, and the system converges to the nominal position. An increase in the size of the ellipse means that the uncertainty grows, hence the

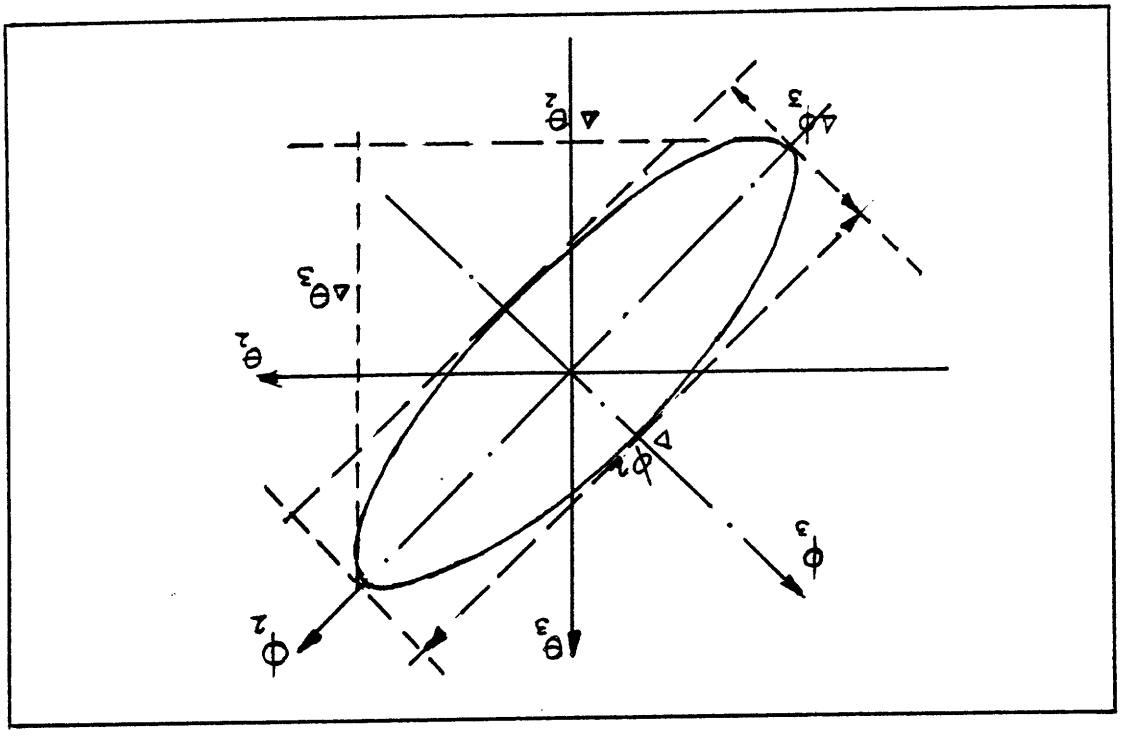

Figure 6-4: The uncertainties related to a rotated ellipse

system is more sensitive to disturbances.

6.3 The Effect of the Initial Conditions

One of the first applications of Set-Theoretic analysis to the study of the propagation of bounded disturbances in multi-linkage systems, was the study of a double pendulum. The pendulum is made of two links connected by a frictionless joint. The masses of the links are concentrated at the midpoints of the links, and the moments of inertia are assumed to be zero (i.e. the masses are point masses). Such a model enabled to study a relatively simple mechanical model, while keeping some of the inherent characteristics of a multi-link system.

The double pendulum is released from an initial state and is affected only by

the field of gravity (no actuator torques at the joints). The initial uncertainty is 0.1 radians in the values of the joint angles, and 0.01 rad/sec in the value of the angular velocities.

Figures 6-5 and 6-6 describe the propagation of the initial uncertainty in the joint space for two different initial positions. In Fig. 6-5 the 1^{st} link makes an angle of 8^0 with the vertical, and the 2^{nd} link makes an angle of 33^0 with the 1^{st} one. A simulation of 1 second shows that the size of the ellipses generally decreases while the orientation of the ellipses remains close to the original orientation. At some points along the trajectory, the ellipse collapses into a line.

Fig. 6-6 shows the propagation of the same initial ellipse from a different initial position. The 1^{st} link is initially at an angle of 36.7^0 with the vertical and the 2^{nd} link makes an angle of 60^0 with the first one. In this case the orientation of the ellipses' axes at any point along the trajectory are close to the directions of the tangent and the perpendicular to the tangent of the trajectory curve. The size of the ellipses decreases during the first part of the motion (as the knee accelerates) and increases later on.

Both figures show one ellipse which is substantially "thinner" than the other. The collapsed ellipses are located at the points where the angular velocity of one of the joints is zero. In Fig. 6-5 the collapsed ellipse occurs at t=0.6 sec.,the collapsed axis is θ_3 and the trajectory indicates that ω_2=0. In Fig. 6-6 the "collapse" occurs at t=1 sec., the collapsed axis is θ_2 and the trajectory indicates that ω_3=0.

A comparison between the two figures shows that case #1 (Fig. 6-5) which describes the smaller oscillations, is less sensitive to initial disturbances, yet the two cases do share some common properties. As a given degree of freedom comes

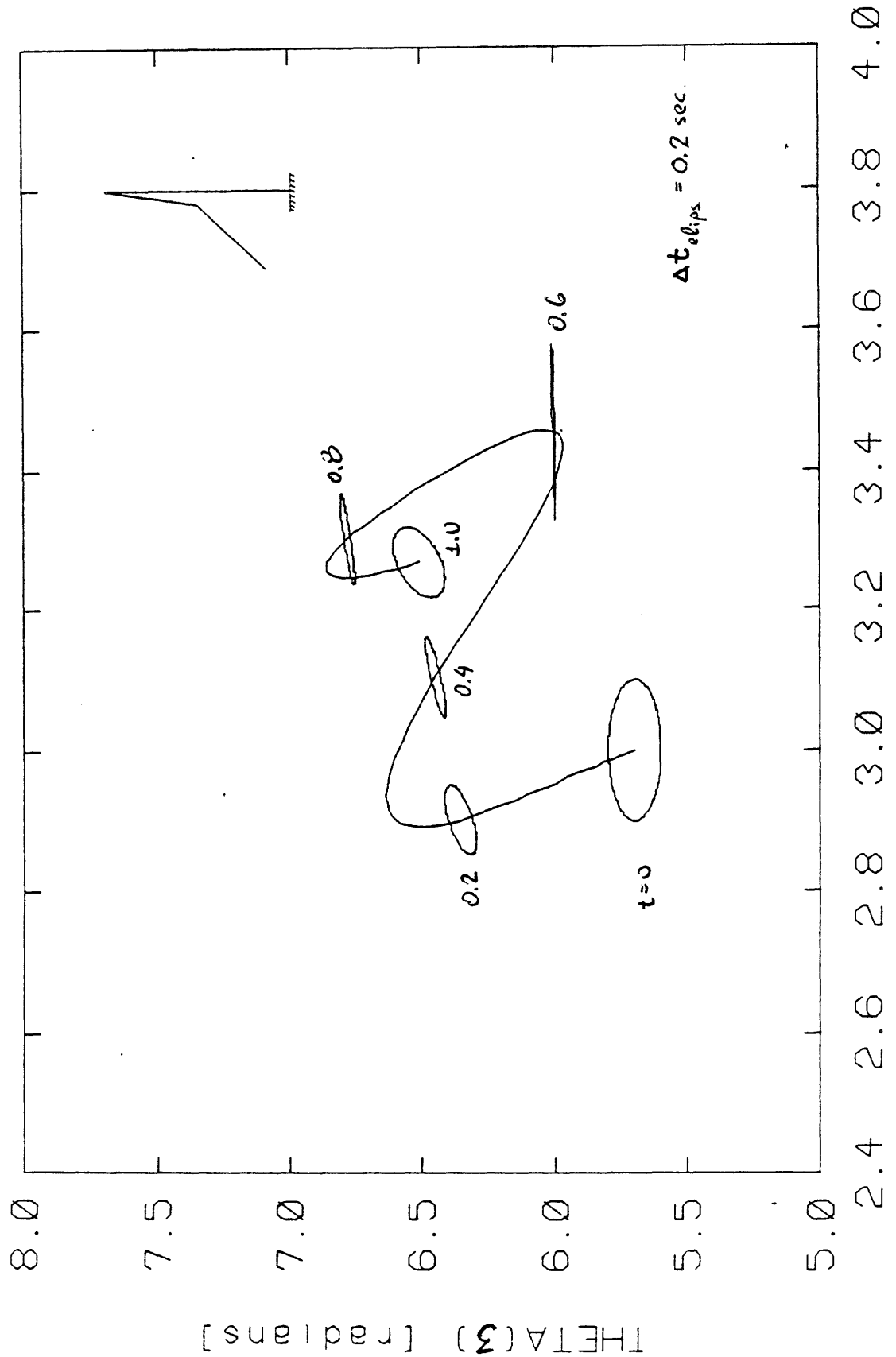

Figure 6-5: Propagation of the ellipses of uncertainty in small oscillations of a double pendulum

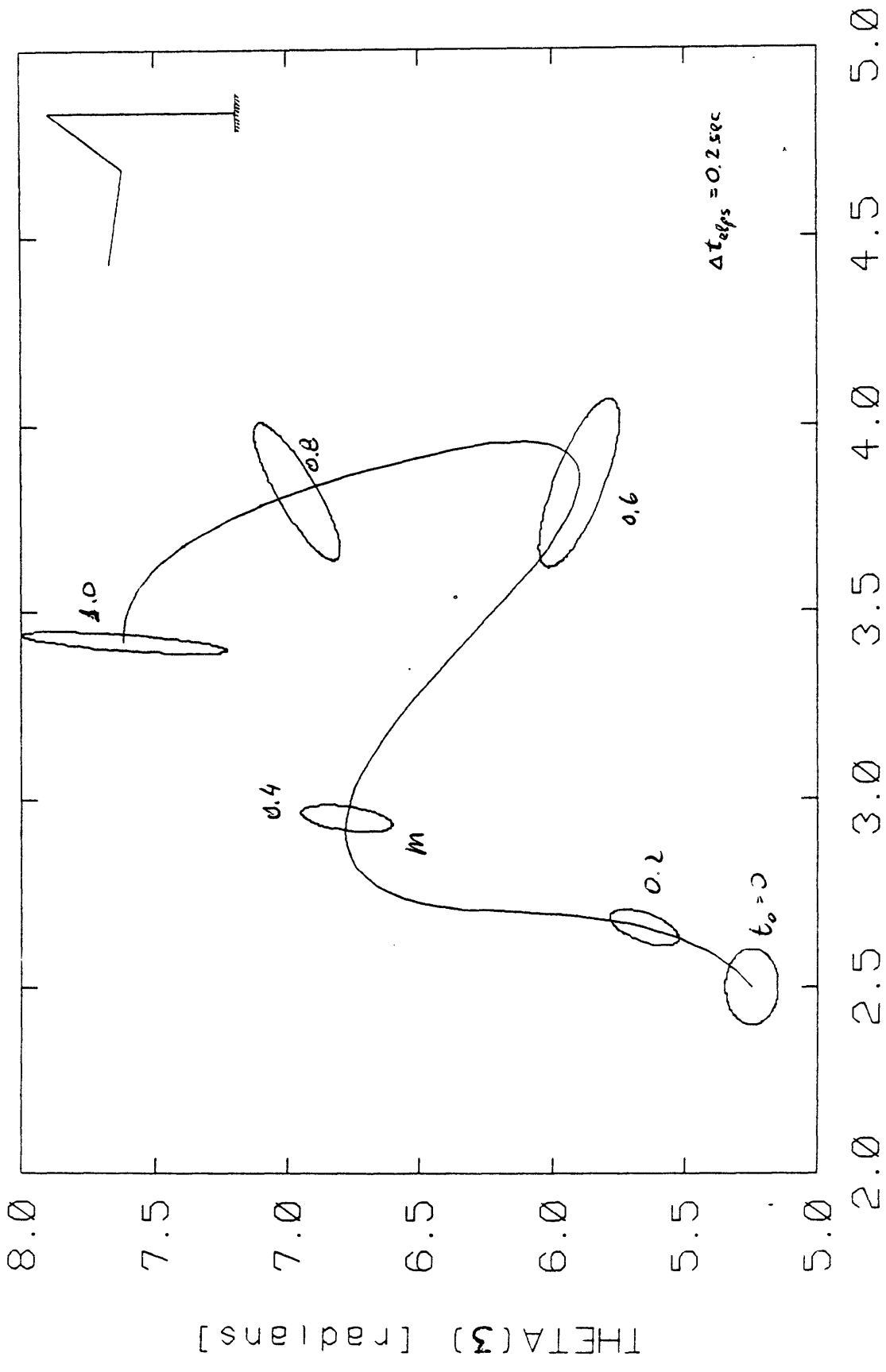

Figure 6-6: Propagation of the ellipses of uncertainty in large oscillations of a double pendulum

to a halt, the uncertainty in the corresponding position grows. This observation is demonstrated by the increase in $\Delta\theta_2$ when ω_2=0, and the increase in $\Delta\theta_3$ when ω_3=0. Using physical reasoning it can be shown that an energy conserving simple pendulum displays a similar behavior, namely: the position uncertainty will reach a maximum, at the point in time when the angular velocity reaches zero. It is quite surprising that the double pendulum presents basically the same behavior, as if this was a system of two uncoupled pendulums.

Figures 6-7 and 6-8 show the transformation of the ellipses from the joint space into the geometric space. Fig. 6-7 stresses the fact that the line uncertainties in the geometric space could come about not only by the collapse of the ellipses in the joint space, but by operating close to singularities as well (i.e. when the knee joint is close to full extension). Hence, the same ellipses in the joint space can transform into either bounded areas or finite line-curves depending on the location of the ellipse in the joint space. The closer the ellipse is to the singularity zone, the "thinner" it becomes.

The information from the joint and geometric spaces can be combined to show the relative contributions of each of the joint uncertainties. In case #1 (the small oscillations), the relative contribution of the knee uncertainty is small, hence the resulting foot uncertainty is generally centered around the hip. In case #2 (the large oscillations) the knee uncertainty contribution is much larger, hence the resulting uncertainty in the geometric space is centered more around the knee. The observation that in case #1 the uncertainty is generally less sensitive to the knee contribution is further exemplified in Figs. 6-9 and 6-10.

Fig. 6-9 describes the effect of reducing the hip position uncertainty by 50% (from 0.1 rad to 0.05 rad). The large axis of the ellipses of uncertainty is generally reduced by 50%. On the other hand reducing the knee position uncertainty by

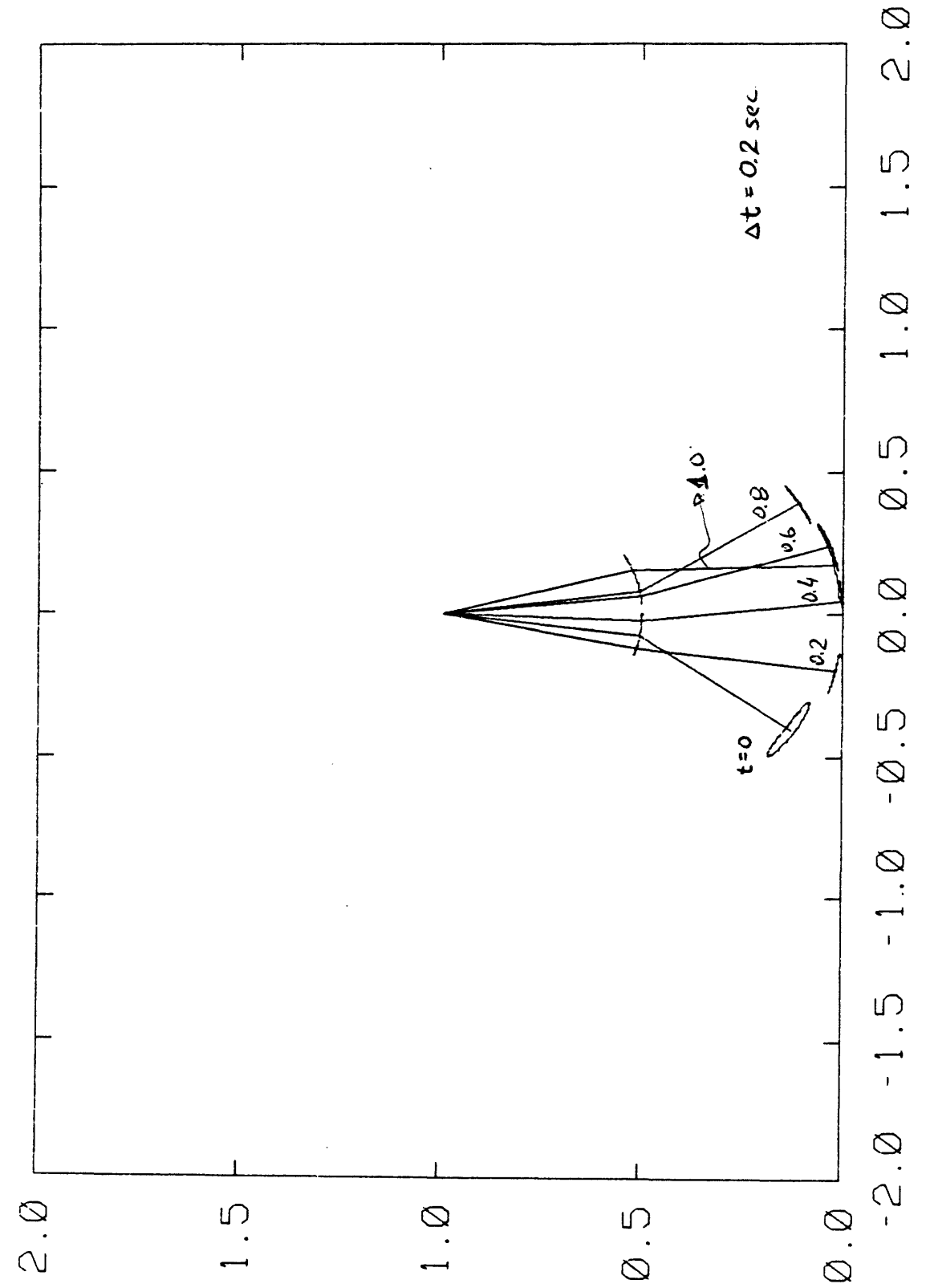

Figure 6-7: Propagation of the uncertainties in the geometric space for small oscillations of a double pendulum

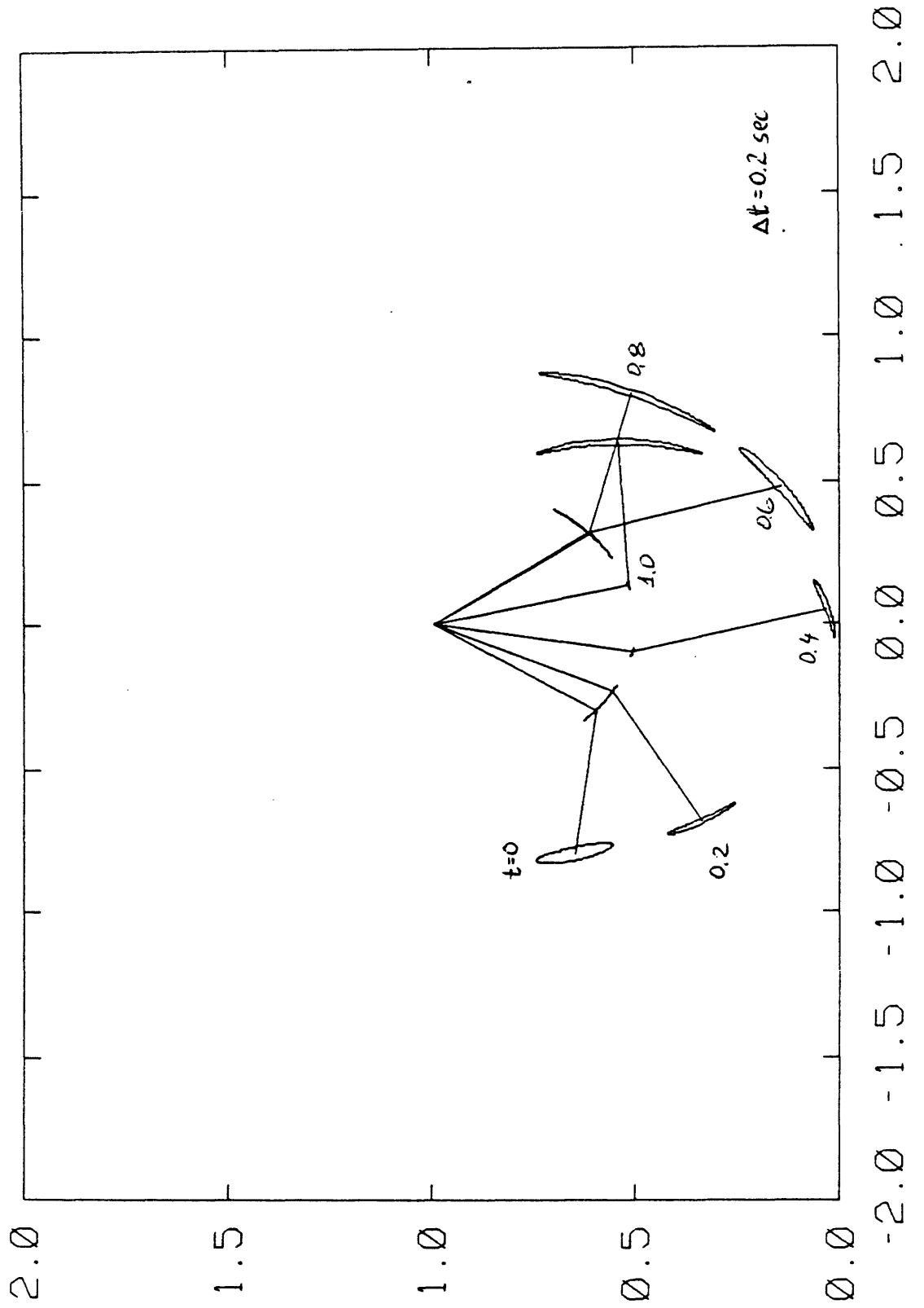

Figure 6-8: Propagation of the uncertainties in the geometric space for large oscillations of a double pendulum

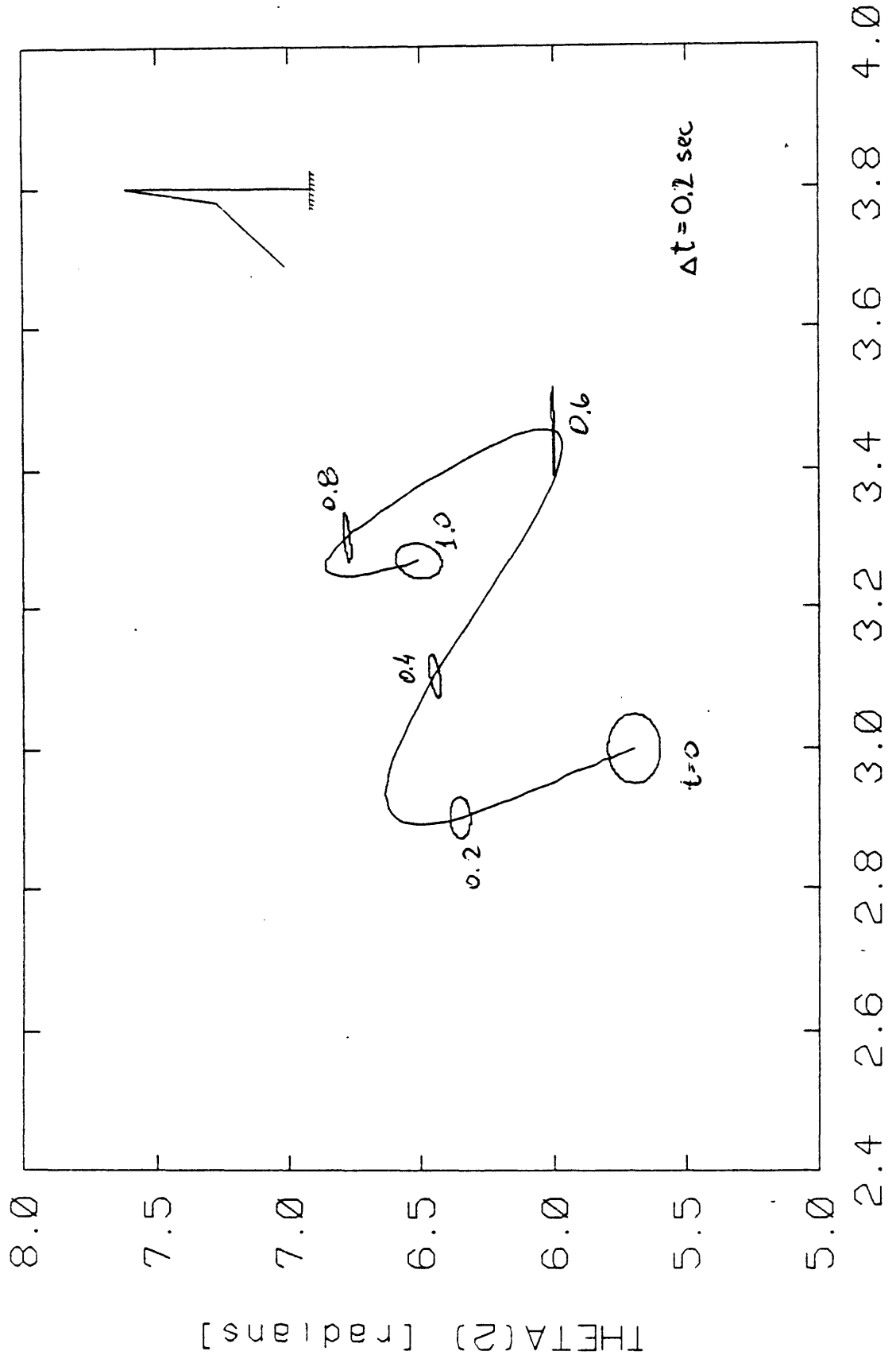

Figure 6-9: The effect of reducing the initial hip angle uncertainty on the propagation of the uncertainties in the joint space

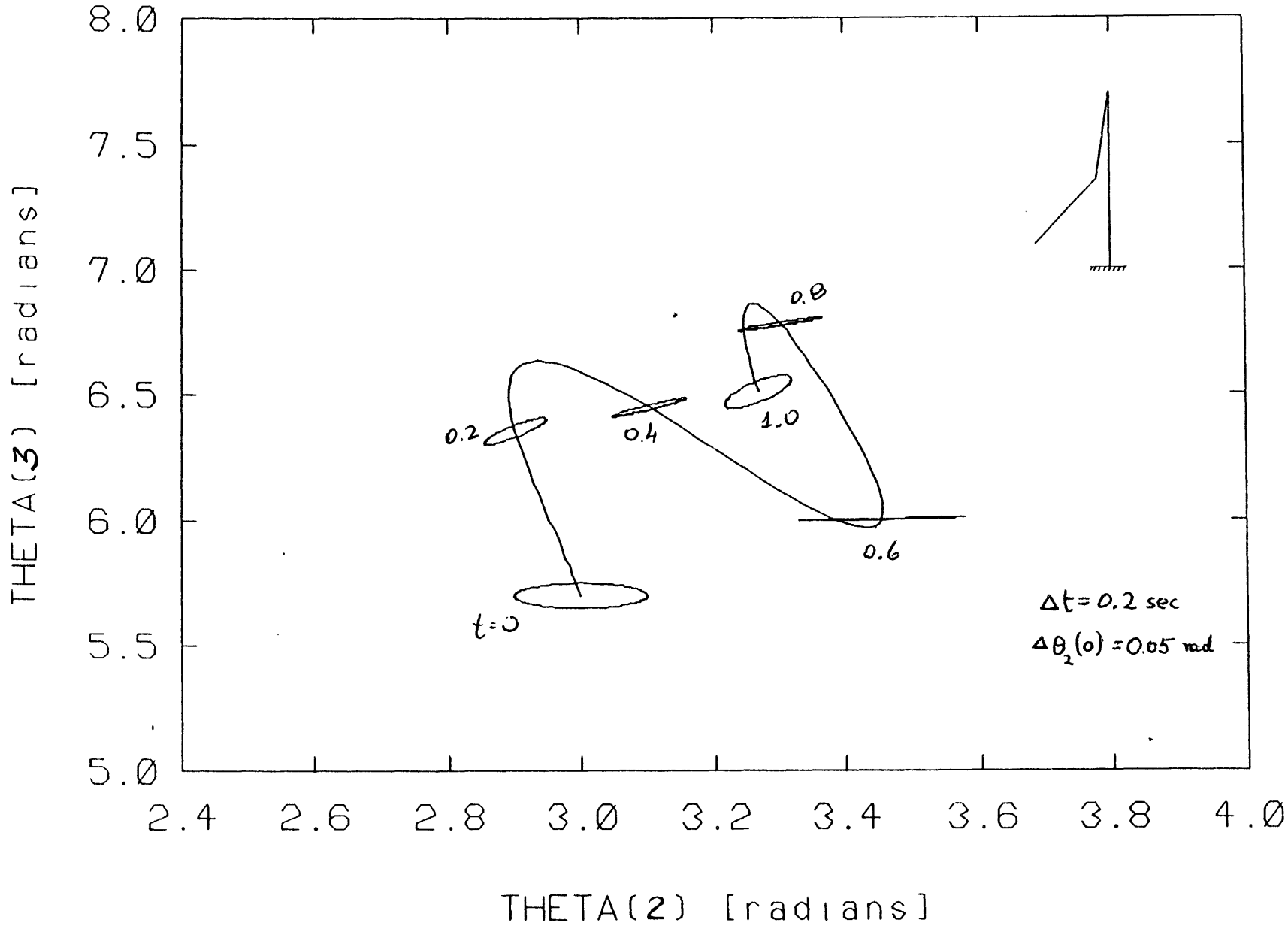

Figure 6-10: The effect of reducing the initial knee angle uncertainty on the propagation of the uncertainties in the joint space

50% while keeping the hip uncertainty constant has a very little effect on the total uncertainty.

The results described in this section are consistent with intuitive notions. The most important one is that small oscillations are less sensitive to disturbances than large oscillations. The physical explanation for that could be the energy changes of the system caused by small position disturbances. Those disturbances will involve smaller potential energy changes if they occur close to the equilibrium position of the double pendulum rather than farther away from that position.

6.4 The Effect of the Constant Torque Actuators

The effect of constant actuators on the propagation of discrete uncertainties, which are introduced at time t=0 is described in this section. The initial uncertainty in all the cases is the same: 0.1 radian on the angles and 0.01 rad/sec on the angular velocities. The sign assignment for the torques corresponds to the sign assignment for the angles.

6.4.1 Small oscillations

The propagation of the initial uncertainties for small oscillations of the double pendulum under different combinations of hip and knee torques, is described in Figs. 6-11 and 6-12. The 1^{st} link initially makes an angle of 8^0 with the vertical, and the 2^{nd} link makes an angle of 33^0 with the 1^{st} one. The initial angular velocities are zero.

Fig. 6-11 describes the trajectory and the propagation of the initial uncertainty under two positive torques: +10 Nt-m at the hip and +1 Nt-m at the

knee. The ellipses are well behaved, and the size changes are relatively small. Notice that the ellipses tend to flatten out near the points where one of the links comes to rest.

Fig. 6-12 describes the trajectory and the disturbance propagation from the same initial conditions, under the effect of two negative torques: -10 Nt-m at the hip and -1 Nt-m at the knee. The ellipses decrease in size during the first swing of the bottom link . They grow substantially after the bottom link comes to a stop and reverses direction. With each cycle the variations in the size of the ellipses tend to grow, which indicates that this is a divergent process.

Figs. 6-13 and 6-14 show the propagation of the uncertainties in the geometric space (for the two cases described above). Fig. 6-13 illustrates two major points:

1. the smaller uncertainties indicate a smaller sensitivity to disturbances
2. as the joint torques cause oscillations which are closer to the static equilibrium (and singular) position, the uncertainties tend to describe portions of arcs, rather than bounded areas.

Fig. 6-14 illustrates the geometric significance of the larger ellipses. The uncertainties are much larger, and the relative contribution of the knee is also larger (as demonstrated by the knee being the center for the geometric shapes describing the foot uncertainties). It is interesting to note that the smallest uncertainty is obtained at the point where the knee and the hip change directions of oscillation.

Fig. 6-15 describes the propagation of the initial uncertainty for a different set of initial conditions. The 1^{st} link is initially at an angle of 36.7^0 with the vertical and the 2^{nd} link makes an angle of 60^0 with the first one. The initial

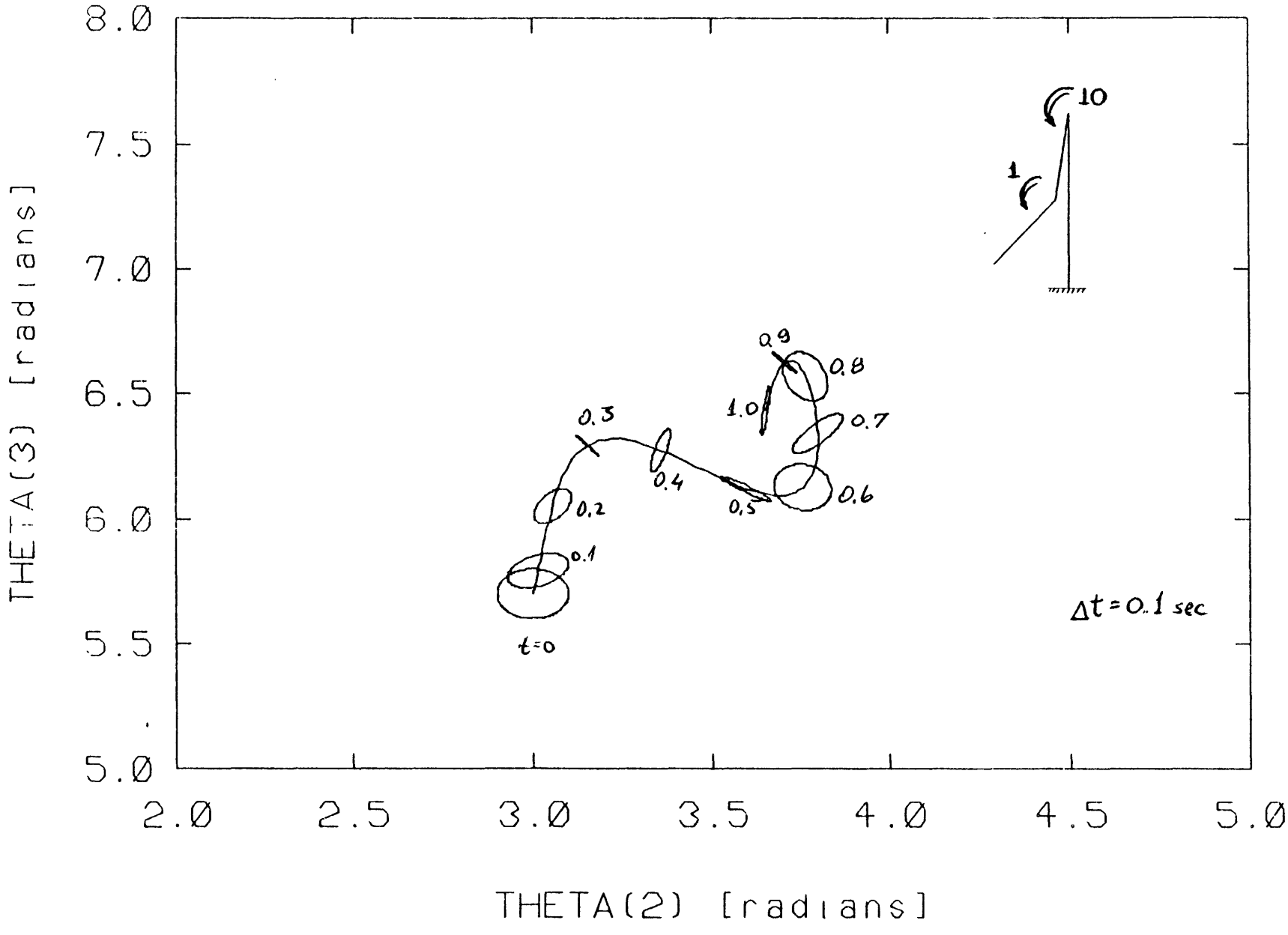

Figure 6-11: Propagation of the ellipses of uncertainty in small oscillations of a double pendulum, under positive actators

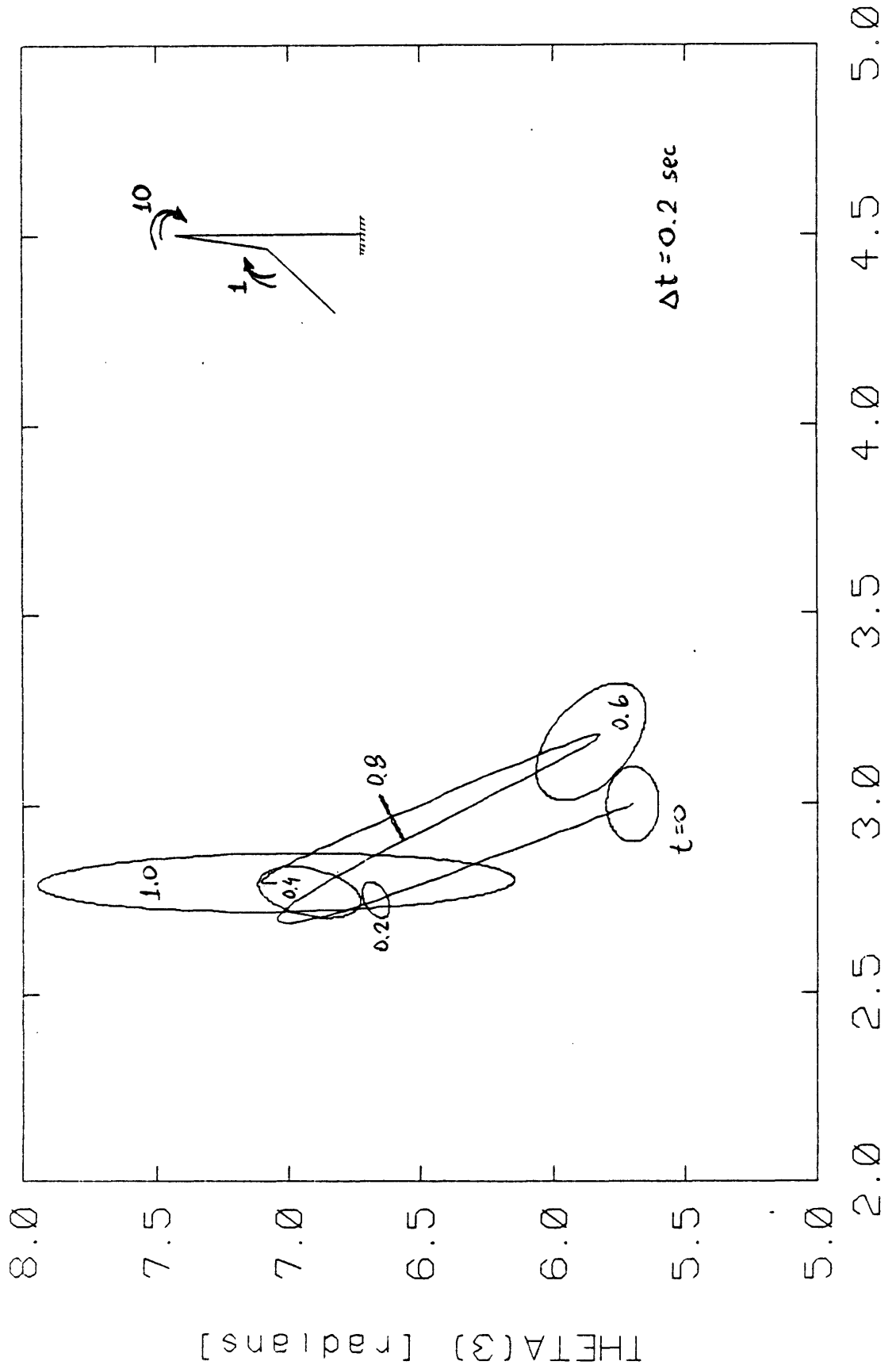

Figure 6-12: Propagation of the ellipses of uncertainty in small oscillations of a double pendulum, under negative actuators

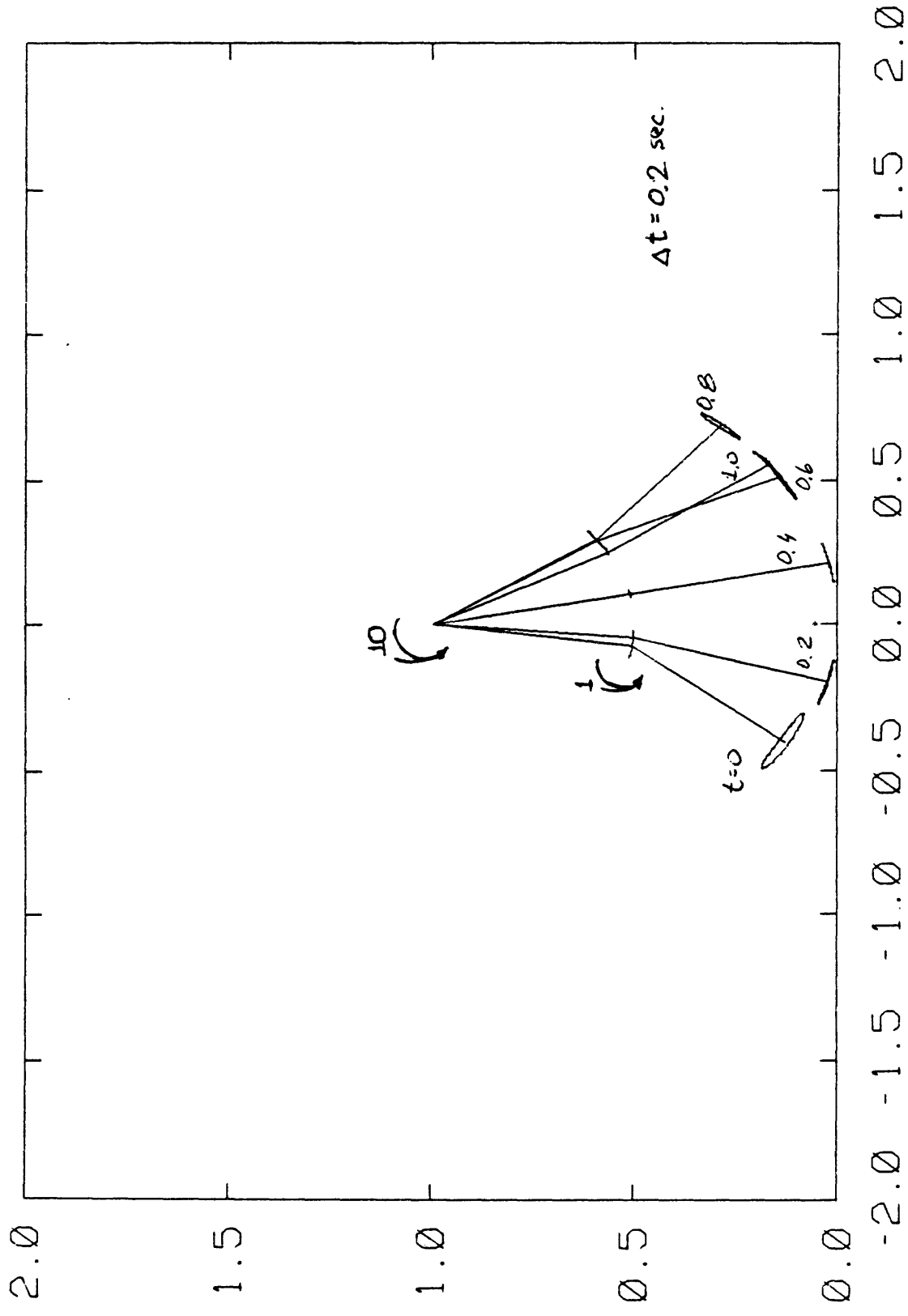

Figure 6-13: Propagation of the uncertainty in small oscillations of a double pendulum, under positive actuators

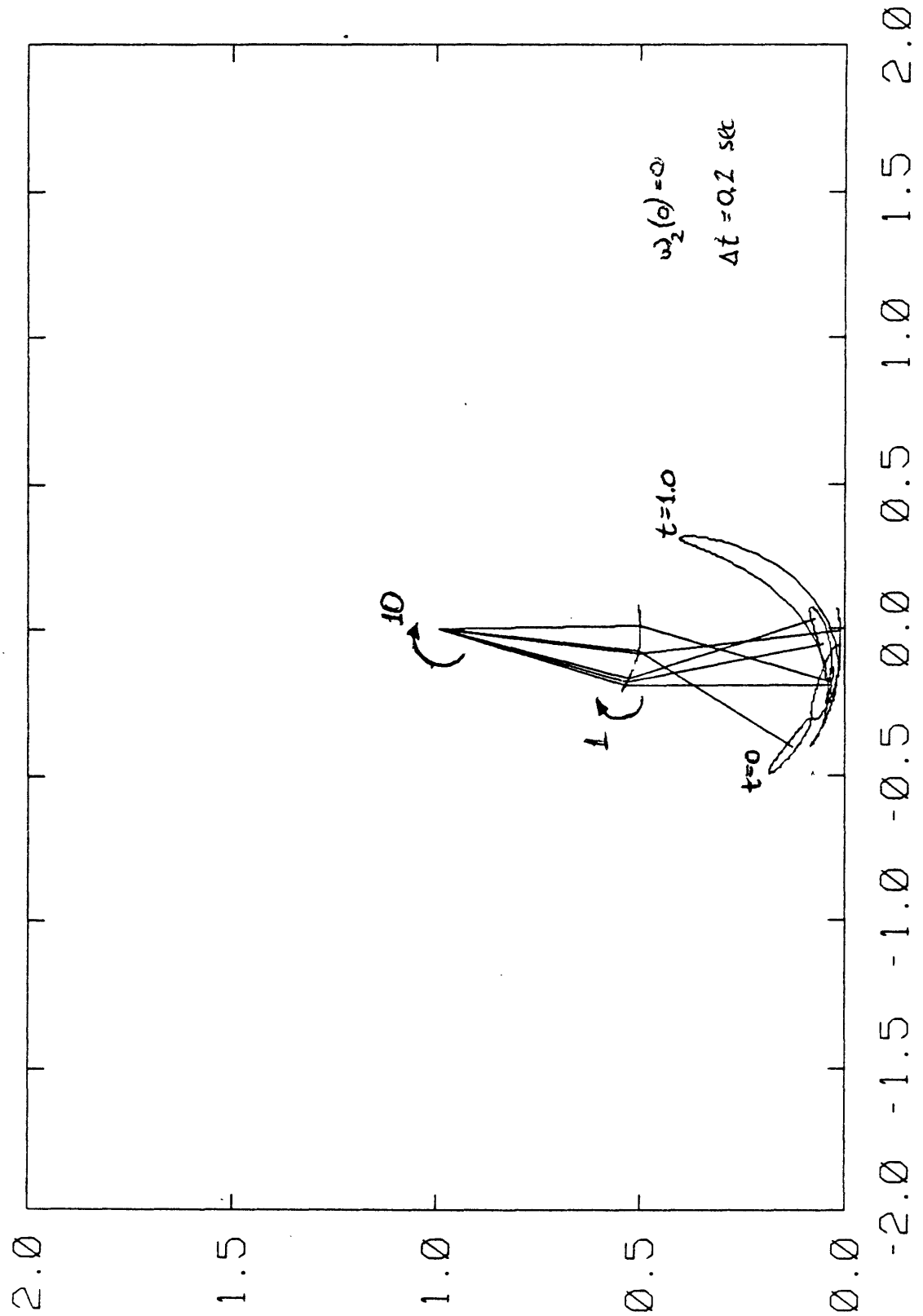

Figure 6-14: Propagation of the uncertainty in small oscillations of a double pendulum, under negative actuators

angular velocities are zero. The hip and knee torques are constant and have the following values: +10 Nt-m at the hip and +1 Nt-m at the knee. Again for this case, as for the case described in Fig. 6-11, the ellipses are well behaved with small changes in the overall size. As the ellipses become thinner and thinner, the uncertainty in the joint space will translate into uncertainties in the geometric domain, which lie along short segments of curves, rather than bounded inside closed areas. This too suggests a smaller sensitivity.

Fig. 6-16 describes the trajectory and the propagation of the initial set of uncertainties for the same initial conditions, but with negative (rather than positive) torques at the joints. The hip torque is now -10 Nt-m and the knee torque is -1 Nt-m. It is clear that the uncertainties are much larger now, but it is interesting to note that the orientation of the ellipses with respect to the trajectory curve is similar to the previous case. The larger ellipses indicate the increased sensitivity to disturbances.

Figs. 6-17 and 6-18 show the propagation of the uncertainties in the geometric space. The figures clearly illustrate the larger sensitivity of the trajectory resulting from negative torques. Fig. 6-17 also points out that:

1. the uncertainties in the foot location become pieces of arcs which are not centered at the knee

2. the smallest uncertainty in the positions of both the knee and the hip is obtained when the knee comes to a stop.

Fig. 6-18 illustrates the geometric significance of the larger ellipses, and also points out the increased contribution of the knee uncertainty, as the centers of the foot uncertainties are much closer to the knee.

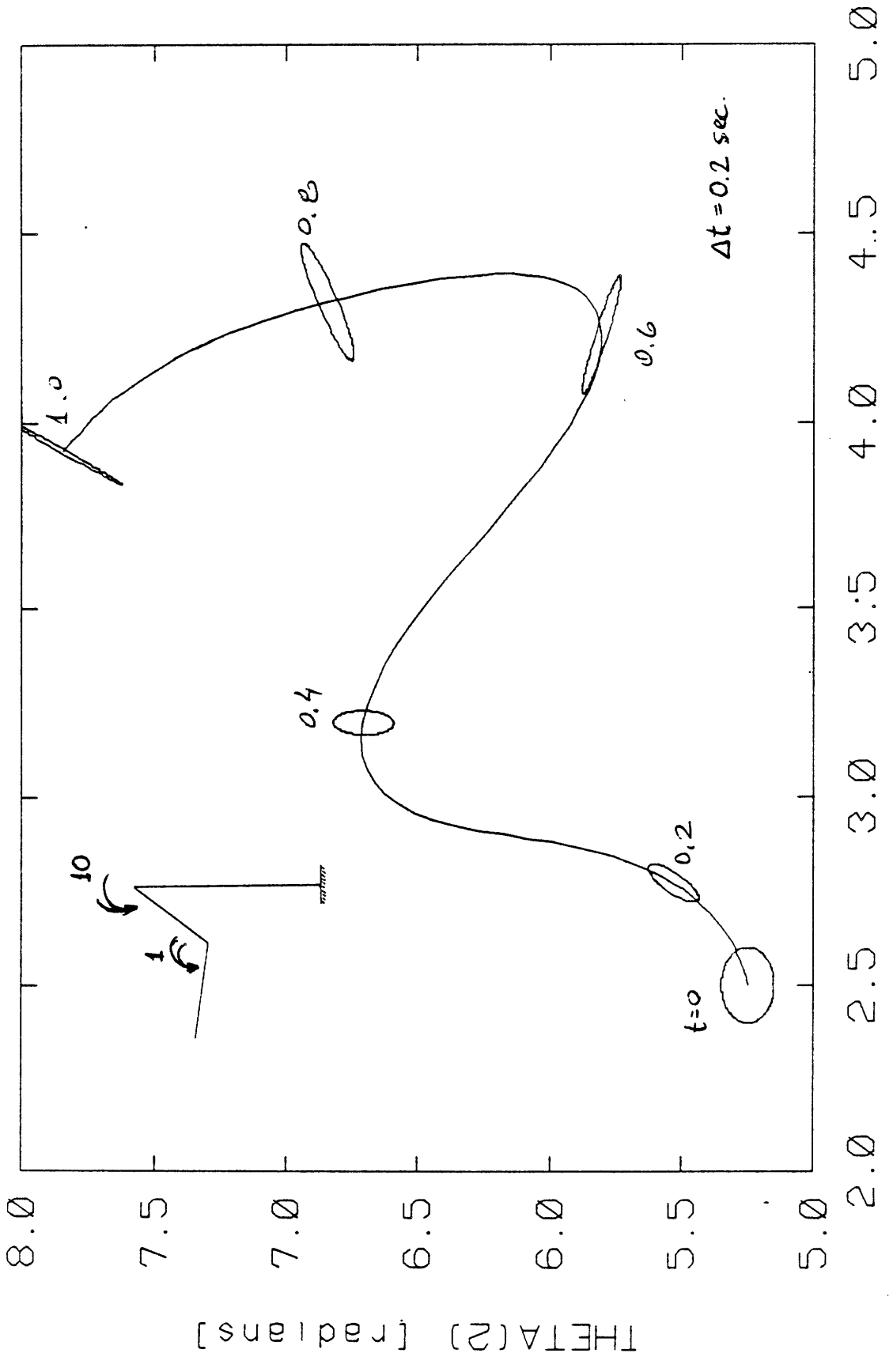

Figure 6-15: Propagation of the ellipses of uncertainty in large oscillations of a double pendulum, under positive actuators

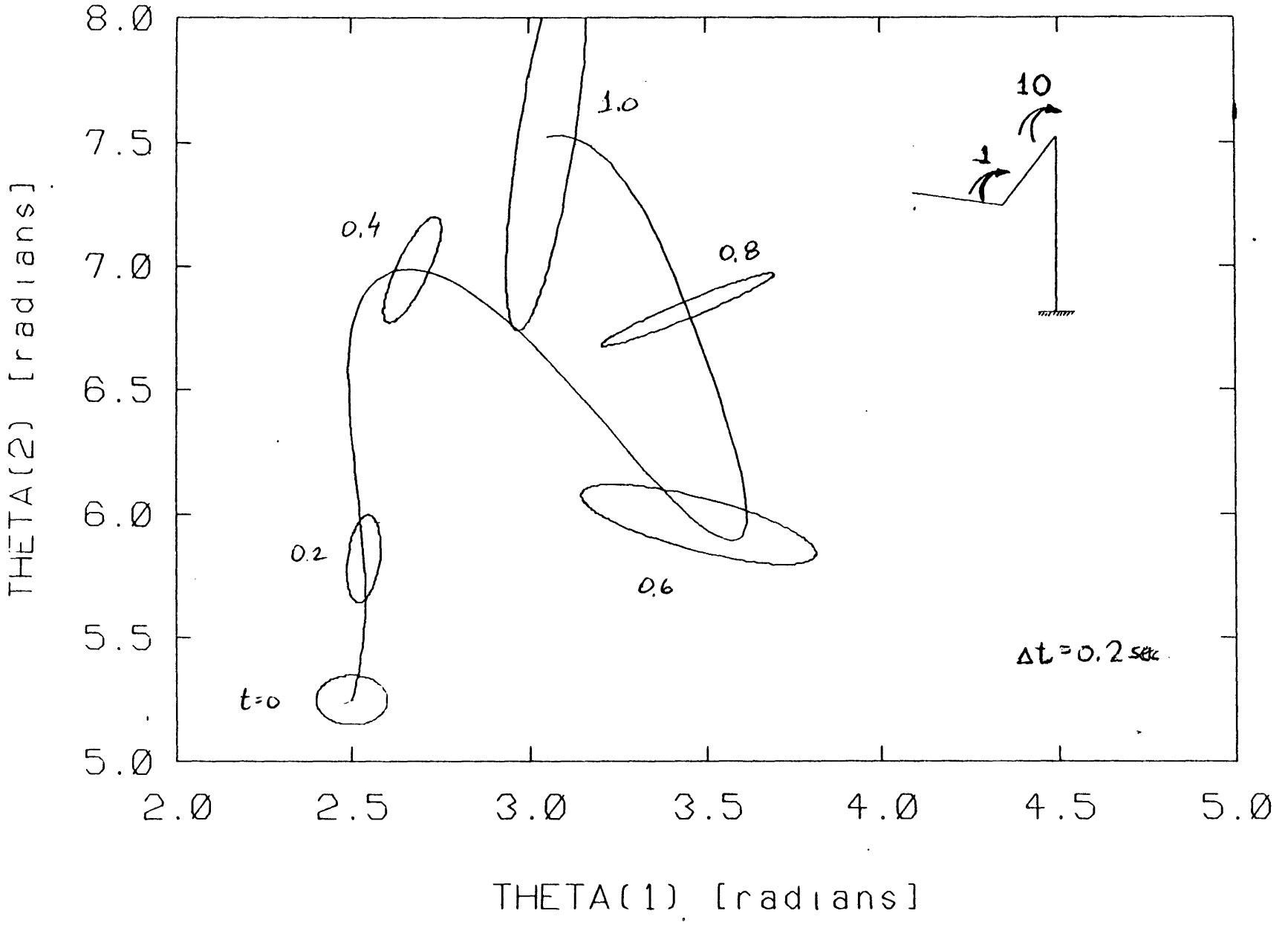

Figure 6-16: Propagation of the ellipses of uncertainty in large oscillations of a double pendulum, under negative actuators

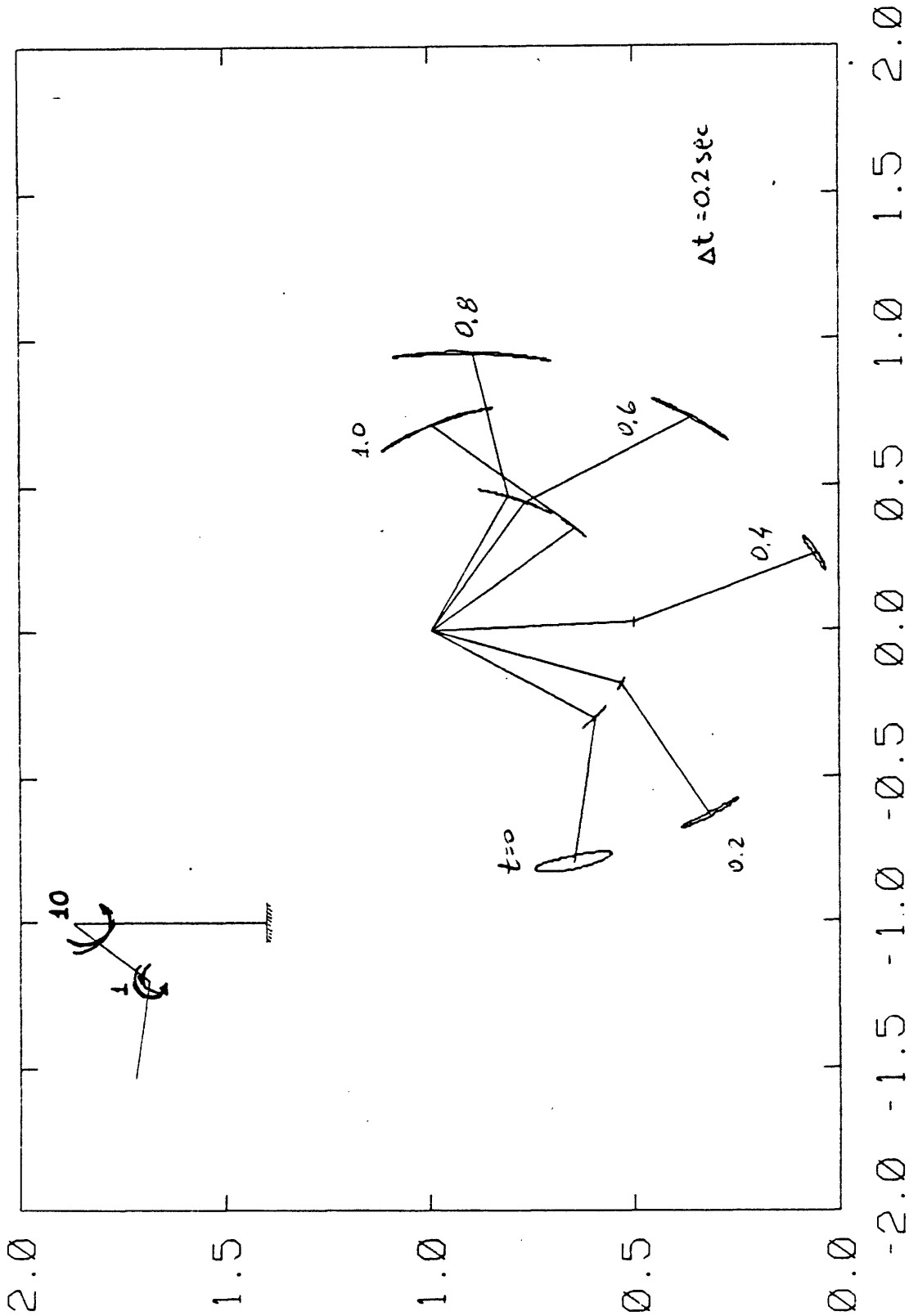

Figure 6-17: Propagation of the uncertainty in large oscillations of a double pendulum, under positive actuators

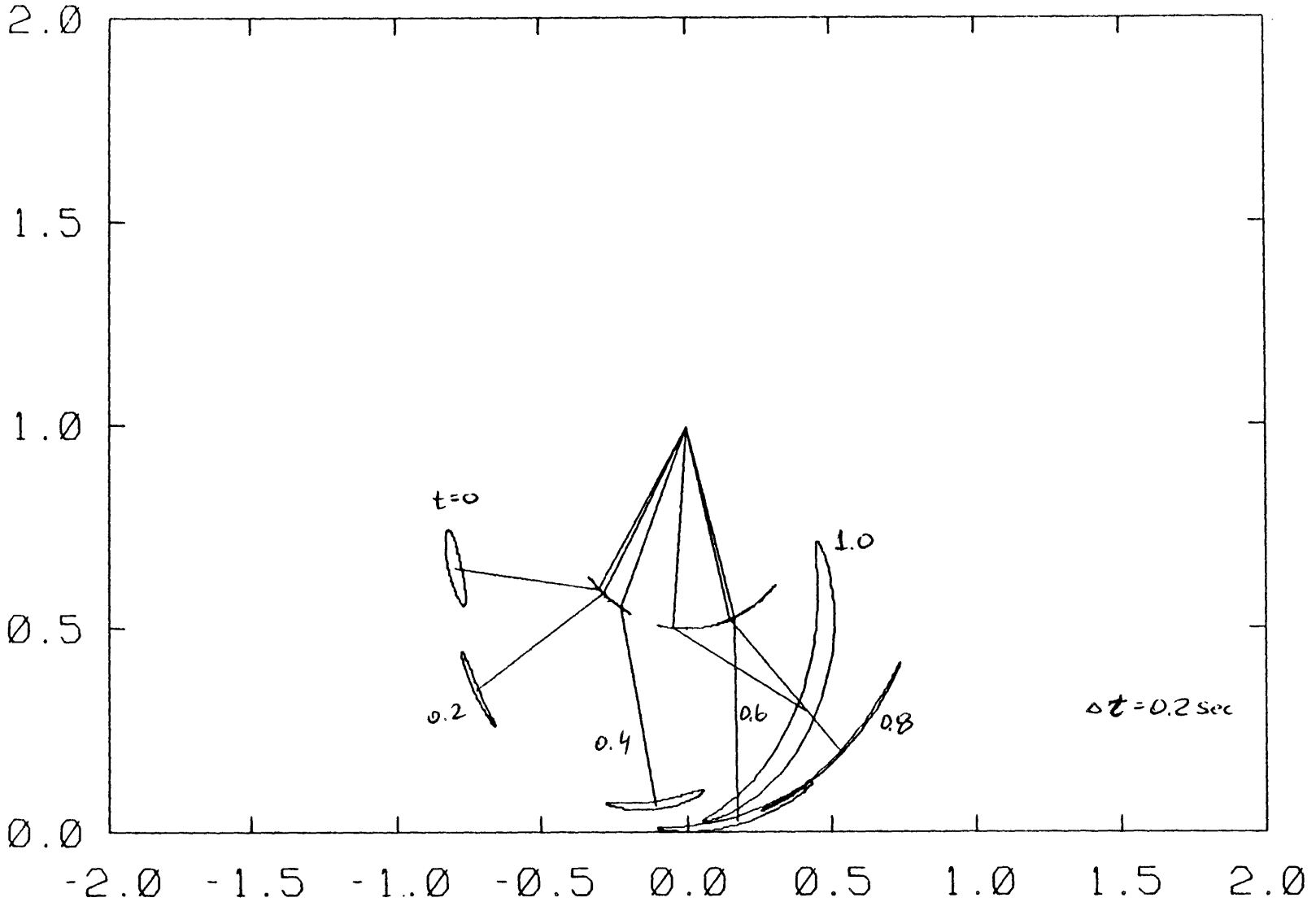

Figure 6-18: Propagation of the uncertainty in large oscillations of a double pendulum, under negative actuators

6.5 The Effect of Continuous Knee Actuator Noise

One of the appealing aspects of Set-Theoretic involves its ability to handle continuous as well as discrete input noise (the proper equations were described in Chapter 5). The major task in such an application is to find a proper value (or a time sequence of values), for the free parameter $\beta(t)$. Recall that $\beta(t)$ is the parameter which specifies (indirectly) the size of the ellipsoids in the equation for the time propagation of the uncertainties in a system subjected to continuous noise (see Chapter 5). Two cases were analyzed: input noise in the knee actuator, and in the hip actuator. In both cases the sensitivity of the ellipses to the value of β was examined.

Fig. 6-19 describes the effect of four different values of β on the propagation of the ellipses, resulting from a continuous noise at the knee. The four cases in that figure were obtained by changing the value of β (β=0.01,0.1,1.0,10.0) for a fixed value of Q (Q=1). From the figure it is clear that β=0.01,10 result in a large overestimation of the size of the ellipses (recall from Chapter 3 that small values of β tend to amplify the effect of the input noise, while large values tend to make the system unstable). The optimal value from this graph is β=1.

Fig. 6-20 describes a similar sequence for the case Q=0.01. This corresponds to a reduction of the maximum noise amplitude (which is equal to the square root of Q) by an order of magnitude, relative to the previous case. The figure shows generally a similar dependence on the value of β. The ellipses are very large for β=0.01, are smallest for the range of values between 0.1 and 1.0, and increases again for β=10 (even though the increase is not as dramatic as before).

It is also interesting to note, that the ellipses converge to those plotted in Fig. 6-15, which described the propagation of initial uncertainties in an undisturbed

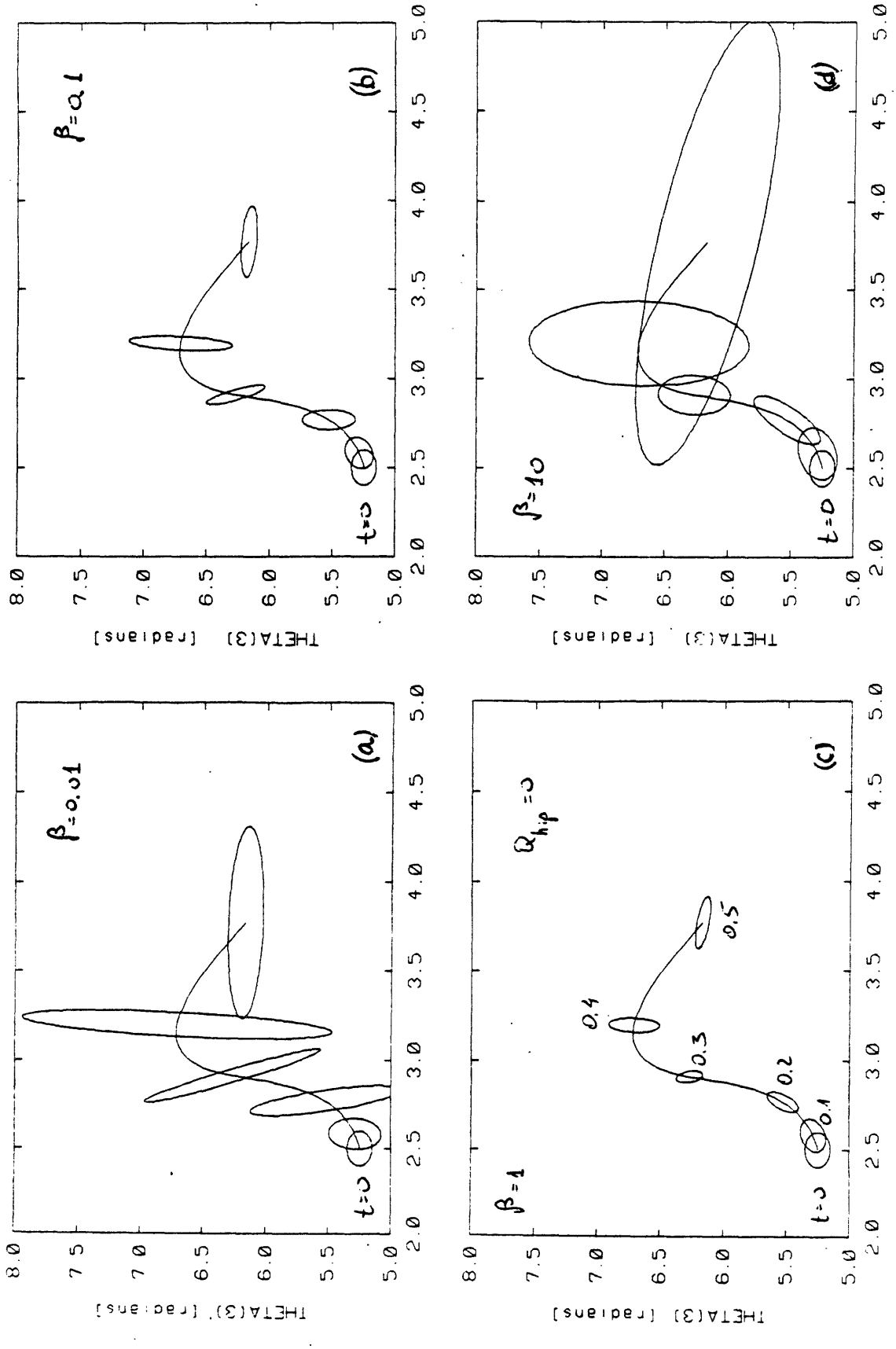

Figure 6-19: The effect of the free parameter $\beta(t)$ (Q=1.0)

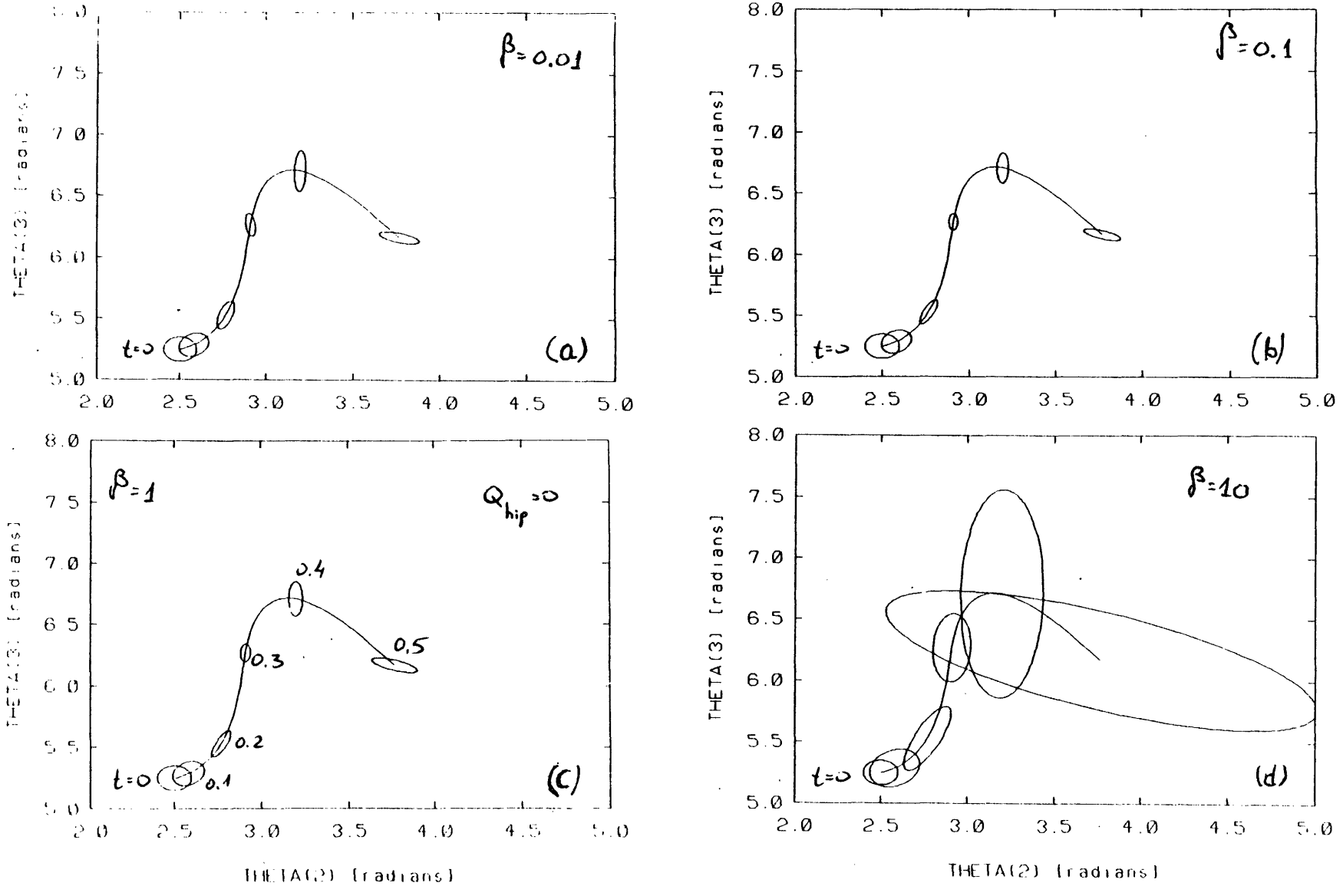

Figure 6-20: The effect of the free parameter $\beta(t)$ (Q=0.01)

system. This result exemplifies the numerical stability of the Set-Theoretic approach for analyzing the effects of noise in such systems.

Figs. 6-21 - 6-22 describe a similar sequance for continuous hip noise. The results show that in this case too, there is a strong dependence on β. β=0.1 seems to be the optimum for both the continuous knee noise, and the continuous hip noise. Notice, that for the hip noise too, the ellipses converge to the undisturbed results (Fig. 6-15). The increased effect of the hip noise (compared to the knee effect) is demonstrated by the increased projections of the ellipses' on the θ_2 axis.

6.6 Summary

This chapter illustrated the application of Set-Theoretic to the analysis of multi-linkage systems. It demonstrated the analytical and numerical techniques that can be used to verify the derivation of the equations.

The propagation of uncertainties in such a system with and without continuous noise sources has been examined on a double pendulum system. The results show that small amplitude oscillations are less sensitive to initial position errors (or uncertainties). The direction of the joint torques generated by the actuators is also of importance, and actuators that tend to counteract the effect of gravity (especially right after the release of the pendulum) tend to increase the sensitivity.

The effect of continuous noise on the position uncertainty was studied and the strong effect of the free parameter β has been demonstrated. The results also suggest that a constant value of β could be chosen, at least for the range of actuators examined. The convergence of the results obtained for very low noise level to the earlier results (where no noise was assumed) exemplify the numerical

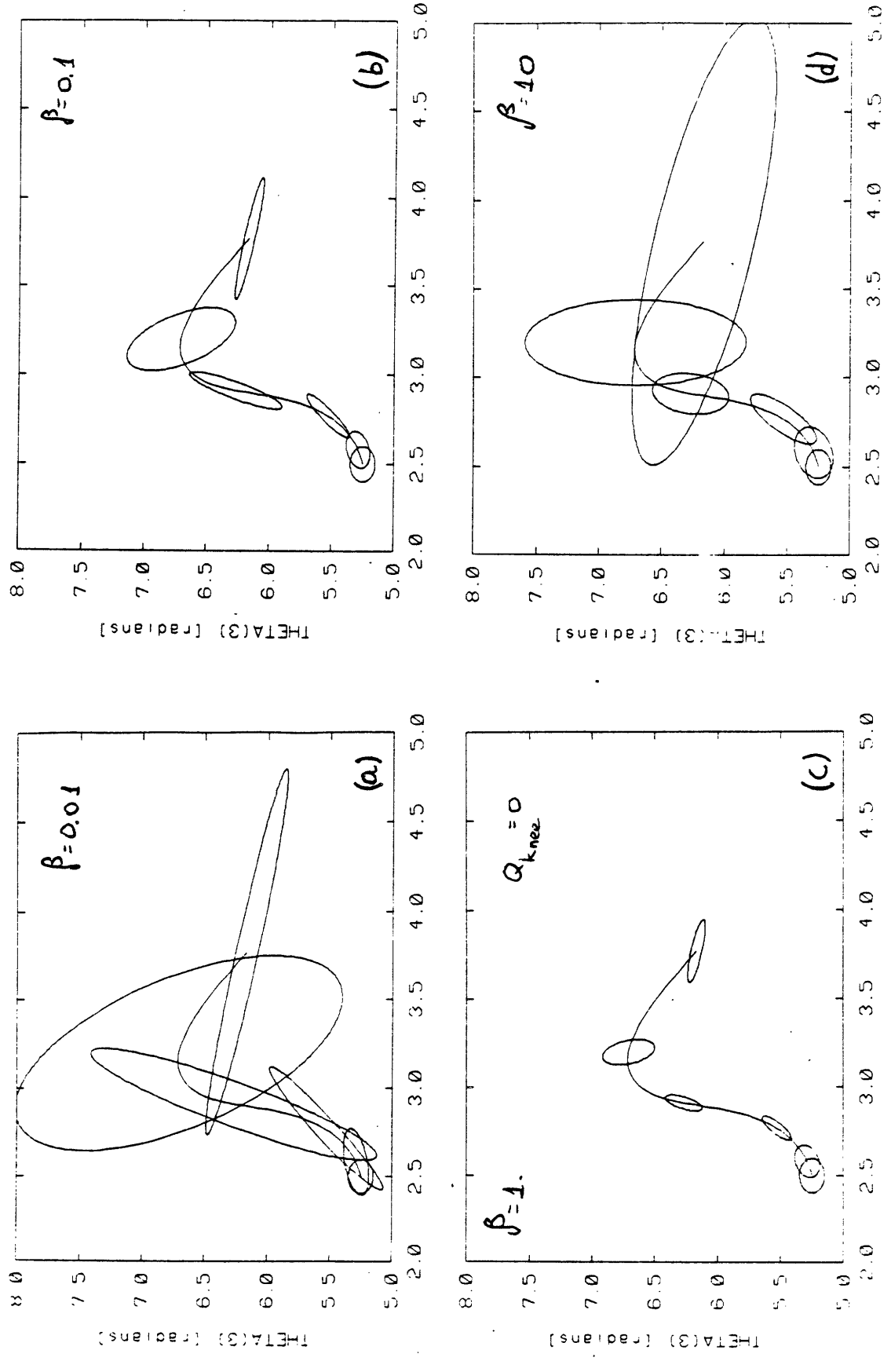

Figure 6-21: The effect of the free parameter $\beta(t)$ (Q=1.0)

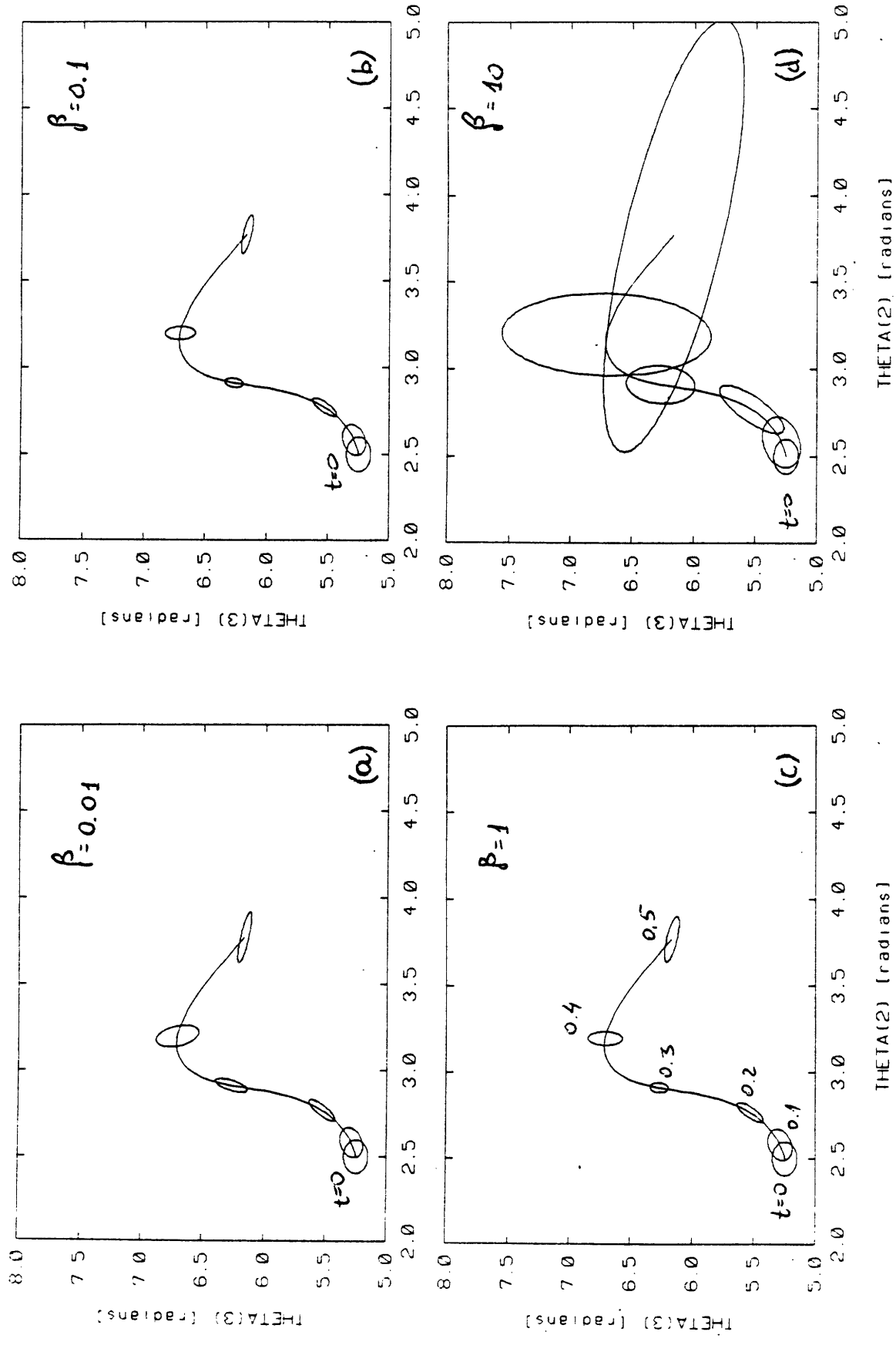

Figure 6-22: The effect of the free parameter $\beta(t)$ (Q=0.01)

stability of the technique.

The next chapter introduces a three-link model of gait, and examines the application of Set-Theoretic analysis to the study of the sensitivity of gait model to disturbances.

Chapter 7
The Application of Set-Theoretic Analysis to Gait Models

7.1 The Sensitivity of Gait Models to Disturbances

The basic question that will be addressed in this section is how does a set of position and velocity disturbances propagate through a given gait model. The model to be analyzed is a simple, three link, frictionless, planar model, described in Fig. 3-1. The leg in stance makes up the first link, the swinging thigh makes the second link, and the swinging shank makes the third link.

The first link moves with a prescribed kinematics. This amounts to the assumption that due to the mass difference between the whole body, whose mass is assumed to be concentrated at the hip, and the swinging leg, the kinematics of the leg in stance is practically unaffected by the dynamics of the swinging leg. Two ideal constant torque actuators are available - at the hip and at the knee. The mass of each link is concentrated at the midpoint of the link, and the moments of inertia are assumed to be zero. The results in this chapter will describe the time propagation of an initial uncertainty (or in other words - the time propagation of an initial set of possible disturbances), under the effect of fixed joint torques.

The results will be described in two planes:

1. joint space

2. geometric space

Recall that the joint space is a space whose coordinates are the joint angles; in this case it is a plane whose coordinates are the two degrees of freedom - $[\theta_2, \theta_3]$. The geometric space is the physical 3D space. As a planar model is discussed in this work, it is made up of the [x, y] coordinates:

- x - longitudinal coordinate (the direction of motion) y - the vertical coordinate

Note that the model does not have hyperextension stops, hence - there is nothing (other than joint torques) to prevent the knee from hyperextension (recall that the "biper" - the mechanical walking biped described in chapter 2 performed the whole gait cycle with hyperextended knees).

Each point in the joint space describes a unique geometric configuration of the swinging thigh and shank with respect to the leg in stance. Hence, it is always possible to transform a point in the joint space into the geometric space (provided that the stance leg position is known)[4].

The mathematical solution of Set-Theoretic analysis enables the examination of the propagation of initial uncertainties in the joint space. Fig. 7-1 describes the trajectory of the swinging leg in the joint space, and the propagation of an initial position uncertainty. Fig. 7-2 is the corresponding geometric space representation. The initial position of the stance leg is indicated by the dashed line. It performs a rotation at constant angular velocity around the its fixed foot position. The geometric coordinates of the fixed foot position are [0; 0]. The constant angular velocity is 1 rad/sec. The initial angular velocity of the swinging thigh is 2.4

---

[4]the opposite is not true, and knowledge of the geometric foot location is not enough to uniquely describe the knee position

rad/sec and that of the shank is 0 (these values were chosen based on the values given in [30]). The initial uncertainty in the angular positions is 0.1 rad/sec (about 5^0), and the initial uncertainty in the angular velocities is 0.01 rad/sec. The ellipses are plotted every 0.05 sec. The stick figures are plotted every 0.1 sec.

The significance of the ellipses in the joint-space is that points which started out inside the initial ellipse, will propagate through the following ellipses as time progresses. It is interesting to note how the size of the ellipses shrinks to a minimum, which occurs near the point where the knee angle reaches a maximum value (at the end of the knee extension phase). As the knee starts to flex - the uncertainty begins to grow.

Fig. 7-2 describes the transformation of the trajectory and the uncertainties from the joint-space into the geometric-space. As there is no uncertainty in the hip position, the knee uncertainties will always be parts of a circular arc centered at the hip. The foot uncertainty has a more complex geometric form, as it depends both on the knee and the hip uncertainties (due to the geometric connectivity constraint of the thigh and the shank).

Two interesting observations can be made:

1. a curve in the joint-space transforms into a curve in the geometric space

2. an ellipse in the joint space can collapse to a curve in the geometric space

The first observation is simply based on the realization that there exists a point to point mapping from the joint-space into the geometric space. Hence, a series of points (which form a curve) in the joint-space will map into a curve in the geometric space. A second observation comes from looking at the way certain

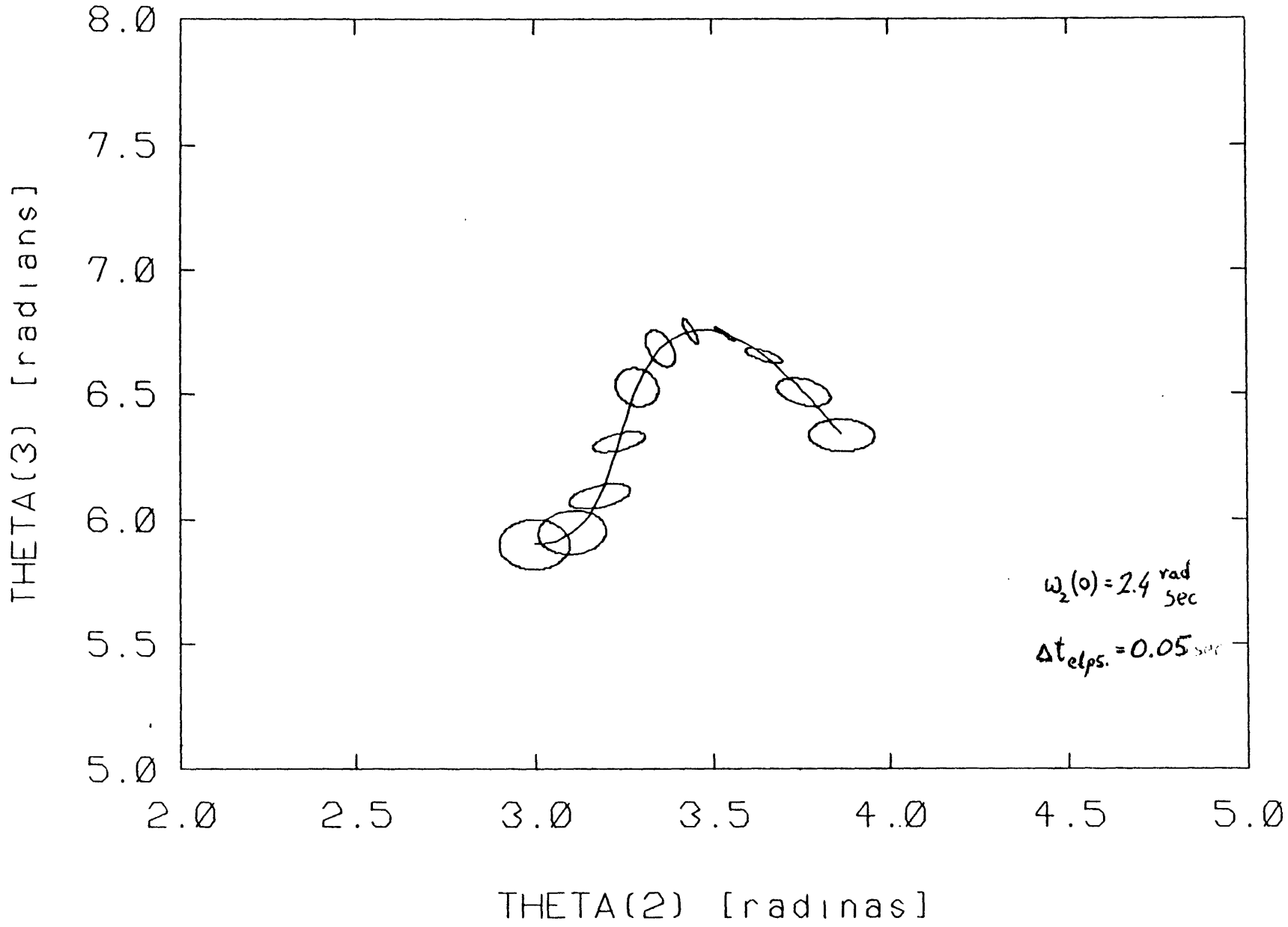

Figure 7-1: The propagation of initial uncertainties in the joint space with no joint torques

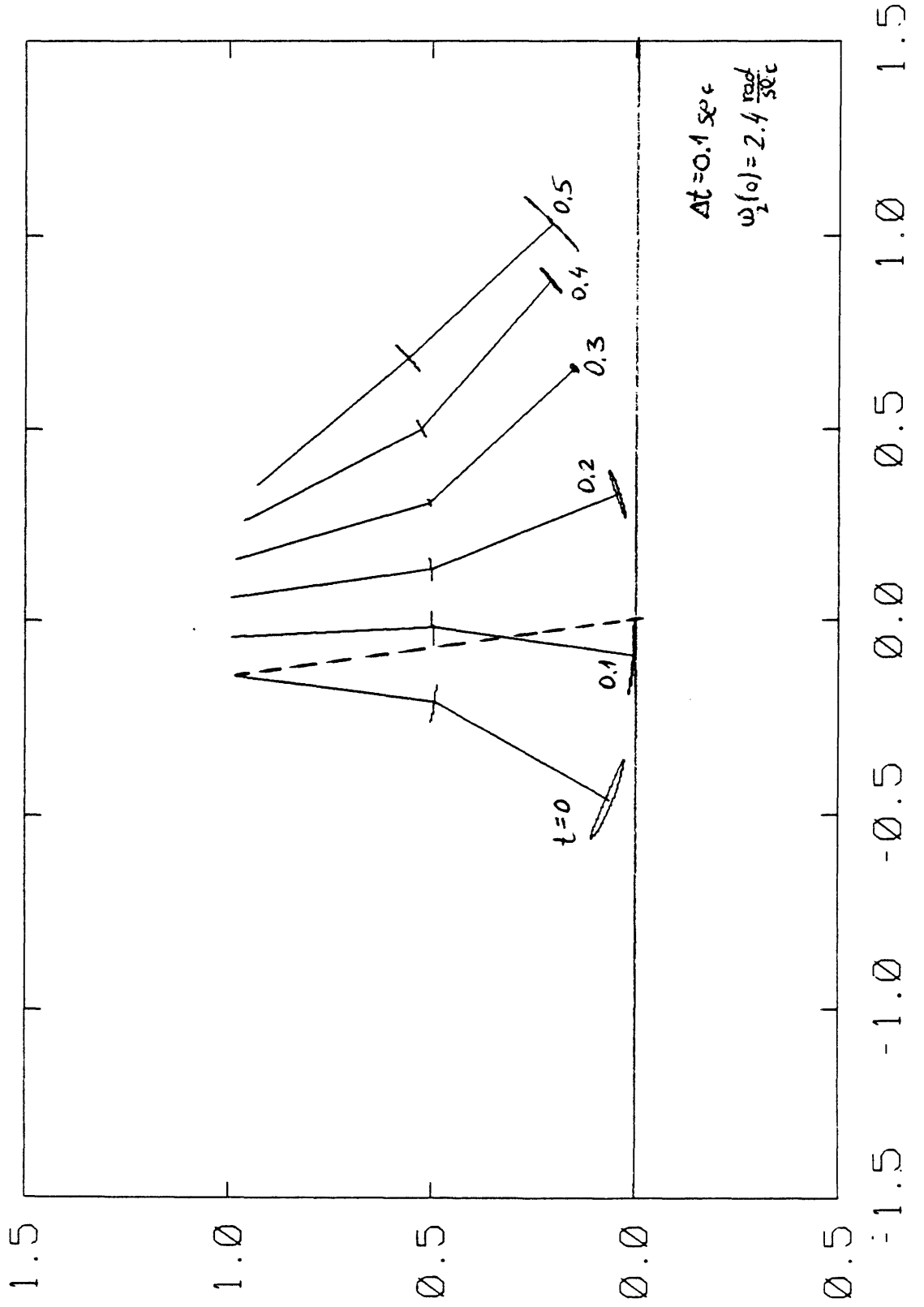

Figure 7-2: The propagation of initial uncertainties in the geometric space with no joint torques

ellipses in the joint-space (e.g. the ellipse at t=0.5 sec) map into the geometric space (the foot uncertainty at t=0.5 sec). This is a manifestation of the geometric connectivity constraints in the geometric space.

Figs. 7-3 and 7-4 show another simulation of the uncertainties, with the same initial conditions but with a constant torque of 1 nt-m at the knee. The smallest uncertainty is again achieved when the knee ends the extension phase (i.e. the knee angular velocity is zero). Notice that the hip uncertainty (the uncertainty in θ_2 goes almost to zero, as reflected in the knee position uncertainty in the geometric space. Also note that the ellipse at t=0.1 sec in the joint space collapses almost to a curve in the geometric space (for the foot position uncertainty).

Figs. 7-5 and 7-6 show the results of changing the direction of the knee actuator (i.e. applying a constant knee torque of -1 nt-m). The same observation, of minimum uncertainty when the knee angular velocity goes to zero, holds in this case too. It is interesting that the uncertainties in the geometric space have shrunk to curves in the geometric space for the duration of the simulation.

Figs. 7-7 and 7-8 describe the results of applying a constant hip torque of 10 nt-m with no knee torque. Under these conditions the knee initially flexes for about 0.4 sec. The minimum uncertainty is again obtained when the knee angular velocity goes to zero. The geometric space stick figures describe a sequence which is closer to real gait. It is especially interesting that the uncertainties are such that they do not violate the geometric constraint created by the floor (which is represented by the horizontal line through 0.0).

In summary, the results described in this section suggest that the process of gait, as described by the above model, minimizes the foot position uncertainty at exactly the state where heel strike and load transfer need to take place. It is also

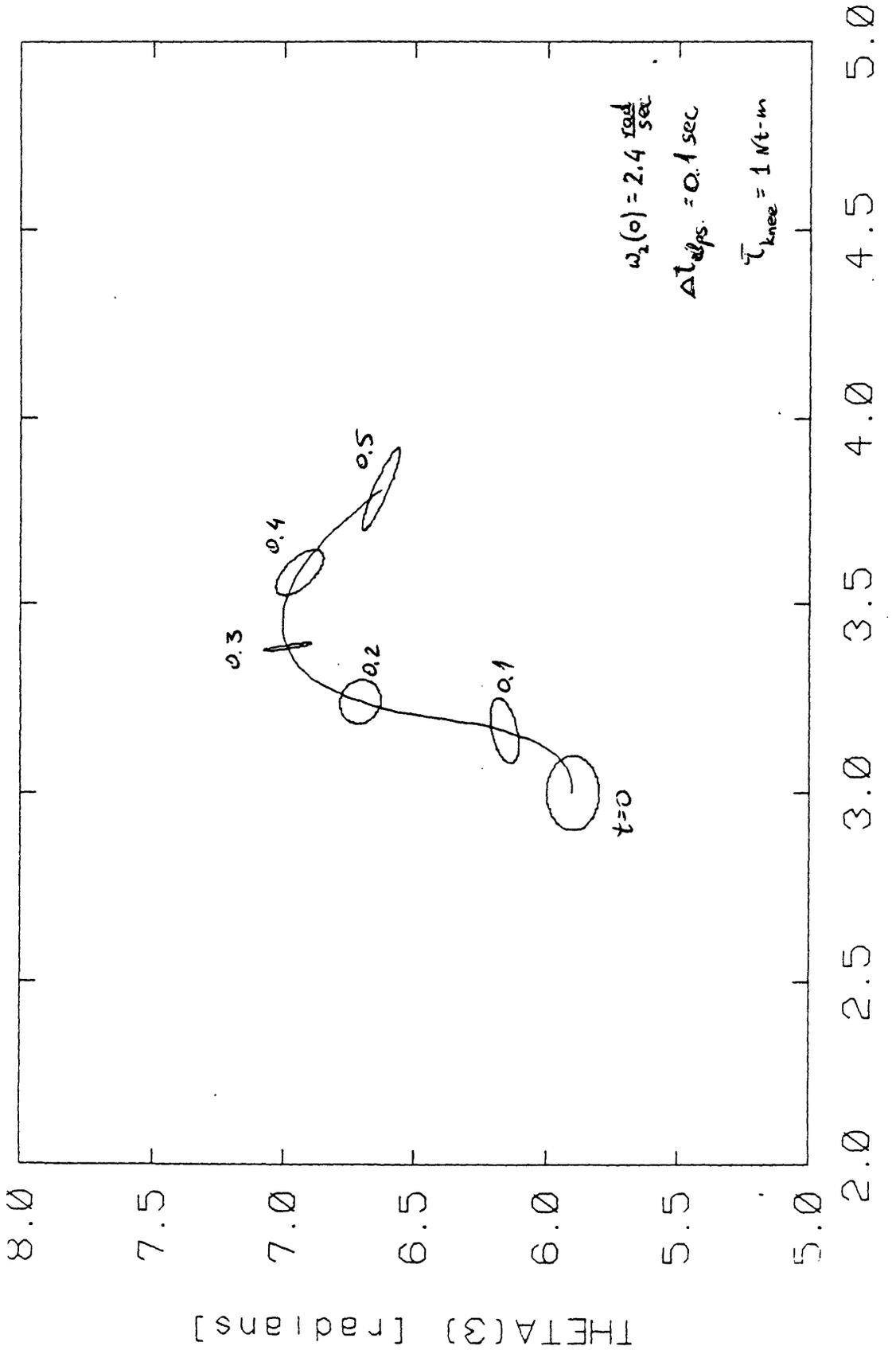

Figure 7-3: The propagation of initial uncertainties in the joint space with a positive knee torque

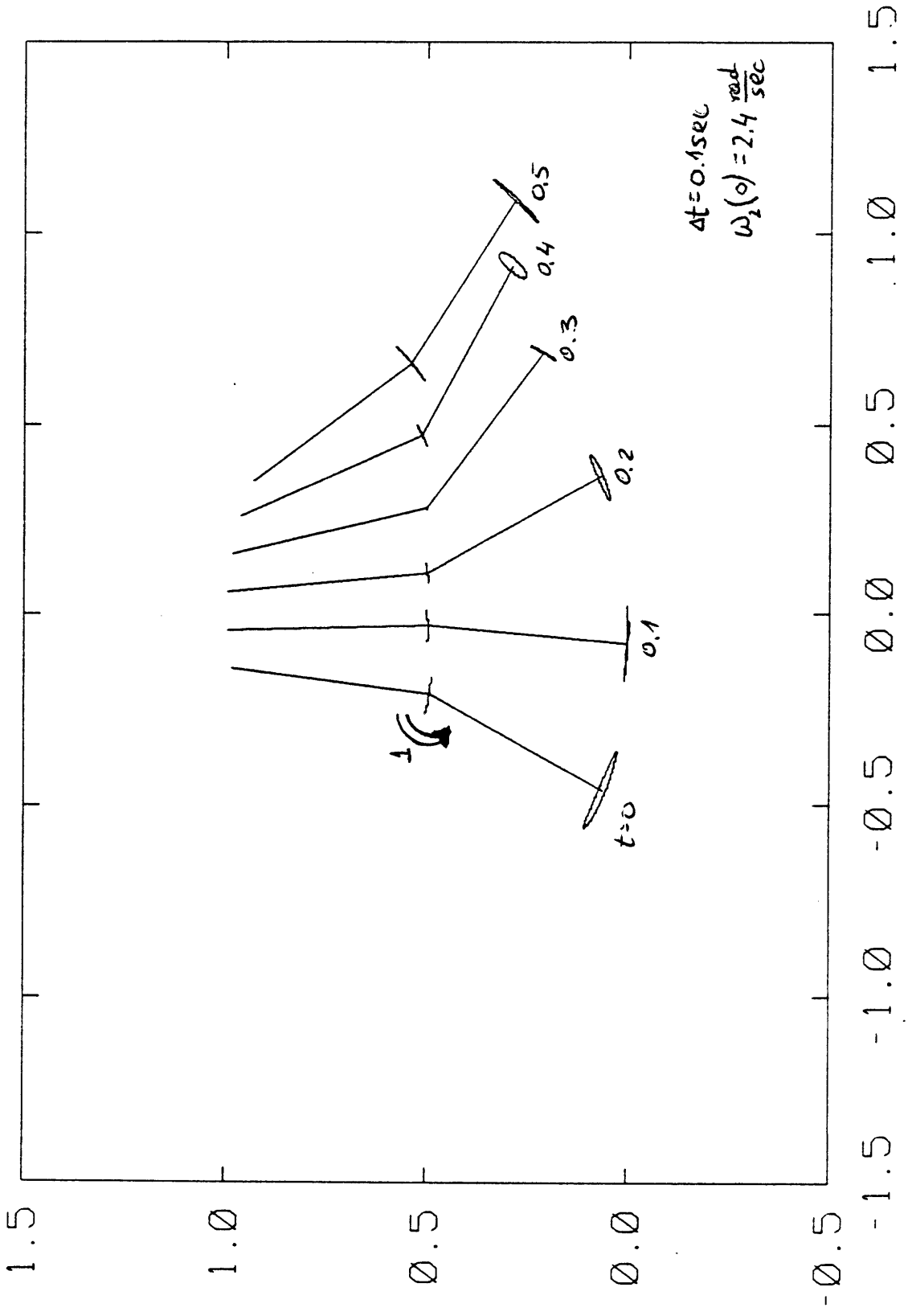

Figure 7-4: The propagation of initial uncertainties in the geometric space with a positive knee torque

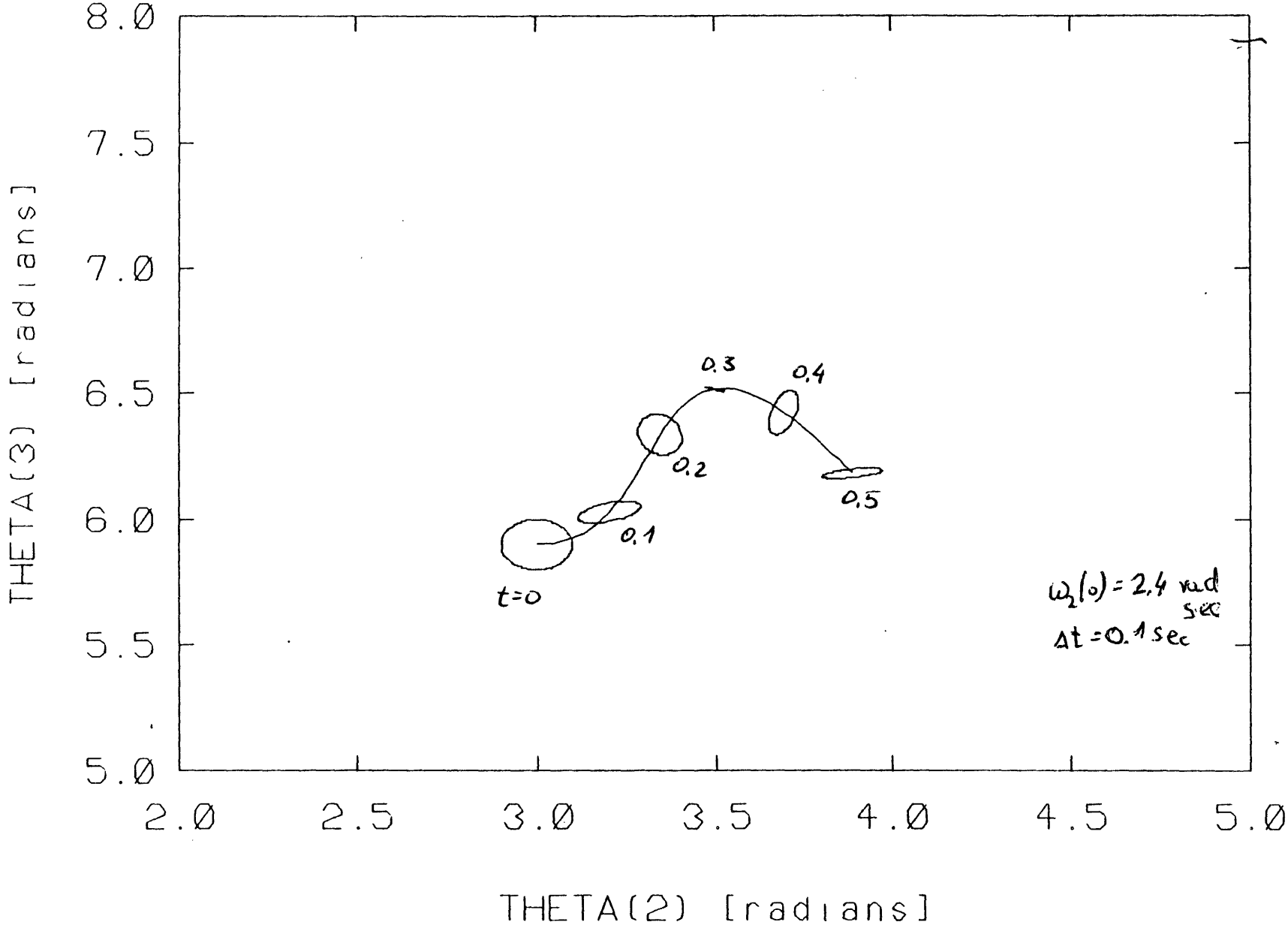

Figure 7-5: The propagation of initial uncertainties in the joint space with a negative knee torque

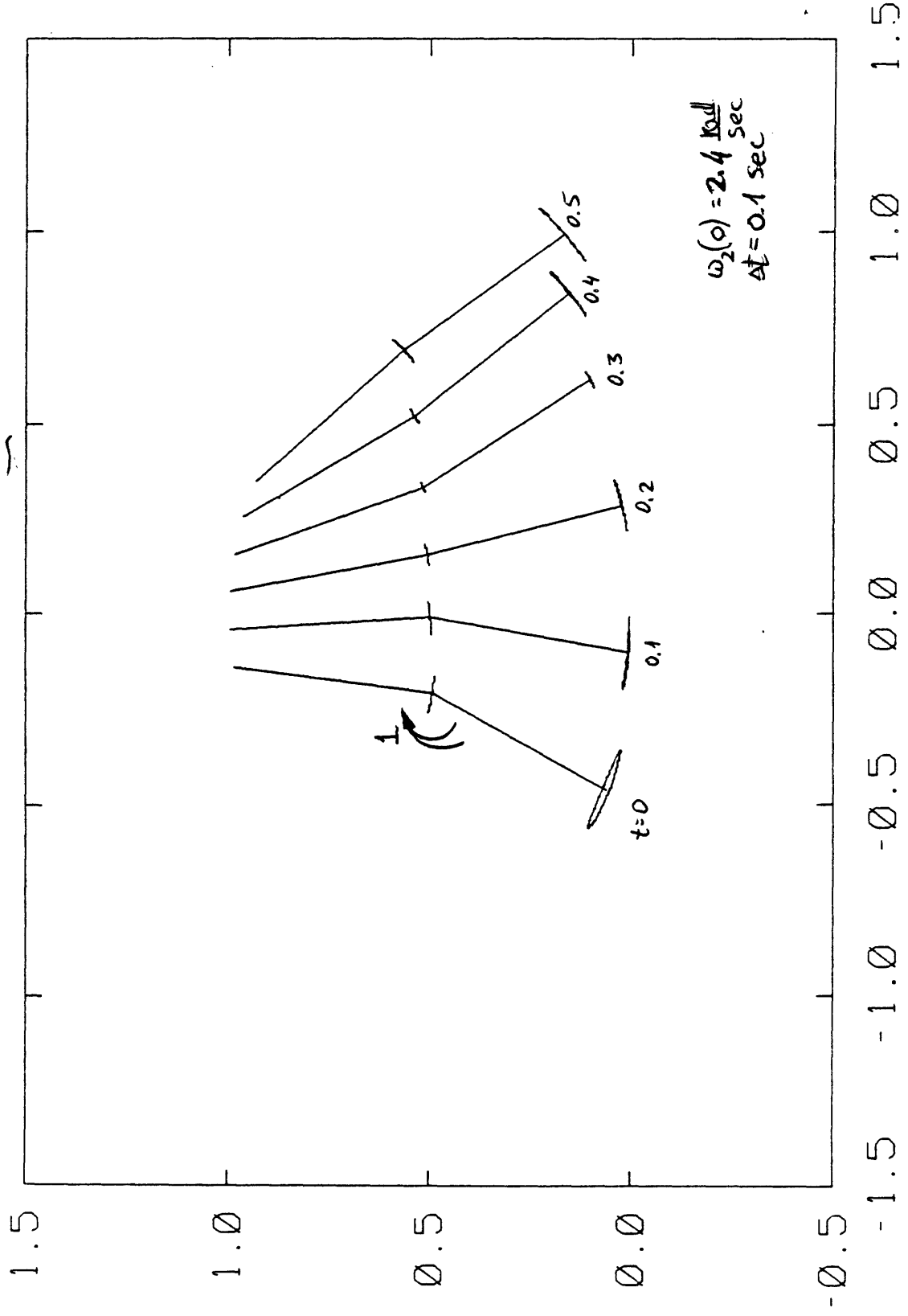

Figure 7-6: The propagation of initial uncertainties in the geometric space with a negative knee torque

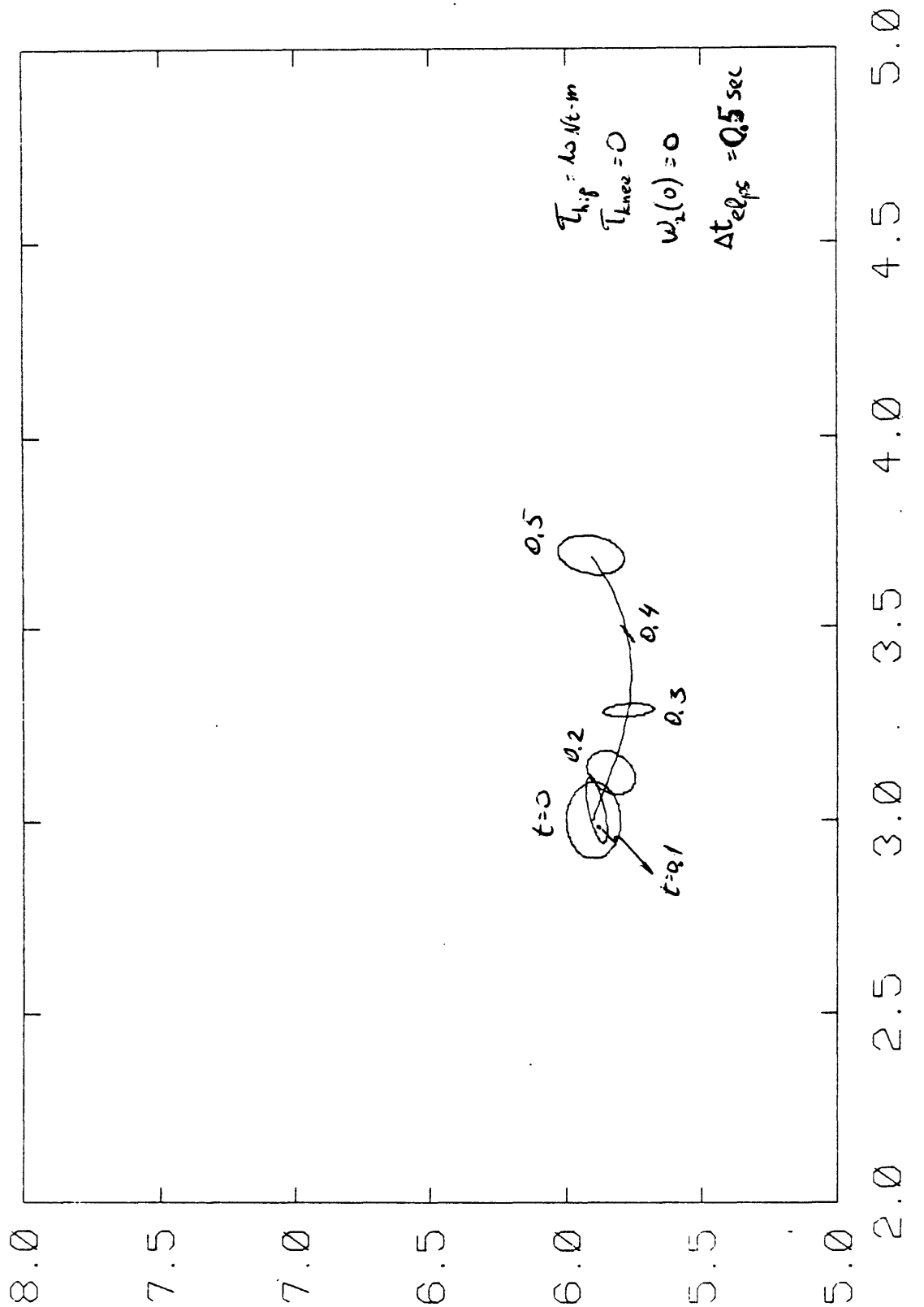

Figure 7-7: The propagation of initial uncertainties in the joint space with a positive hip torque

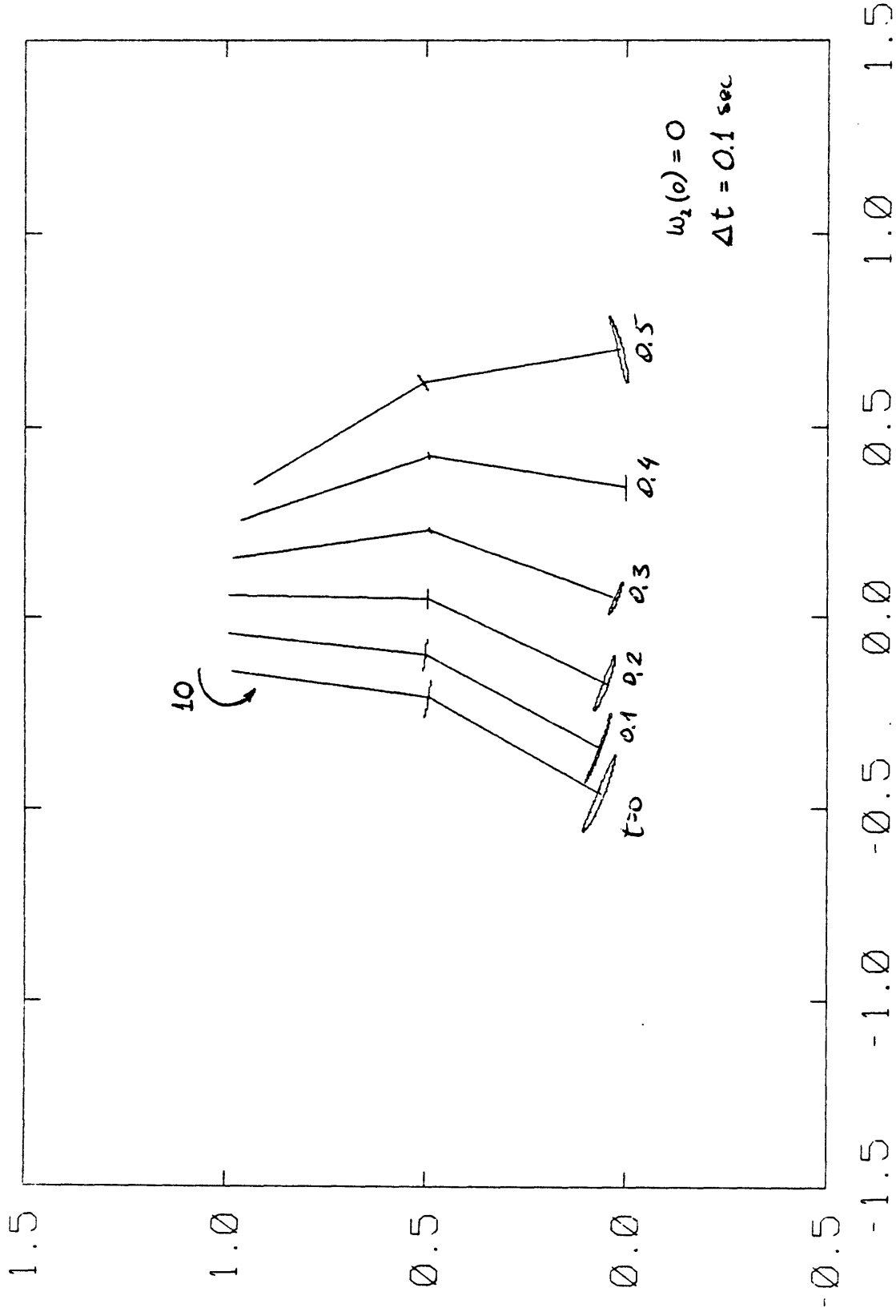

Figure 7-8: The propagation of initial uncertainties in the geometric space with a positive hip torque

interesting to note, that due to the geometric coupling between the shank and the thigh, uncertainties described by ellipses in the joint-space may collapse into curves in the geometric space. Hence, the possible foot locations will be along a curve, rather than inside a bounded area.

7.2 Propagation of Uncertainties During Obstacle Avoidance Maneuvers

Figs. 7-9 and 7-10 show the same stance leg kinematics and the same initial position of the swinging leg as in the previous section. The initial angular velocity of the swinging links is zero. The hip and knee actuators (20nt-m and -5 nt-m respectively) are turned on for 0.1 sec and then turned off. Note that at t=0.4 the knee position uncertainty shrinks almost to zero (reflecting the small hip angle uncertainty in the joint-space). This creates a foot location uncertainty which is close to a circular arc centered at the knee.

Connecting the extremum points of the foot uncertainties creates a tube which contains the possible trajectories. Note that the cross-section of the tube changes with time. Initially (up to 0.2 sec) the uncertainty is mostly orthogonal to the trajectory, whereas later on the uncertainty (at a given time) becomes more along the trajectory.

In Figs. 7-11 and 7-12 the hip actuator has been increased to 30 nt-m and the knee actuator changed to -15 nt-m. The uncertainties are much larger in this case, but there is an interesting ramification of the geometric coupling between the two degrees of freedom (θ_2 and θ_3) in the geometric space. If the only uncertainty in the system is that of θ_2, the foot could have made contact as low as point A. It is "due" to the uncertainty in θ_3, and the fact that the ellipse in the joint space is <u>not</u> aligned with the axes, that the uncertainty in the vertical direction is much smaller.

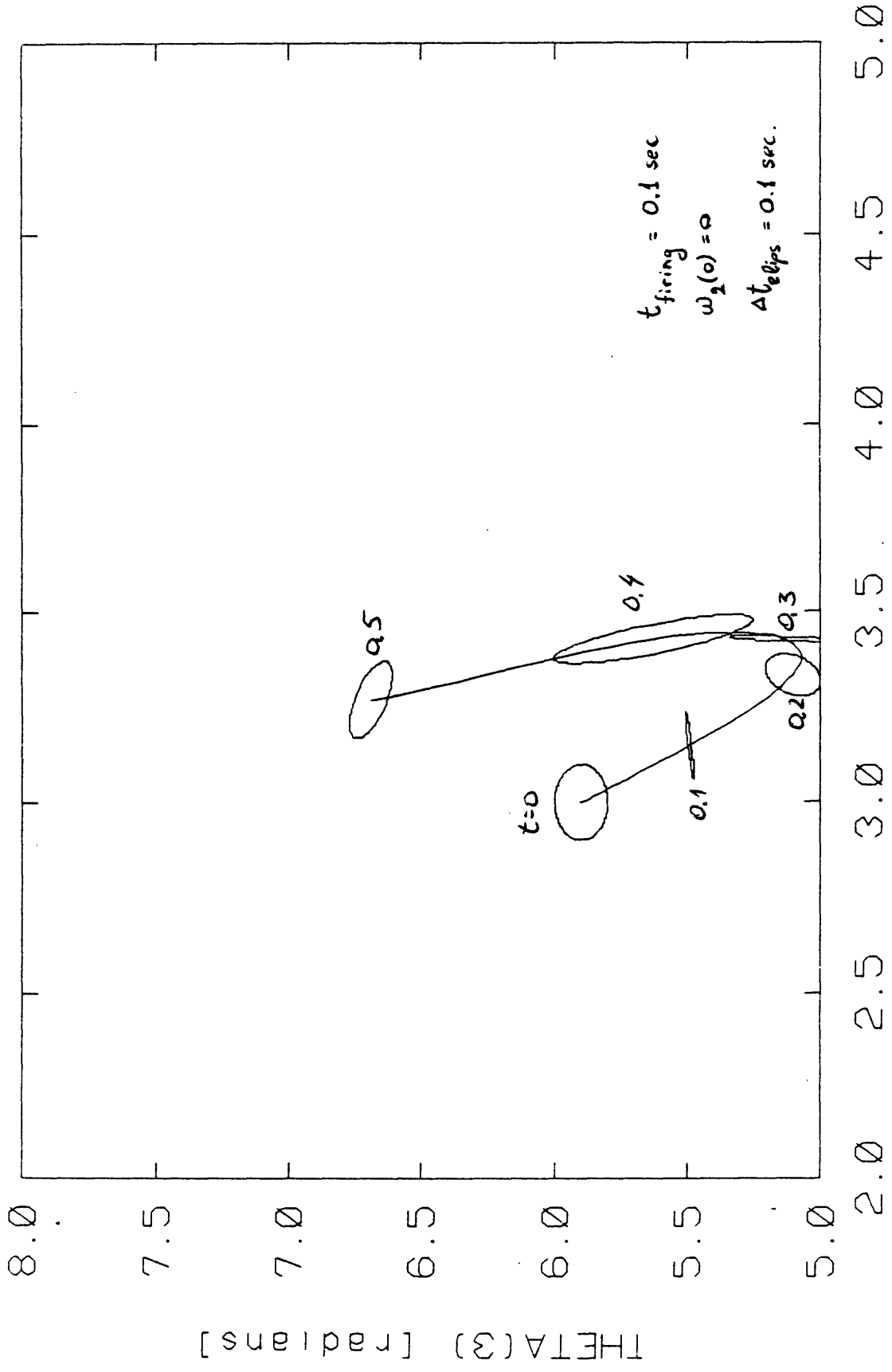

Figure 7-9: The propagation of initial uncertainties in the joint space with a "short firing" of small joint torques

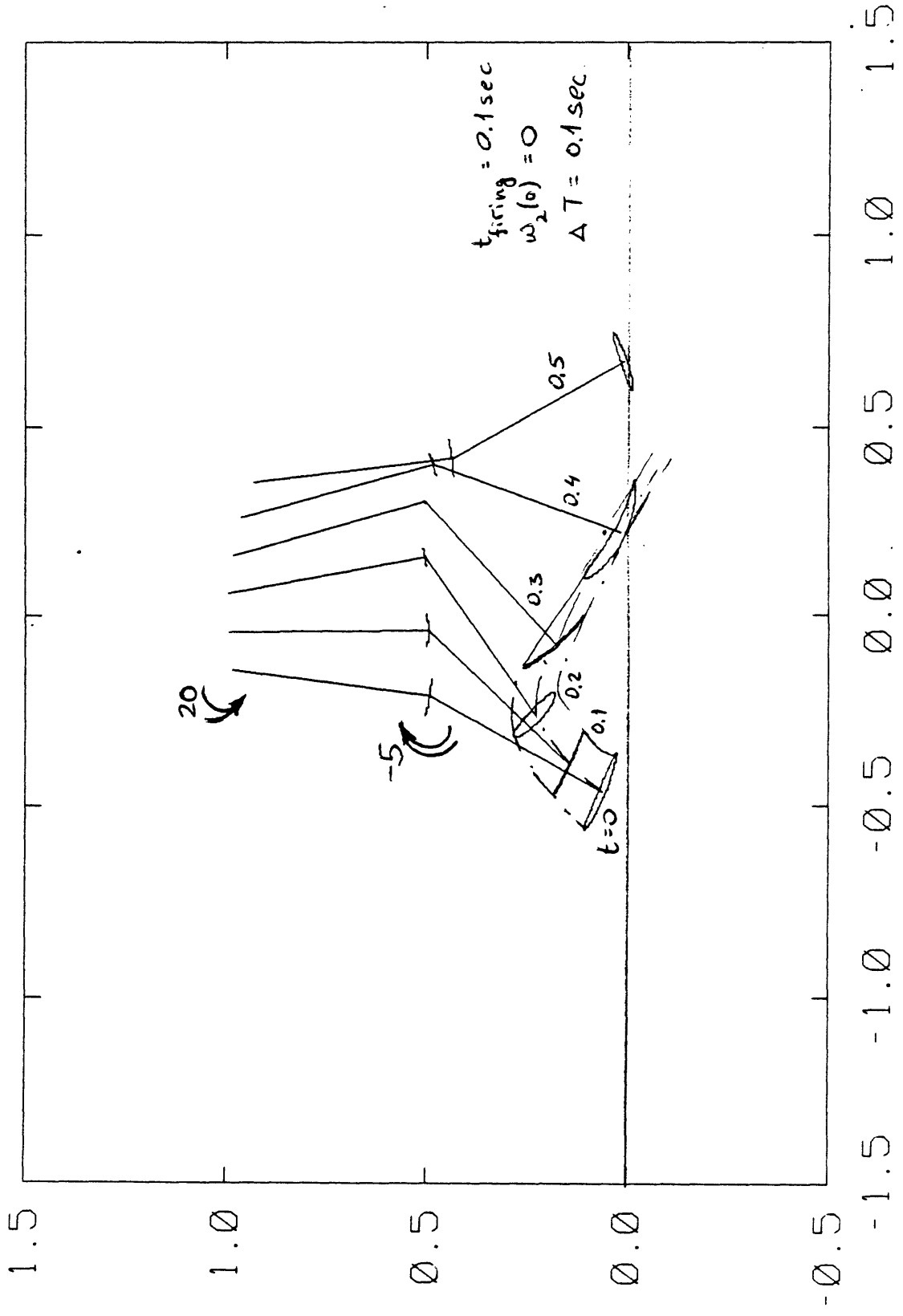

Figure 7-10: The propagation of initial uncertainties in the geometric space with a "short firing" of small joint torques

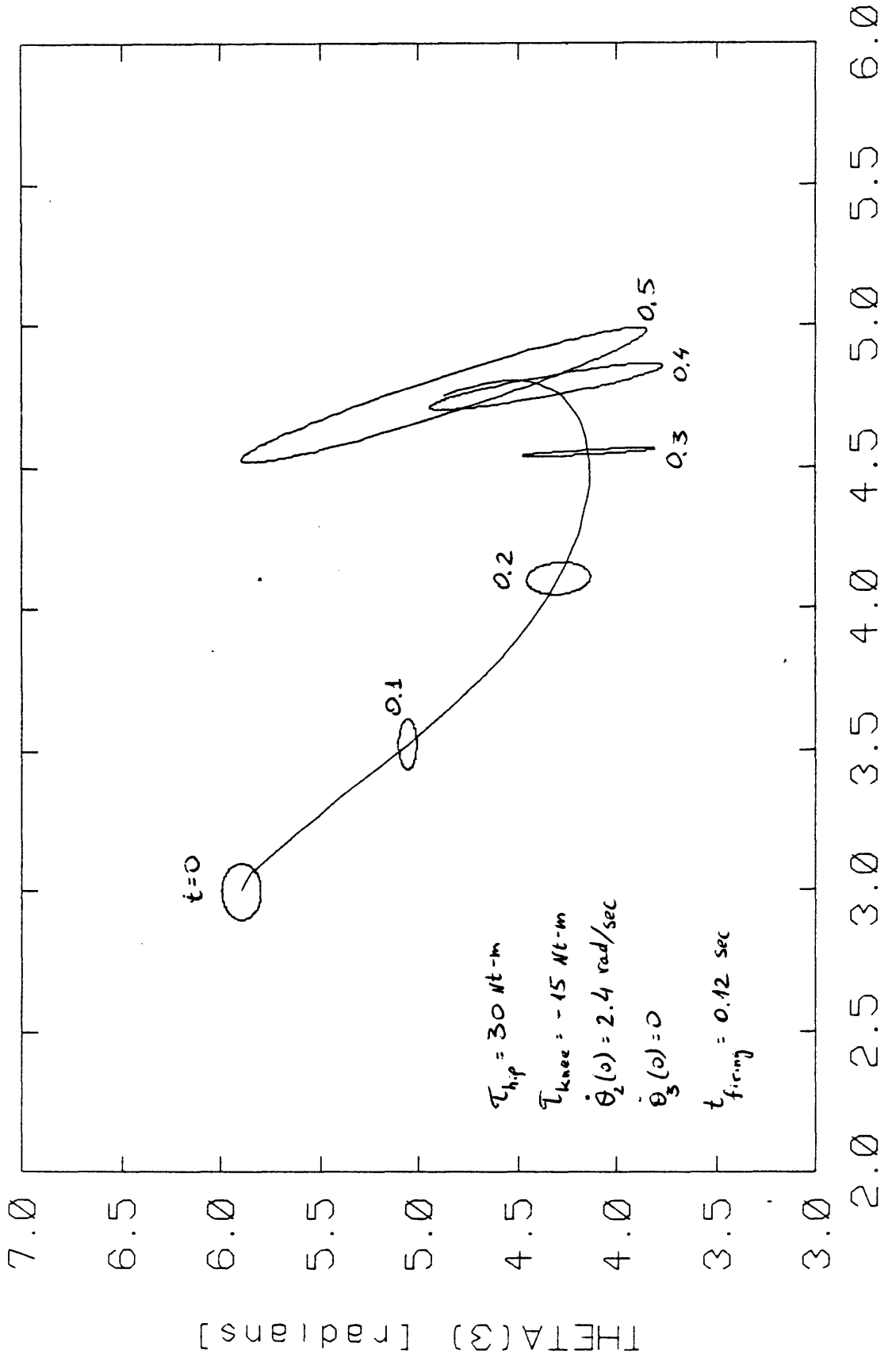

Figure 7-11: The propagation of initial uncertainties in the joint space with a "short firing" of large joint torques

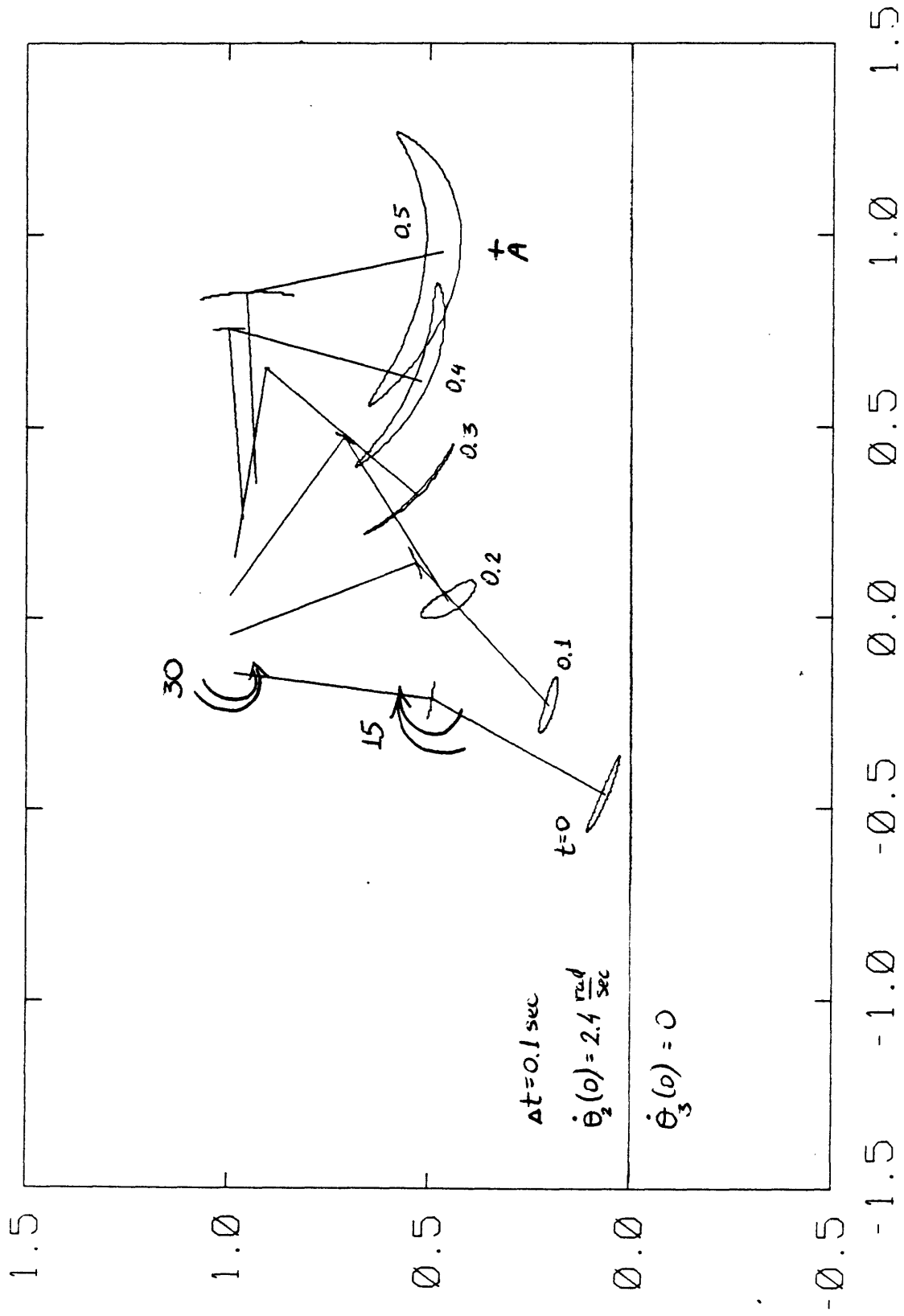

Figure 7-12: The propagation of initial uncertainties in the geometric space with a "short firing" of large joint torques

This observation suggests an interesting benefit for reflexive mechanisms which are aimed at overcoming vertical obstacles (recall the cat's placement reflex discussed in chapter 6). This would mean that under open-loop control, the system "trades off" uncertainties along its trajectory against uncertainties orthogonal to the trajectory.

Chapter 8
Conclusions and Future Work

8.1 Major Conclusions

This thesis describes the first application of Set-Theoretic analysis to the dynamics of multi-link systems in general, and to gait modelling in particular. The basic advantage of using Set-Theoretic (as opposed to other analytical tools) is its ability to handle sets. That enables a system analyst to study the response of a given dynamic system to unknown disturbances. The only information that is required is the upper bound of the disturbances, but no information on the statistical properties is required. The basic concept to be kept in mind is the concept of unknown-but-bounded, which is equivalent to the concept of a closed set: variables could exist anywhere inside the set, but cannot exist outside it.

Set-Theoretic analysis describes the time propagation of sets of states, and as such is a very useful tool in examining the sensitivity of dynamic systems to disturbances. The mathematical approach that has been adopted in this work uses ellipsoids to describe the sets in the state space. Symbolic linearization of the state equations around a nominal trajectory was used to generate the time propagation of the sets. Due to the mathematical complexity involved in obtaining a linearization of the state equations, an automated procedure (based on the symbolic language manipulator - MACSYMA) has been developed.

8.1.1 Practical limitations

The automated procedure successfully generated the linearized state equations of a three-link model. The first link moves with a known kinematics in an inertial reference system, with a double-pendulum hinged to it (which represents a two degree of freedom system). An attempt to apply the procedure to a three degree of freedom system failed at the stage of linearizing the state equations (due to computer memory limitations). This represents one of the limits which need to be considered in any future work.

Another practical limitation involves the size of the FORTRAN terms generated at the final stage of the automated procedure described above. This stage involves the transformation of the algebraic terms, generated in the linearization process, into the FORTRAN terms needed for the numerical integration routines. The limit involves the number of continuation lines accepted by the compiler, at the compilation stage. Some of the terms were more than 100 lines long, and they had to be broken down to sections no longer than about 20 lines in order to achieve a successful compilation.

8.1.2 Time propagation of uncertainties in a double pendulum

The time propagation of initial disturbances in a double pendulum was studied. The first observation concerns the numerical stability of Set-Theoretic analysis. The numerical simulations proved to be numerically stable under a broad range of initial conditions, initial uncertainties and actuator torques. Hence, Set-Theoretic appears to be a numerically suitable tool to study such a coupled, non-linear system.

The results show, that as expected, the system is much more sensitive to

disturbances at the hip than at the knee. The system is also more sensitive to disturbances when the nominal oscillations are large. When an angular velocity of a given degree of freedom became zero, the uncertainty in its angular position increased (which is always the case for a single pendulum).

The effect of constant torque actuators on the propagation of initial disturbances was studied. Using the physiological nomenclature - a combination of flexive hip torques and extensive knee torques were less sensitive than the opposite combination (extension at the hip and flexion at the knee). This result holds for small as well as large amplitude oscillations of the double pendulum.

Studying the effect of continuous actuator noise demonstrated the increase in the uncertainties. It also demonstrated the strong effect of the free parameter β, and the need to optimize its value in any study of continuous noise. The relationship between the nominal value of the angular velocity, and the position uncertainties persisted for the case of continuous noise.

8.1.3 The application of Set-Theoretic analysis to gait research

A new organizational framework for the study of control issues in gait research has been introduced. The role of Set-Theoretic as a general tool for examining the sensitivity of theoretical gait models has been discussed and illustrated on a simple 3-link, 2 degrees of freedom model.

The analysis of the sensitivity of the above model to initial disturbances (analyzed by studying the propagation of initial uncertainties) reveals that over a wide range of initial conditions, the uncertainty goes to a minimum when the angular velocity of the knee goes to zero (the end of the swing phase). This suggests that the natural geometric coupling between the thigh and the shank of

the swinging leg are beneficial in order to achieve convergence to the nominal position of heel strike and load transfer.

Another useful result was obtained in analyzing the response of the "placement reflex" reaction (i.e. applying large flexive torques at the hip and the knee for a short period of time). It appears that the geometric coupling causes smaller uncertainties in the orthogonal direction to the trajectory. This means that without any sophisticated closed-loop controllers, obstacles of large height variation can be successfully negotiated.

An interesting suggestion arises when a detailed analysis of the "placement reflex" is done. As was described in Chpater 2, the leg position seems to play a modulator role in that reflex: during swing phase, the "placement reflex" which involves hip and knee flexion takes place, whereas an inverse response occurs during stance phase. As the advantageous aspects of the flexive reponse during swing phase have been demonstrated, an interesting strategy for artificial locomotion (for prosthesis as well as walking mechanisms) emerges.

Such a strategy would suggest, that locking the joint (e.g. the knee joint in the "M.I.T. knee" - see [16]), is a useful strategy ONLY during stance phase. A different strategy should be applied during swing phase, which would take advantage of the natural hip flexion response, and will add to that a strong knee flexion for a short period of time. It seems that such a response will be more along the lines of the natural response to disturbances, as well as taking advantage of the inherent properties of a multi-linkage system (as exemplified by the uncertainty propagation in the obstacle avoidance simulations).

As a matter of fact, since the modulated reflex as described above does not depend on the gait process (it can be triggered while the leg is at rest), a unified

response to disturbances during standing and walking emerges. The input signal required for such a strategy is only the hip position, and based on this input, the knee position controller could be referenced to either the fully extended position (when the hip is extended), or to a flexive response - if the hip is flexed.

8.2 Future work

Since this work is the first at "marrying" Set-Theoretic analysis and multi-linkage systems, a major part of the thesis deals with the development and testing of the necessary tools for such an implementation. Once it is established that indeed Set-Theoretic analysis can be used as an analytic tool for the study of such systems, the door will be open for future research.

Future extensions can deal with two different aspects:

1. experimental studies
2. theoretical extensions

8.2.1 Experimental studies

Chapter 5 describes the numerous analytical and computational methods that have been carried out in this study. It is clear, though, that the test of the results will have to involve experimental work.

Studies on the disturbance propagation in multi-linkage systems can be performed on mechanical pendulums, driven by electrical motors (the actual model discussed in this work will have to be modified, to include the motor dynamics). The experiments will involve measurements of the propagation of disturbances through the system, and will compare those results to the theoretical predictions.

The same experiments can be carried out in the area of biomechanics. The propagation of disturbances can be studied in tasks of arm movement, or in gait studies. By using different models of controllers on the theoretical models (and different models of actuators), correlations could be found between the theoretical models and the experimental results. Such studies can be an invaluable source of information on the function of the local (e.g. spinal) disturbance handling mechanisms (the third level of movement control as discussed in chapter 6).

Locomotion (walking and running) can be studied especially with reference to the global strategies used by the human being to recover from disturbances. Such studies will be a direct extension of Nashner's studies (which dealt only with the ankle joint response), and could carry a wealth of information on the properties of the human recovery control system. Issues like step size control, dynamic decoupling between the leg in stance and the leg in swing can be studied by disturbing the legs in a controllable manner.

Different kinds of disturbances can be studied. The one which will most closely resemble the present disturbance propagation study, will be a stumbling experiment. Such a study could involve the introduction of controlled disturbances to the swinging leg. Another kind of disturbance can be the continuous disturbance source. This could be, for example, a pnematic device which could introduce controlled disturbances by changing its thrust. The third kind of disturbances are those that originate at the leg in stance. These can be vertical or horizontal disturbances, aimed at simulating the effects of slipping or walking on a non-solid surface (like sand).

Similar issues exist in arm physiology and control. The application of Set-Theoretic analysis to such systems presents a new mathematical formulation aimed at studying the fidelity of this control system (i.e. what is the target area for a

given pointing task, and what are the properties of a theoretical control model required to achieve the same fidelity.

8.2.2 Theoretical extensions

The present application of Set-Theoretic to multi-linkage systems uses the linearized form of the state equations. This work has established that the limit for an automatic procedure, which generates the symbolic version of the linearized state equations is reached for a 3-link 2 degrees of freedom system. Naturally, the following questions should be addressed.

1. Can other algorithms (different than Paul's) be used for a more efficient generation of the above equations?

2. Can numerical differentiation replace the symbolic differentiation for the purpose of creating the linearized state equations?

3. As Paul's algorithm (as well as others) result in the dynamic equations in the implicit form (with respect to the state variables), how can Set-Theoretic be modified to deal with implicit state equations?

4. How can mechanical stops and other highly nonlinear effects which are common in multi-linkage systems be integrated into the analysis?

As discussed in the chapter describing the historical development of Set-Theoretic, this work presents the first and necessary step for future developments in the area. Just as the very first works in the application of Set-Theoretic to linear systems dealt with aspects of estimation theory, and the time propagation of uncertainties in linear systems, this work presents the equivalent extension to the non-linear systems of the kind of multi-linkage mechanisms.

Following the developments of Set-Theoretic applications to linear systems, two major problems have to be solved, in order for Set-Theoretic to become a

viable tool in the control of multi-linkage systems:

1. the inverse problem

2. the optimal control problem

The inverse problem can be described in the following manner: given a target zone (in the state space) and constraints on the actuators and the outputs, what is the time sequence of control sets that could get the system from an initial set, subject to the bounded sets of disturbances, to within the target zone. The result of such a solution will be the time sequence of allowable control sets, which will get the system (in the face of the bounded disturbances), from its original set to the final (required) set, without violating any of the control and output constraints.

The optimal control problem is strongly tied to the results of the inverse problem. Conceptually, this is a problem of finding the control sequence within the sets of allowable controls, which will maximize the tolerance of the system for disturbances. This has the potential of becoming a major control design tool for multi-linkage systems, especially for devices which are normally subject to noise (vibrations for example).

Finally, I would like to stress that the general tool of Set-Theoretic could be applied to other dynamic systems, like precision manufacturing for example. Terms like target zone (final tolerance), bounded disturbances and constraints appear over and over in other dynamic systems. Extending the use of Set-Theoretic analysis to other fields, may prove to be a benefitial.

Bibliography

[1] Alexander R. McN.
Allometry of the Limbs of Antelopes (Bovidae).
J. Zool. Lond. 183:125-146, 1977.

[2] Alexander, R. McN.
Walking and Running.
American Scientist 72(4):348-354, 1984.

[3] Antonsson, E. K.
A Three-Dimensional Kinematic Acquisition and Intersegmental Dynamic Analysis System for Human Motion.
PhD thesis, M.I.T., June, 1982.

[4] Beckett, R. and Chang, K.
An Evaluation of the Kinematics of Gait by Minimum Energy.
J. Biomech. 1:147-159, 1968.

[5] Beletskii, V. V. and Golubitskaya, M. D.
Model Problem of Bipedal Locomotion with Vertical Uncomfortableness.
Vestnik Moskovskogo Universiteta, Mekhanika 36(3):62-68, 1981.
Translated from Russian.

[6] Bendat, J. S. and Piersol, A.G.
Random Data: Analysis and Measurement Procedures.
Wiley - Interscience, 1971.

[7] Bressler, B. and Frankel, J. P.
The Forces and Moments in the Leg During Level Walking.
Trans. ASME 72:27-36, Jan, 1950.
Presented at the 1948 Annual Meeting, New York, N.Y., Nov 28-Dec 3, 1948, Paper No. 48-A-62.

[8] Chow, C. K. and Jacobson, D. H.
Studies of Human Locomotion via Optimal Programming.
Mathematical Biosciences 10:239-306, 1971.

[9] Denavit J. and Hartenberg, R. S.
A Kinematic Notation for Lower-Pair Mechanisms Based on Matrices.
ASME Journal of Applied Mechanics :215-221, Jun, 1955.

[10] Frank A. A.
An Approach to the Dynamic Analysis and Synthesis of Biped Locomotion Machines.
Medical and Biological Engineering 8:465-476, 1970.

[11] Franklin, G. F. and Powell, J. D.
Digital Control of Dynamic Systems.
Addison-Wesley Publishing Co., 1980.

[12] Glover, J. D. and Schweppe F. C.
Control of Linear Dynamic Systems with Set-Constrained Disturbances.
IEEE Trans. in Autom. Control AC-16(5), Oct, 1971.

[13] Glover J. D.
Control of Systems with Unknown-but-Bounded Disturbances - Application to Electric Power Systems.
PhD thesis, EE Dept., M.I.T., January, 1971.

[14] Gray, J.
Animal Locomotion.
Wiedenfeld and Nicholson, London, 1968.

[15] Grillner, S.
Locomotion in Vertebrates: Central Mechanisms and Reflex Interaction.
Physiol. Rev. 55:247-304, 1975.

[16] Grimes, D. L.
An Active Multi-Mode Above-Knee Prosthesis Controller.
PhD thesis, ME Dept., M.I.T., June, 1979.

[17] Gubina F., Hemami H. and McGhee R. B.
On the Dynamic Stability of Biped Locomotion.
IEEE Transactions on Biomedical Engineering BME-21(2):102-108, Mar, 1974.

[18] Hemami H. Chen B.
Stability Analysis and Input Design of a Two-Link Planar Biped.
The International Journal of Robotics Research 3(2):93-100, 1984.

[19] Hirose, S.
A Study of Design and Control of Quadruped Walking Vehicle.
The International Journal of Robotics Research 3(2):113-133, 1984.

[20] Hnyilicza, E.
A Set-Theoretic Approach to State Estimation.
Master's thesis, EE Dept., M.I.T., Jun, 1969.

[21] Kahan W.
Circumscribing an Ellipsoid About an Inter-Section of Two Ellipsoids.
Can. Math. Bull. 2(3):437-441, 1968.

(22) ASME-NYAS.
A Versatile Walking Truck, 1968.
Transportation Engineering Conf., Washington D.C.

[23] Marey, E. J.
A Treatise on Terrestrial and Aerial Locomotion.
Appleton-Century-Crofts, New York, 1874.

(24) Second International Symposium on External Control of Human Extremities, Dubrovnik, Yugoslavia.
Finite State Control of Quadruped Locomotion, 1966.

[25] McGhee R. B.
Some Finite State Aspects of Legged Locomotion.
Mathemetical Biosciences 2:57-66, 1968.

[26] McMahon, T. A.
Muscles, Reflexes and Locomotion.
Princeton University Press, Princeton, New Jersey, 1984.

[27] Miura, H. and Shimoyama, I.
Dynamic Walk of a Biped.
The International Journal of Robotics Research 3(2):60-74, 1984.

[28] Mochon, S. and McMahon, T. A.
Ballistic Walking.
J. Bionech. 13:49-57, 1980.

[29] Mochon, S. and McMahon, T. A.
Ballistic Walking: an Improved Model.
Math. Biosci. 52:241-260, 1981.

[30] Mochon, S.
Ballistic Walking: a Mathematical Model of Human Locomotion.
PhD thesis, Harvard University, April, 1980.

[31] Moore R. L.
Adaptive Estimation and Control for Nuclear Power Plant Load Changes.
PhD thesis, EE Dept., M.I.T., May, 1971.

[32] Morawski, J. M.
A Simple Model of Step Control in Bipedal Locomotion.
IEEE Transactions on Biomedical Engineering BME-25(6):544-549, Nov, 1978.

[33] Murray, M. P., Drought, A. B. and Kory, R. C.
Walking Patterns of Normal Men.
Journal of Bone and Joint Surgery 46-A(2):335-360, Mar, 1964.

[34] Murray, M. P., Kory, R. C., Clarkson, B. H. and Sopic, S. B.
Comparison of Free and Fast Speed Walking Patterns of Normal Men.
Am. Jour. of Physical Medicine 45(1):1966, 1966.

[35] Muybridge, E.
The Human Figure in Motion.
Dover, New York, 1955.
Abridgements of the original work, published in 1887.

[36] Nashner, L. M.
Balance Adjustments of Humans Perturbed While Walking.
Journal of Neurophysiology 44(4):650-663, Oct, 1980.

[37] Nubar, Y. and Contini R.
A Minimal Principle in Bio-Mechanics.
Bull. Math. Biophys. 23:377-390, 1961.

[38] Ogata, K.
Modern Control Engineering.
Prentice-Hall, Inc., Englewood Cliffs, N.J., 1970.

[39] Ozguner, F., Tsai, S. J. and McGhee, R. B.
An Approach to the Use of Terrain - Preview Information in Rough Terrain Locomotion by a Hexapod Walking Machine.
The International Journal of Robotics Research 3(2):134-146, 1984.

[40] Paul R. P.
Robot Manipulators: Mathematics, Programming and Control.
M.I.T. Press, Cambridge, Mass., 1981.

[41] Raibert, M. H., Brown, H. B. and Chepponis, M.
Experiments in Balance with a 3D One - Legged Hopping Machine.
The International Journal of Robotics Research 3(2):75-92, 1984.

[42] Schlaepfer, F. and Schweppe F.
Continuous Time State Estimation Under Disturbance Bounded by Convex Sets.
IEEE Trans. in Autom. Control AC-17:197-206, Apr, 1972.

[43] Schlaepfer F.
Set-Theoretic Estimation of Distributed Parameter Systems.
Technical Report ESL-R-413, M.I.T., Cambridge, Mass., Jan, 1970.

[44] Schultz, D. G. and Melsa, J. L.
State Functions and Linear Control Systems.
McGraw-Hill Book Co., 1967.

[45] Schweppe, F. and Knudsen, H.
The Theory of Amorphous Cloud Trajectory Prediction.
IEEE Trans. Inform. Theory IT-14(3):415-427, May, 1968.

[46] Schweppe F. C.
Recursive State Estimation: Unknown but Bounded Errors and System Inputs.
IEEE Trans in Autom. Control AC-13:22-29, Feb, 1968.

[47] Schweppe, F.C.
Uncertain Dynamic Systems.
Prentice-Hall Inc., Englewood Cliffs, New Jersey, 1973.

[48] Shiller, Z.
Optimal Dynamic Trajectories and Modeling of Robotic Manipulators.
Master's thesis, ME Dept., M.I.T., Jun, 1984.

[49] Simon, S. R., Paul, I. L., Mansour, J., Munro, M. Abernethy, P. J. and Radin, E. L.
Peak Dynamic Force in Human Gait.
Journal of Biomechanics 14(12):817-822, 1981.

[50] Sira-Ramirez, H. J.
Set-Theoretic Control of Large - Scale Uncertain Systems.
PhD thesis, EE Dept., M.I.T., 1977.

[51] Stein, J. L.
Design Issues in the Stance Phase Control of above knee Prostheses.
PhD thesis, ME Dept., M.I.T., January, 1983.

[52] Tomovic, R. and McGhee, R. B.
A Finite State Approach to the Synthesis of Bioengineering Control Systems.
IEEE Transactionss on Human Factors in Electronics HFE-7(2):65-69, Jun, 1966.

(53) ASME.
Optimal Trajectory Controls for Systems of Coupled Rigid Bodies, 1971.
Presented at the 1971 ASME Int. Design Automation Conf., Ontario, Canada, Paper 71-Vibr-82.

[54] Townsend M. A. and Seireg, A. A.
Effect of Model Complexity and Gait Criteria on the Synthesis of Bipedal Locomotion.
IEEE Transactions on Biomedical Engineering BME-20(6):433-444, Nov, 1973.

[55] Townsend, M. A.
Optimal Trajectories and Controls for Systems of Coupled Rigid Bodies with Application to Biped Locomotion.
PhD thesis, M.E. Dept., The University of Wisconsin, 1971.

[56] Usoro, P. B.
Set-Theoretic Control Synthesis and Application.
PhD thesis, ME Dept., M.I.T., 1979.

[57] Vukobratovic M., Frank A. A. and Juricic, D.
On the Stability of Biped Locomotion.
IEEE Transactions on Bio-Medical Engineering BME-17(1):25-36, Jan, 1970.

[58] Vukobratovic M. and Juricic D.
Contribution to the Synthesis of Biped Gait.
IEEE Transactions on Bio-Medical Engineering BME-16(1):1-6, Jan, 1969.

[59] Vukobratovic, M. and Stokic, D.
Significance of Force - Feedback in Controlling Arificial Locomotion - Manipulation Systems.
IEEE Transactions on Biomedical Engineering BME-27(12):705-713, Dec, 1980.

[60] Winter, D. A. and Robertson, D. G. E.
Joint Torque and Energy Patterns in Normal Gait.
Biollogical Cybernetics 29:137-142, 1978.

[61] Winter, D. A.
Overall Principle of Lower Limb Support During Stance Phase of Gait.
Journal of Biomechanics 13:923-927, 1980.

[62] Witsenhausen, H. S.
Minimax Control of Uncertain Systems.
Technical Report ESL-R-269, Electronic Systems Lab., M.I.T., Cambridge, Mass., May, 1966.

[63] Witsenhausen, H. S.
A Minimax Control Problem for Sampled Linear Systems.
IEEE Trans. in Autom. Control AC-13:5-21, Feb, 1968.

[64] Witsenhausen, H. S.
Set of Possible States of Linear Systems Given Perturbed Observations.
IEEE Trans. in Autom. Control AC-13:556-558, Oct, 1968.

[65] Zarrugh, M. Y.
Kinematic Prediction of Intersegment Loads and Power at the Joints of the Leg in Walking.
Journal of Biomechanics 14(10):713-725, 1981.